

NACA TN 2289

NATIONAL ADVISORY COMMITTEE FOR AERONAUTICS

TECHNICAL NOTE 2289

ELASTIC CONSTANTS FOR CORRUGATED-CORE
SANDWICH PLATES

By Charles Libove and Ralph E. Hubka

Langley Aeronautical Laboratory
Langley Field, Va.



Washington
February 1951

TECHNICAL NOTE 2289

ELASTIC CONSTANTS FOR CORRUGATED-CORE

SANDWICH PLATES

By Charles Libove and Ralph E. Hubka

SUMMARY

The sandwich plate consisting of corrugated sheet fastened between two face sheets is considered. Application of existing theories to the analysis of such a sandwich plate requires the knowledge of certain elastic constants. Formulas and charts are presented for the evaluation of these constants. The formulas for three of these constants were checked experimentally and found to give values in close agreement with the experimental values.

INTRODUCTION

A type of sandwich plate for which practical use has recently been found in airplane-wing construction consists of a corrugated metal sheet fastened, at its crests and troughs, to two ordinary metal sheets (see, for example, fig. 1). The main advantage of this type of sandwich is that the corrugated-sheet core not only serves to separate the faces and, thereby, to achieve high flexural stiffness, but it also carries a share of any compressive loading applied parallel to the corrugations and any edgewise shear loading. This type of sandwich has been called cardboard-box construction (reference 1) and also double-skin construction. It is referred to herein as corrugated-core sandwich plate.

Plate theories applicable to the symmetrical type of corrugated-core sandwich, illustrated in figure 1(a), have been developed in reference 2 for flat plates and in reference 3 for curved plates.^a These theories are essentially homogeneous orthotropic-plate theories extended to include deflections due to transverse shear, which can be significant for the corrugated-core sandwich plate because of the relatively flexible core.

^aThe precedent established in reference 4 of referring to sandwich plates of the type shown in figure 1(a) as symmetrical is adhered to herein. The type of corrugation shown in this figure is also called symmetrical.

Application of the general sandwich-plate theories of references 2 and 3 to any particular type of sandwich requires a knowledge of certain elastic constants for that type of sandwich plate. These constants describe the distortions associated with simple loadings. They include two transverse shear stiffnesses D_{Q_x} and D_{Q_y} , two bending stiffnesses D_x and D_y , a twisting stiffness D_{xy} , two stretching moduli E_x and E_y , a shearing modulus G_{xy} , two Poisson's ratios μ_x and μ_y associated with bending, and two Poisson's ratios μ'_x and μ'_y associated with stretching.

The purpose of the present paper is to present formulas for evaluating these elastic constants for the corrugated-core type of sandwich plate. For the sake of completeness, formulas are also developed for evaluating the additional elastic constants that would be needed for a rigorous extension of the sandwich-plate theories to the unsymmetrical type of sandwich. These additional constants, denoted by C_{xx} , C_{xy} , C_{yx} , C_{yy} , and T , describe coupling - for example, the curvatures produced by extensional forces. The derivation and formulas for the transverse shear stiffness D_{Q_y} are essentially the same as those given in reference 4 for the case in which interference between corrugation flats and face sheets is neglected, but are extended slightly to include the effects of stretching of the corrugation (in addition to bending) and the prevention of anticlastic curvature in the elements of the sandwich plate. The former effect can be important when the sandwich cross section approaches a truss; the latter, because the length of the sandwich plate parallel to the corrugation axis is several times the corrugation pitch. The results obtained for the bending and twisting stiffnesses D_x , D_y , and D_{xy} for the symmetrical sandwich correspond to the slightly less precise formulas of reference 5. (Transverse shear stiffness was not evaluated in this reference. A slight difference in definition of the symbols D_x and D_y exists between reference 5 and the present paper.)

Because the formulas developed are generally rather involved, charts are presented for one of them, the transverse shear stiffness D_{Q_y} , and approximations are given for several of the others, together with the results of numerical investigations of the accuracy of these approximations. In calculating the charts and in investigating the accuracy of approximate formulas, a family of corrugation shapes consisting of straight lines and circular arcs was considered. The bend radii of the corrugation, measured to the center line, were generally taken as 0.18 times the corrugation depth h_c , but departures from this value were also considered, as were departures from symmetry.

As a check on the formulas, bending and twisting tests were run on samples of a corrugated-core sandwich plate. Experimental values of bending stiffness D_y , transverse shear stiffness D_{Qy} , and twisting stiffness D_{xy} were obtained and compared with the theoretical values.

The function of the elastic constants in a sandwich-plate theory is first briefly described. A section follows in which the formulas for the elastic constants for the corrugated-core sandwich are summarized. The tests and comparison between theory and experiment are then described, a discussion section follows, and a section of concluding remarks ends the body of the paper. The symbols used in the body of the paper are listed and defined in appendix A. A number of them are also defined in the text where they first appear. Appendixes B to E contain the theoretical derivations.

THE FUNCTION OF THE ELASTIC CONSTANTS IN SANDWICH-PLATE THEORY

The sandwich-plate theories of references 2 and 3 are based on a structural idealization of the sandwich as a plate of continuous construction with material which is orthotropic with respect to the mutually perpendicular x-, y-, and z-directions. The modulus of elasticity in the z, or thickness, direction is assumed to be infinite; that is, local buckling of the faces is not considered and the over-all thickness is assumed to remain constant. Straight material lines normal to the middle surface are assumed to remain straight, but not necessarily normal to the middle surface, during distortion of the plate.

This idealized structure can adequately represent a corrugated-core sandwich plate of either the symmetrical or unsymmetrical type for many practical purposes, provided the core has sufficient stiffness to keep the over-all thickness of the plate essentially constant and provided the plate width (perpendicular to the corrugation axis) is many times the corrugation pitch. If the symmetrical type of sandwich (fig. 1(a)) is to be represented, then the elastic properties of the idealized-plate material may be regarded as varying symmetrically about the middle surface through the thickness. In order to represent the behavior of the unsymmetrical type of sandwich (fig. 1(b)), the elastic properties of the idealized-plate material must be thought of as varying nonsymmetrically with respect to the middle surface.

The behavior of a differential element of the idealized sandwich plate under load can be described by a set of force-distortion relationships. For an element of the symmetrical type of idealized sandwich

(fig. 1(a)), subjected to forces and moments as shown in figure 2(a), these relationships, as developed in references 2 and 3, are

$$\frac{\partial^2 w}{\partial x^2} = -\frac{M_x}{D_x} + \frac{\mu_y}{D_y} M_y + \frac{1}{D_{Q_x}} \frac{\partial Q_x}{\partial x} \quad (1)$$

$$\frac{\partial^2 w}{\partial y^2} = \frac{\mu_x}{D_x} M_x - \frac{M_y}{D_y} + \frac{1}{D_{Q_y}} \frac{\partial Q_y}{\partial y} \quad (2)$$

$$\epsilon_x = \frac{N_x}{E_x} - \frac{\mu'_y}{E_y} N_y \quad (3)$$

$$\epsilon_y = -\frac{\mu'_x}{E_x} N_x + \frac{N_y}{E_y} \quad (4)$$

$$\frac{\partial^2 w}{\partial x \partial y} = \frac{M_{xy}}{D_{xy}} + \frac{1}{2} \frac{1}{D_{Q_x}} \frac{\partial Q_x}{\partial y} + \frac{1}{2} \frac{1}{D_{Q_y}} \frac{\partial Q_y}{\partial x} \quad (5)$$

$$\gamma_{xy} = \frac{N_{xy}}{G_{xy}} \quad (6)$$

where $\frac{\partial^2 w}{\partial x^2}$, $\frac{\partial^2 w}{\partial y^2}$, and $\frac{\partial^2 w}{\partial x \partial y}$ are the curvatures and twist of the middle surface and ϵ_x , ϵ_y , and γ_{xy} are the strains of the middle surface. The quantities D_x , D_y , μ_x , and so on which appear in the coefficients of the loading terms are the elastic constants. Each constant describes a distortion produced by a simple loading. For example, if all loadings are zero except M_x , then, according to equation (1), $-\frac{1}{D_x}$ is the amount of curvature in the x-direction produced per unit of M_x .

The behavior of the unsymmetrical type of sandwich (fig. 1(b)) is more complex than that of the symmetrical type. In particular, a certain amount of coupling among the distortions may be expected; for example, extensional forces may in general produce curvatures as well as extensions. The same type of coupling can be expected in a symmetrical sandwich subjected to unsymmetrical loading. In setting up force-distortion relationships for an element of the unsymmetrical type of sandwich, the loading on the element will be generalized as shown in figure 2(b). The forces N_x , N_y , and N_{xy} are no longer assumed to be applied in the middle plane; each has an arbitrary plane of application, denoted

by I, II, and III, respectively. The strains ϵ_x , ϵ_y , and γ_{xy} are measured in these same respective planes. The force-distortion relationships for the element are then given by the following generalization of equations (1) to (6):

$$\frac{\partial^2 w}{\partial x^2} = -\frac{M_x}{D_x} + \frac{\mu_y}{D_y} M_y + \boxed{C_{xx}N_x + C_{xy}N_y} + \frac{1}{D_{Q_x}} \frac{\partial Q_x}{\partial x} \quad (1')$$

$$\frac{\partial^2 w}{\partial y^2} = \frac{\mu_x}{D_x} M_x - \frac{M_y}{D_y} + \boxed{C_{yx}N_x + C_{yy}N_y} + \frac{1}{D_{Q_y}} \frac{\partial Q_y}{\partial y} \quad (2')$$

$$\epsilon_x = \boxed{-C_{xx}M_x - C_{yx}M_y} + \frac{N_x}{E_x} - \frac{\mu'_y}{E_y} N_y \quad (3')$$

$$\epsilon_y = \boxed{-C_{xy}M_x - C_{yy}M_y} - \frac{\mu'_x}{E_x} N_x + \frac{N_y}{E_y} \quad (4')$$

$$\frac{\partial^2 w}{\partial x \partial y} = \frac{M_{xy}}{D_{xy}} + \boxed{TN_{xy}} + \frac{1}{2} \frac{1}{D_{Q_x}} \frac{\partial Q_x}{\partial y} + \frac{1}{2} \frac{1}{D_{Q_y}} \frac{\partial Q_y}{\partial x} \quad (5')$$

$$\gamma_{xy} = \boxed{2TM_{xy}} + \frac{N_{xy}}{G_{xy}} \quad (6')$$

The boxed terms are the terms that have been added to express the coupling behavior. The coefficients C_{xx} , C_{xy} , and so on in the boxed terms are the coupling elastic constants. The presence of each coupling elastic constant in two equations is a consequence of the

reciprocity theorem for elastic structures. (Further consequences of the reciprocity theorem are that $\frac{\mu_x}{D_x} = \frac{\mu_y}{D_y}$ and $\frac{\mu'_x}{E_x} = \frac{\mu'_y}{E_y}$.)

Through a proper choice of locations for planes I, II, and III, some uncoupling may be effected for any given sandwich. Plane I may be chosen so that C_{xx} or C_{yx} is zero, plane II so that C_{xy} or C_{yy} is zero, and plane III so that T is zero. Thus, in general, three of the coupling elastic constants may be made equal to zero. In special

cases, proper choice of locations of planes I, II, and III will result in still further uncoupling. For the symmetrical sandwich, of course, choosing these planes to coincide at the middle surface of the plate causes all the coupling constants to vanish.

THEORETICAL RESULTS

Elastic Constants for Symmetrical Sandwich

In appendixes B to E, derivations are made of formulas for the elastic constants for the general corrugated-core sandwich plate. The formulas obtained are now given in reduced form for use in conjunction with the force-distortion equations (1) to (6) for the symmetrical sandwich plate. Generally, the subscript C denotes the core, and the subscripts 1 and 2 denote the lower and upper faces, respectively. In this section, however, only symmetrical sandwiches are considered and the subscript 1 is used for both faces. It should be kept in mind, therefore, that the definitions of many of the terms appearing in the following formulas for the elastic constants apply only to the symmetrical type of sandwich.

Bending stiffnesses.- The formulas obtained in appendix B for the bending stiffnesses D_x and D_y are

$$D_x = \overline{EI}_x \quad (7)$$

$$D_y = \frac{\overline{EI}_y}{1 - \mu_1^2 \left(1 - \frac{\overline{EI}_y}{\overline{EI}_x} \right)} \quad (8)$$

where

$$\overline{EI}_x = E_C \overline{I}_C + \frac{1}{2} E_1 t_1 h^2$$

$$\overline{EI}_y = \frac{1}{2} E_1 t_1 h^2$$

- μ_1 Poisson's ratio of face sheet material
- E_1 modulus of elasticity of face sheet material, psi
- E_C modulus of elasticity of core material, psi

\bar{I}_C	moment of inertia, per unit width, of corrugation cross-sectional area about middle plane, inches ³
t_1	thickness of each face sheet, inches
h	distance between middle surfaces of face sheets, inches

For practical sandwiches, the moment of inertia \bar{I}_C contributed by the core is often small compared with the moment of inertia which the faces contribute to cross sections perpendicular to the corrugations. In such cases, $\frac{\bar{EI}_y}{\bar{EI}_x}$ is very nearly unity, and the following approximation to equation (8) may be made

$$D_y \approx \bar{EI}_y \quad (8')$$

This approximation implies a neglect of the restraining effect of the corrugation on the Poisson expansion or contraction of the face sheets. Results of a numerical survey of the accuracy of this approximation are given in table I for the symmetrical sandwich $\left(\frac{t_1}{t_2} = 1.00\right)$ of the common type shown at the top of the table. The table gives the ratio of the approximate value of D_y , as computed from equation (8'), to the exact value of D_y , as computed from equation (8). The error in the approximate value is seen to be small over a large part of the range of configurations considered and, in extreme cases, no more than 6 percent.

Poisson's ratios associated with bending.- The formulas obtained for the Poisson's ratios associated with bending μ_x and μ_y are (see appendix B)

$$\mu_x = \mu_1 \quad (9)$$

$$\mu_y = \mu_x \frac{D_y}{D_x} \quad (10)$$

Extensional stiffnesses.- The formulas obtained in appendix B for the extensional stiffnesses E_x and E_y , reduced to the symmetrical case, are

$$E_x = \bar{EA}_x \quad (11)$$

$$E_y = \frac{\overline{EA}_y}{1 - \mu_1^2 \left(1 - \frac{\overline{EA}_y}{\overline{EA}_x}\right)} \quad (12)$$

where

$$\overline{EA}_x = E_C \overline{A}_C + 2E_1 t_1$$

$$\overline{EA}_y = 2E_1 t_1$$

\overline{A}_C

area, per unit width, of corrugation cross section perpendicular to corrugation axis, inches

If, once again, the restraining effect of the corrugation on the Poisson expansion or contraction of the faces is neglected (that is, \overline{A}_C is taken as zero and, therefore, $\frac{\overline{EA}_x}{\overline{EA}_y}$ as 1), equation (12) gives the following approximation:

$$E_y \approx \overline{EA}_y \quad (12')$$

The error in this approximation is somewhat larger than the error obtained in the approximation to D_y , since the contribution of the core to \overline{EA}_x is relatively larger than its contribution to \overline{EI}_x . The error is indicated in table I, where numerical values of the ratio of the approximate to the exact values are tabulated.

Poisson's ratios associated with extension.- The formulas obtained (appendix B) for the Poisson's ratios associated with extension μ'_x and μ'_y are

$$\mu'_x = \mu_1 \quad (13)$$

$$\mu'_y = \mu'_x \frac{E_y}{E_x} \quad (14)$$

Twisting stiffness.- The following formula was obtained in appendix C for the twisting stiffness D_{xy} :

$$D_{xy} = 2\overline{GJ} \quad (15)$$

where

$$\overline{GJ} = \frac{1}{2} G_1 t_1 h^2$$

G_1 shear modulus of elasticity of face sheet material, psi

The stiffness D_{xy} is independent of the properties of the core since symmetry requires that the shear flow in the corrugated-core sheet be zero.

Horizontal shear stiffness.- The horizontal shear stiffness G_{xy} is given (see appendix C) by

$$G_{xy} = \overline{GA} \quad (16)$$

where

$$\overline{GA} = \frac{G_C t_C^2}{A_C} + 2G_1 t_1$$

G_C shear modulus of elasticity of core material, psi

t_C thickness of corrugated-core sheet, inches

Transverse shear stiffness in planes perpendicular to corrugation axis.- The transverse shear stiffness in planes perpendicular to the corrugation axis D_{Qy} is given (see appendix D) by the formula

$$D_{Qy} = Sh \left(\frac{E_C}{1 - \mu_C^2} \right) \left(\frac{t_C}{h_C} \right)^3 \quad (17)$$

where

h_C depth of corrugation, measured vertically from center line at crest to center line at trough (see fig. D5 of appendix D), inches

μ_C Poisson's ratio of core material

S nondimensional coefficient depending upon shape of corrugation, relative proportions of sandwich cross section, and the material properties of the component parts

Formulas for evaluating S are derived in appendix D. Because of the complexity of these formulas, a number of charts were computed which give S directly for the common type of sandwich with corrugation cross-sectional shape consisting of straight lines and circular arcs.

The charts of figure 3 are for the case in which the core and faces have the same material properties. They give S for a wide range of geometric proportions but are restricted to the value 0.18 for $\frac{R_{C1}}{h_C}$, where R_{C1} is the corrugation center-line bend radius. This restriction was made primarily for computational convenience, but it is generally consistent with corrugation shapes that have been considered for sandwich construction. The effect on S of departing from the value 0.18 for $\frac{R_{C1}}{h_C}$ can be estimated from figure 4(a), where a number of curves of S are given for values of $\frac{R_{C1}}{h_C}$ of 0.12 and 0.24 as well as 0.18. Cross plots based on the charts of figure 3 would indicate that S becomes relatively insensitive to the ratio $\frac{h_C}{t_C}$ at higher values of this ratio. For that reason $\left(\frac{t_C}{h_C}\right)^3$ was not included in the coefficient S in equation (17).

The effect on S of using a core material of different modulus than the face material may be estimated from figure 4(b). Curves of S are plotted for values of $\frac{E_C}{E_1}$ of 0.23 (magnesium core, steel faces) and 4.30 (steel core, magnesium faces) along with the basic curves, from figure 3, for $\frac{E_C}{E_1} = 1.00$. The value of S is seen to be relatively insensitive to large differences in elastic modulus between the core and the face sheets.

If both departures from the conditions of figure 3 occur simultaneously (that is, $R_{C1} \neq 0.18h_C$ and $E_C \neq E_1$), the effect on S may be obtained approximately by superposing the individual effects as determined from figures 4(a) and 4(b).

For symmetrical configurations not covered by the charts of figure 3, 4(a), or 4(b), S may be computed from equation (D19) of

appendix D, used in conjunction with the auxiliary equations (D20) and (D15), with k_y and k_z taken as 1. If, besides being symmetrical, the corrugation center line consists of straight lines and circular arcs, then equations (D22) and (D23) or (D24) may be used instead of equations (D15). This system of equations was used to compute the charts previously described.

Transverse shear stiffness in planes parallel to corrugation axis.- A general formula for the transverse shear stiffness in planes parallel to the corrugation axis D_{Q_x} , as derived in appendix E, is

$$D_{Q_x} = \frac{G_C I t_C h}{p \int_0^l Q ds} \quad (18)$$

where

- I moment of inertia of width $2p$ of cross section parallel to yz-plane, taken about centroidal axis parallel to y-axis, inches⁴
- $2p$ corrugation pitch, inches
- l length of one corrugation leg measured along the center line, inches (see fig. E-3)
- s coordinate measured along center line of corrugation leg, inches (see fig. E-3)

The quantity Q is the static moment about the centroidal axis (middle plane for symmetrical sandwich) of the cross-hatched area in figure E-1. If materials having different moduli of elasticity are used for the core and faces, a transformed cross section should be used in computing I and Q .

An approximate formula, which is more practicable, is obtained if, in the derivation, a bending moment M_x is assumed to be resisted only by the face sheets. The assumption leads to constant shear flow in the corrugation, and the following approximation is thus obtained:

$$D_{Q_x} \approx \frac{G_C t_C h^2}{p l} = \frac{G_C t_C^2}{A_C} \left(\frac{h}{p} \right)^2 \quad (18')$$

The results of a numerical investigation of the accuracy of equation (18') as compared with equation (18) are given in table I.

Elastic Constants for General Case

The general formulas for the elastic constants derived in appendixes B to E are now to be discussed. These formulas, used in conjunction with the force-distortion equations (1') to (6'), describe the distortions of an element of either the symmetrical or unsymmetrical sandwich plate loaded as shown in figure 2(b). The symbols appearing in the formulas are defined in appendix A.

Elastic constants associated with flexure and extension.- General formulas for the constants associated with flexure and extension D_x , D_y , μ_x , μ_y , E_x , E_y , μ'_x , μ'_y , C_{xx} , C_{xy} , C_{yx} , and C_{yy} are given by equations (B25) to (B36) of appendix B. These formulas apply to a sandwich with arbitrarily shaped corrugation, in which the upper and lower face sheets may differ in thickness, modulus of elasticity, and Poisson's ratio and in which the loading planes I and II are arbitrarily chosen.

Appreciable simplification of the formulas results from the practical assumption that the Poisson's ratios of the upper- and lower-face sheet materials are equal ($\mu_2 = \mu_1$). Equations (B25') to (B36') then apply.

It is evident from both sets of these equations (B25) to (B36) and (B25') to (B36') that the values of the constants associated with extension (E_x , E_y , μ'_x , μ'_y) and the coupling constants (C_{xx} , C_{xy} , C_{yx} , C_{yy}) are dependent upon the location of planes I and II in which the stretching forces N_x and N_y , respectively, are applied. If these forces are applied at the centroids of the transformed cross sections of the sandwich (that is, $k_I = k_{\overline{EI}_x}$ and $k_{II} = k_{\overline{EI}_y}$), then further simplification of the formulas takes place. Equations (B25') to (B36') reduce to equations (B25'') to (B36'').

The approximations to D_y and E_y given for the symmetrical sandwich by equations (8') and (12') may also be assumed to apply to the unsymmetrical sandwich when $k_{II} = k_{\overline{EI}_y}$ and $\mu_2 = \mu_1$. When these approximate expressions are used, however, \overline{EI}_y and \overline{EA}_y should be evaluated from their general formulas as given in appendix A or from equations (B20) of appendix B. Table I gives the results of a numerical investigation of the accuracy of the approximate expressions for D_y and E_y for the unsymmetrical sandwich ($\frac{t_1}{t_2} = 0.80$ and 0.50). The errors

resulting from use of the approximate expressions are seen to be of the same order for the unsymmetrical sandwich as for the symmetrical sandwich.

Elastic constants associated with twisting and horizontal shear.- Formulas for the constants associated with twisting and horizontal shear D_{xy} , G_{xy} , and T are given by equations (C35), (C36), and (C37) in appendix C. The values of G_{xy} and T depend upon the location of plane III in which the horizontal shear force is applied. Locating the horizontal shear force at the shear center of the cross section (that is, letting $k_{III} = k_{\overline{GJ}}$, where $k_{\overline{GJ}}$ is defined by equation (C31) or in the symbol list of appendix A) causes the coupling constant T to vanish and simplifies the expression for G_{xy} . The formulas for this case are equations (C35'), (C36'), and (C37').

As for the constants associated with flexure and extension, a simplification in the formula for D_{xy} occurs if the corrugation is completely neglected. Equation (C35) then gives the following approximation:

$$D_{xy} = 2\overline{GJ} \approx h^2 \frac{(G_1 t_1)(G_2 t_2)}{G_1 t_1 + G_2 t_2} \quad (19)$$

The results of a numerical survey of the accuracy of this approximation are given in table I. The error incurred through the use of the approximate formula is seen to be generally quite small. For the symmetrical

case $\left(\frac{t_1}{t_2} = 1\right)$, no error at all results from neglect of the core since symmetry requires the corrugation shear flow to be zero.

Transverse shear stiffness in planes perpendicular to corrugation axis.- Equation (17) which gives the transverse shear stiffness D_{Qy} for the symmetrical sandwich also applies to the unsymmetrical sandwich provided the coefficient S is obtained from formulas or charts which apply specifically to the unsymmetrical sandwich. Figure 3 gives extensive charts for evaluating S for a symmetrical sandwich with faces and core of the same material and with the corrugation center line consisting of straight lines and circular arcs, the latter having a radius of curvature of $0.18h_c$. Figure 4(a) shows the effect of using a radius of curvature other than $0.18h_c$, and figure 4(b), the effect of using core material different from that of the faces. The rest of figure 4 is devoted to showing separately the effects on S of two departures from symmetry for a sandwich that is otherwise the same as that considered in figure 3. Figure 4(c) is for a case in which the nonsymmetry is due to the core and consists in the lower and upper flats

being of unequal width; figure 4(d) applies when the core is symmetrical but the faces are of unequal thickness. No chart is given for the case in which the core is symmetrical and the face thicknesses equal but in which the nonsymmetry arises from the use of a different material for the lower face than for the upper face. However, for nonsymmetry of this type, S can generally be obtained quite accurately by assuming, first, that both faces are of the upper-face material and, next, that both faces are of the lower-face material and averaging the two values S_1 and S_2 thus obtained in the following manner:

$$\frac{1}{S^3} = \frac{1}{2} \left(\frac{1}{S_1^3} + \frac{1}{S_2^3} \right)$$

or

$$S = \frac{1.26 S_1 S_2}{\sqrt[3]{S_1^3 + S_2^3}}$$

In general, when the upper face is different from the lower face, either in thickness or material or both, S can be determined approximately by averaging in the previously described manner the two values obtained by first assuming that both faces are the same as the upper face and next that both faces are the same as the lower face. The error in such an approximation will generally be less than 3 percent.

For an unsymmetrical sandwich not covered by the charts, S may be evaluated from equation (D17) used in conjunction with the auxiliary equations (D18) and (D15); if the corrugation itself is symmetrical, then some simplification results from taking $k_y = k_z = 1$ in the auxiliary equations.

If the corrugation center line consists of straight lines and circular arcs, then equations (D21) and (D23) or (D24) may be used instead of equations (D15). If, in addition, the corrugation is symmetrical and if k_y and k_z are taken as 1 in equations (D18), then equations (D22) may replace equations (D21).

Transverse shear stiffness in planes parallel to corrugation axis.-
Equations (18) and (18') for the evaluation of the transverse shear stiffness D_{Q_x} for a symmetrical sandwich also apply to the unsymmetrical sandwich. The error of the approximate formula (equation (18')) when applied to the unsymmetrical sandwich is indicated in table I.

EXPERIMENTAL EVALUATION OF D_y , D_{Q_y} , AND D_{xy}

General Summary

The elastic-constant formulas that were thought to need experimental verification were those which depended to a large extent in their derivation upon the assumption that the thickness of the core remains essentially constant or that the corrugation cross section is undistorted. Among these, the formulas for D_y , D_{Q_y} , and D_{xy} were selected for checking because these constants could be experimentally evaluated through simple bending and twisting tests on sandwich beams and panels as described schematically in appendix A of reference 2.

The test sandwich was of the symmetrical type. The core consisted of a readily available Alclad 24S-T36 aluminum-alloy standard circularly corrugated sheet having a nominal thickness of 0.032 inch and a nominal over-all depth of 3/4 inch. The faces were of 24S-T3 aluminum-alloy sheet having a nominal thickness of 0.064 inch. Two test specimens were used: A beam for the evaluation of D_y and D_{Q_y} and a panel for the evaluation of D_{xy} . Although blind riveting was necessary only on one side of the panel, it was used on both sides in order to maintain symmetry. On the beam driven rivets were used in both faces since the beam was relatively narrow.

The results of the tests and comparisons with theory are summarized in the following table. In computing the theoretical values the following properties were assumed: $E_1 = E_2 = 10,500,000$ pounds per square inch, $E_C = 10,300,000$ pounds per square inch, and $\mu_1 = \mu_2 = \frac{1}{3}$.

	D_y (in.-lb)	D_{Q_y} (lb/in.)	D_{xy} (in.-lb)
Range of experimental values	221,000 224,000	4010 4310	182,000
Theoretical value	220,000	^a 4300	177,000

^aComputed with $\mu_1 = \mu_2 = \mu_C = 0$ because the beam tested was relatively narrow and Poisson curvatures were therefore assumed to be unrestrained.

Test and Analysis

Evaluation of D_y . - The dimensions of the test beam are shown in figure 5(a). The beam was supported on two knife edges as shown in figures 5(b) and 5(c) and loaded near the ends so as to obtain a region of pure bending moment between supports. The supports were placed 19.05 inches apart for one test (the test which yielded the value of 221,000 in.-lb for D_y) and loads P were applied in increments of 5 pounds up to a maximum of 25 pounds and then removed in the same increments; in a second test (which yielded the value of 224,000 in.-lb for D_y), the supports were placed 24.56 inches apart and loads P were applied in increments of 5 pounds up to a maximum load of 30 pounds and removed in the same increments. Deflections of the beam were measured at the locations shown in figure 5(b) with gages having a sensitivity of 0.0001 inch.

Despite the fact that spacer blocks were inserted in the sandwich at the supports to prevent local distortion, downward displacements of the upper face were observed immediately above the supports. These displacements, on the order of 2 to 4 percent of the maximum deflections at the center of the beam, were probably caused primarily by thickness change of the beam, since gages placed directly on the supports showed no support displacements. In correcting for the upper-face sheet displacements above the supports, the vertical displacement of the "middle surface" of the sandwich at each support was taken as one-half of the face-sheet displacement. The deflections at points away from the supports were then referred to the straight line connecting the middle-surface points immediately above the supports. Away from the supports, gages placed in contact with the lower-face sheet showed that no thickness change occurred in the beam and that the deflection of the upper face could therefore be taken as the deflection of the middle surface. The deflections varied linearly with applied load.

The described manner of correcting the deflection for the distortions above the supports resulted in calculated values of D_y which were practically independent of the choice of station whose deflection was used in the calculation. The calculated values of D_y were obtained from the deflection curve drawn through the corrected deflections at the gage stations. The following formula, based on the assumption of a uniform beam subjected to constant moment Pd , was used:

$$D_y = \frac{(Pd)y_s(L - y_s)}{2bw_s} \quad (20)$$

where

P	load applied at each end of beam, pounds (see fig. 5(b))
d	distance between the load and support, inches (see fig. 5(b))
y_s	distance from left support to any station, inches
w_s	deflection at station y_s , inches
L	distance between supports, inches (see fig. 5(b))
b	width of beam, inches (1.92 in.)

This formula was applied at three stations, $y_s = \frac{L}{3}$, $\frac{L}{2}$, and $\frac{2}{3}L$. The three values thus obtained differed from one another by no more than 2 percent in any test; the average of the three values was taken as the true value of D_y .

Evaluation of D_{Q_y} .-- The beam test specimen and span lengths used in evaluating D_{Q_y} were the same as those used in evaluating D_y (see figs. 6(a) and 6(b)). The beam was subjected to several different lateral loadings, each being of a type to produce transverse shear. These loadings are illustrated schematically in figure 6(a) and the experimental values of D_{Q_y} obtained from each test are also given. A photograph of a typical test setup is shown in figure 6(b). Deflections were measured between the supports at six stations for the shorter span and at eight stations for the longer span and also immediately above the supports.

As in the tests for D_y , slight downward displacements of the upper face were observed immediately above the supports. These displacements were generally of the order of 1 to 2 percent of the maximum deflection at the center of the beam but in two cases were as high as 3 and 5 percent, respectively, at the right support. The measured deflections were corrected for the distortions above the supports in the manner described for D_y . The deflections varied linearly with the applied load.

The corrected measured deflections were used to plot deflection curves for the beam as a whole, from which values of D_{Q_y} were computed. The following formula, based on the assumption of a uniform beam and a

uniform running lateral load, was used to calculate D_{Q_y} for those cases in which a number of equally spaced lateral loads were applied to the beam:

$$D_{Q_y} = \frac{L - y_s}{\frac{2w_{sb}L}{Pny_s} - \frac{1}{12D_y} [L^3 - y_s^2(2L - y_s)]} \quad (21)$$

where

- P load applied at each crest or each trough of corrugation, pounds (see fig. 6(a))
- n number of loads P applied to the beam (see fig. 6(a))
- D_y bending stiffness per unit width of the beam, inch-pounds
(taken as 221,000 in.-lb when $L = 19.05$ in. and
224,000 in.-lb when $L = 24.56$ in.)

The following formula was used for the case of a concentrated central load:

$$D_{Q_y} = \frac{1}{\frac{2w_{sb}}{Py_s} - \frac{1}{24D_y} (3L^2 - 4y_s^2)} \quad (22)$$

where

- P load on the beam, pounds

The deflections substituted in these formulas were the deflections at values of y_s of $0.2L$, $0.4L$, $0.6L$, and $0.8L$. Thus, the formulas yielded four values for each test. These values differed from one another at the most by 11 percent and their average was taken as the true value of D_{Q_y} for the sandwich.

Evaluation of D_{xy} . - A sandwich panel, 59.84 inches long by 21.11 inches wide, was twisted to determine D_{xy} . The faces of the panel were bent up along the edges to form flanges to which were bolted, on two sides and one end of the panel, three steel plates of $\frac{1}{8}$ -inch nominal thickness and 3-inch width. (See figs. 7(a) and 7(b).) A somewhat wider steel plate was placed at the remaining end and it was,

in turn, bolted to a rigid backstop with sufficient clearance to permit warping of the plate out of its plane. To the steel plate at the opposite end of the panel was bolted an aluminum-alloy loading plate (not shown) to which the torque was applied. The steel plates were bolted to the sides of the panel in order to help achieve a state of pure twist in the panel. Strain gages were placed back-to-back on the faces and corrugation legs across the width at the midlength of the panel in order to determine to what extent a state of pure twist (that is, constant face shear stress and zero corrugation shear stress) had been achieved. The dimensions of the panel are shown in figure 7(c).

Loads were applied in increments of 2000 inch-pounds up to a maximum of 10,000 inch-pounds and removed in the same increments. Deflections of the panel were measured at seven stations across the width at each of four stations along the length (see fig. 7(d)), the stations starting approximately 12 inches from the supported end and spaced approximately 12 inches apart. The measured deflections varied linearly both across the width and along the length and were proportional to the applied load. From the measured deflections, the twist $\frac{\partial^2 w}{\partial x \partial y}$ was computed. The twisting stiffness D_{xy} was then obtained from the formula:

$$D_{xy} = \frac{M_{xy}}{\frac{\partial^2 w}{\partial x \partial y}} = \frac{\frac{1}{2b}(T - T')}{\frac{\partial^2 w}{\partial x \partial y}} \quad (23)$$

where

b width of panel (21.11 in.)

T applied torque, inch-pounds

T' torque required to twist side plates, pound-inches²

$$\left(2 \left[\frac{1}{3} (3) \left(\frac{1}{8} \right)^3 (11,000,000) \right] \frac{\partial^2 w}{\partial x \partial y} = 43,000 \frac{\partial^2 w}{\partial x \partial y} \right)$$

(see reference 6, equation (156))

The linearity of the deflections across the width and along the length indicated that a state of nearly pure twist was being achieved. The strain-gage measurements tended to confirm the existence of this state of pure twist. They showed that, except in the first two cells near each edge of the panel, the face shear stresses were very nearly uniform across the width, with only one value departing as much as 8 percent from the average. In the same region, the corrugation-leg shear stresses were generally less than 1.5 percent of the face shear stresses.

In order to investigate whether the use of side plates was necessary to the experimental evaluation of D_{xy} , the test was repeated with the side plates removed. The shear-stress distribution across the width became considerably nonuniform; the deflections were still linear across the width but departed slightly from linearity along the length. The test value of D_{xy} , based on the twist in the central portion of the panel, was only about 0.85 as large as the experimental value obtained with the side plates on. This result indicates that side plates are desirable in order to minimize edge effects and achieve a state of pure twist when testing for D_{xy} .

DISCUSSION

Formulas have been presented for evaluating the elastic constants of a corrugated-core sandwich plate of either the symmetrical or unsymmetrical type. The formulas are rather comprehensive and precise, but reductions to several important special cases have been made and practical approximations to a number of the formulas have been given. Tests have been run to verify the formulas for three of the more important constants and, indirectly, the basic assumptions in their derivations.

The formulas given are limited to plates stressed in the elastic range and not subject to local buckling. Engineering adaptation of the results to cases involving plasticity and local buckling can probably be made; however, attempts at such an adaptation were beyond the scope of the present study.

Each component of the sandwich (face sheet or core sheet) is assumed to be composed of homogeneous isotropic material. In actual construction this assumption may be violated by the presence of perforations in one sheet to facilitate the driving of rivets in the other sheet. In evaluating the elastic constants the presence of the perforations can be accounted for approximately by assuming a homogeneous face sheet of reduced modulus.

When values of the elastic constants for a given corrugated-core sandwich plate are substituted in equations (1) to (6) or (1') to (6'), the resulting equations describe approximately the distortions of an element of the plate under load. The distortions are described only approximately, because the actual plate does not behave in quite the manner assumed for the idealized plate. In particular, straight material lines in the thickness direction will not remain straight under the presence of shear but will tend to warp. In evaluating the transverse shear stiffness D_{Q_x} or D_{Q_y} theoretically, therefore, the problem arises of choosing an average straight line through the warped one in order to define a transverse shear strain for the cross section. Fortunately, for most sandwiches the plausible range for choosing this straight line is small and causes only a slight ambiguity in extending the definition of D_{Q_x} or D_{Q_y} to an actual plate. For the corrugated-core sandwich as analyzed in appendixes D and E, the average straight line was taken as the one passing through corresponding material points in the middle surfaces of the face sheets. This line has the minimum deviation from the true warped line (as determined by least squares) provided the core is ignored and is probably satisfactory whenever the effective contribution of the core to the total cross-sectional moment of inertia is small. The tendency of the originally straight lines to warp introduces a further complication inasmuch as any restraint against such warping (due to the mutual interference of adjacent parts of the plate) will tend to increase the transverse shear stiffness. Such restraint will be small except in the region of concentrated loads. In the theoretical derivations, the conservative assumption was therefore made that there is no restraint at all against warping. Since the tendency of originally straight lines in the thickness directions to warp is a function of the type of loading, experimental values of D_{Q_x} or D_{Q_y} , as determined through beam tests, should, in principle, vary according to the type of spanwise loading distribution used. The variations observed in the tests to determine D_{Q_y} , however, (see fig. 6(a)) seemed to be caused more by scatter and other factors than by the type of load distribution.

Since the primary application of the elastic constants will probably be to sandwich-plate theory, it should be mentioned that the force-distortion equations (1) to (6) or (1') to (6') represent one component of such a theory. If to these equations are added the differential equations of equilibrium of the element shown in figure 2 and equations relating strains and displacements, the combination of equations will constitute a complete formulation of a sandwich-plate theory. The force-distortion equations (1) to (6) have been presented before in references 2 and 3, but the generalized equations (1') to (6'), which include coupling terms, are believed to be new. The relative importance

of the coupling terms for the corrugated-core sandwich has not been rigorously evaluated; it would depend upon the degree of nonsymmetry of the cross section and the type of problem under consideration. There is reason to believe, however, that in most cases the effect of coupling will be slight. For a sandwich having faces of the same Poisson's ratio but different thicknesses and having a core moment of inertia and area which approach zero, locating the loading planes I, II, and III at the centroidal plane between the two faces will cause all the coupling constants to vanish. Since the core of practical corrugated-core sandwiches will probably contribute only a small part to the total area of the cross section and a smaller part to the moment of inertia, the coupling constants will very likely be unimportant for properly chosen locations of planes I, II, and III. In such cases and for some problems neglecting the coupling terms in equations (1') to (6') may be sufficiently accurate.

CONCLUDING REMARKS

In order to facilitate application of an existing sandwich-plate theory to the corrugated-core type of sandwich, formulas and charts have been presented for the evaluation of the necessary elastic constants. Both the symmetrical and unsymmetrical types of corrugated-core sandwich have been considered, and the extensions of the existing sandwich-plate theory required to make it strictly applicable to the unsymmetrical type are indicated.

The formulas and charts presented are limited to plates stressed in the elastic range, which are not subject to local buckling. The formulas are rather comprehensive and precise, but reductions to several important special cases have been made. Practical approximations to a number of the formulas have been investigated numerically and found to be sufficiently accurate for most practical cases.

The formulas for three of the elastic constants were checked experimentally and found to give values in close agreement with experiment.

Langley Aeronautical Laboratory
National Advisory Committee for Aeronautics
Langley Field, Va., November 20, 1950

APPENDIX A

SYMBOLS AND DEFINITIONS

plane I	plane in which N_x acts and in which ϵ_x is measured, parallel to faces
plane II	plane in which N_y acts and in which ϵ_y is measured, parallel to faces
plane III	plane in which N_{xy} acts and in which γ_{xy} is measured, parallel to faces

General Sandwich Symbols

C_{xx}	coupling elastic constant representing curvature in x-direction $\frac{\partial^2 w}{\partial x^2}$ produced per unit of N_x applied; also strain in x-direction ϵ_x per unit of $-M_x$, pound ⁻¹
C_{xy}	coupling elastic constant representing curvature in x-direction $\frac{\partial^2 w}{\partial x^2}$ produced per unit of N_y applied; also strain in y-direction ϵ_y per unit of $-M_x$, pound ⁻¹
C_{yy}	coupling elastic constant representing curvature in y-direction $\frac{\partial^2 w}{\partial y^2}$ produced per unit of N_y applied; also strain in y-direction ϵ_y per unit of $-M_y$, pound ⁻¹
C_{yx}	coupling elastic constant representing curvature in y-direction $\frac{\partial^2 w}{\partial y^2}$ produced per unit of N_x applied; also strain in x-direction ϵ_x per unit of $-M_y$, pound ⁻¹
D_{Q_x}, D_{Q_y}	transverse shear stiffnesses, per unit width, of a beam cut from plate in the x- and y-directions, respectively, pounds per inch

D_x, D_y	bending stiffnesses, per unit width, of a beam cut from plate in x- and y-directions, respectively, inch-pounds
D_{xy}	twisting stiffness of unit-width and unit-length element cut from plate, with edges parallel to x- and y-axes, inch-pounds
E_x, E_y	extensional stiffnesses of plate in x- and y-directions, respectively, pounds per inch
G_{xy}	shear stiffness of plate in xy-plane, pounds per inch
M_x, M_y	resultant bending-moment intensities in x- and y-directions, respectively, pounds
M_{xy}	resultant twisting-moment intensity with regard to x- and y-directions, pounds
N_x	intensity of resultant normal force acting in x-direction in plane I, pounds per inch
N_y	intensity of resultant normal force acting in y-direction in plane II, pounds per inch
N_{xy}	intensity of resultant shear force acting in x- and y-directions in plane III, pounds per inch
Q_x, Q_y	intensities of transverse resultant shear acting on cross sections parallel to yz-plane and xz-plane, respectively, pounds per inch
T	coupling elastic constant representing twist $\frac{\partial^2 w}{\partial x \partial y}$ produced per unit of N_{xy} applied; also one-half the shear strain γ_{xy} per unit of M_{xy} , pound ⁻¹
u, v, w	displacements in x-, y-, and z-directions, respectively, inches
x	coordinate, measured parallel to corrugation direction, inches
y	coordinate, measured parallel to faces and perpendicular to corrugation direction, inches
z	coordinate, measured perpendicular to faces, inches
γ_x, γ_y	shear strains associated with Q_x and Q_y , respectively

- γ_{xy} shear strain, with respect to x- and y-directions, of plane III
- ϵ_x, ϵ_y strains of plane I in x-direction and of plane II in y-direction, respectively
- μ_x, μ_y Poisson's ratios associated with bending in x- and y-directions, respectively
- μ'_x, μ'_y Poisson's ratios associated with extension in x- and y-directions, respectively

Corrugated-Core Sandwich Symbols

- \bar{A}_C area per unit width of corrugation cross section parallel to yz-plane, inches
- A_1 area, in width $2p$, lying between corrugation center line and lower-skin center line (see fig. C4 of appendix C), square inches
- A_2 area, in width $2p$, lying between corrugation center line and upper-skin center line (see fig. C4 of appendix C), square inches

- a_1, a_2
 - b_1, b_2
 - c_1, c_2
 - d_1, d_2
 - e_1, e_2
 - f_1, f_2
 - g_1, g_2
 - j_1, j_2
 - k_1, k_2
 - R_{C1}, R_{C2}
 - R_{i1}, R_{i2}
 - α_1, α_2
 - β_1, β_2
- } dimensions of corrugation cross section consisting of straight lines and circular arcs (see fig. D5 of appendix D)

b width of test beam or panel, inches

- B_3, B_4, B_6, B_7 nondimensional parameters in formula for S (equation (D19)) for a symmetrical corrugated-core sandwich, defined by equations (D20)
- C_1, C_2, \dots, C_7 nondimensional parameters in formula for S (equation (D17)) for a corrugated-core sandwich, defined by equations (D18)
- d distance between load and support of test beam, inches
- E_1, E_2 moduli of elasticity for lower and upper faces, respectively, psi
- E_C modulus of elasticity of corrugated-core sheet material, psi
- E'_C stretching modulus of elasticity of corrugated-core sheet material, used in derivation of D_{Qy} , psi
- \overline{EA}_x extensional stiffness of corrugated-core sandwich plate in x-direction (bending in x-direction prevented), pounds per inch $(E_1 t_1 + E_C \bar{A}_C + E_2 t_2)$
- \overline{EA}_y extensional stiffness of corrugated-core sandwich plate in y-direction (restraining effect of corrugation ignored; bending in y-direction prevented), pounds per inch $(E_1 t_1 + E_2 t_2)$
- \overline{EI}_x bending stiffness, per unit width, of a beam cut from corrugated-core sandwich plate in x-direction, inch-pounds $\left(E_C \bar{I}_C + \left[E_1 t_1 k \overline{EI}_x^2 + E_C \bar{A}_C (k \bar{C} - k \overline{EI}_x)^2 + E_2 t_2 (1 - k \overline{EI}_x)^2 \right] h^2 \right)$
- \overline{EI}_y bending stiffness, per unit width, of a beam cut from corrugated-core sandwich plate in y-direction (restraining effect of corrugation ignored), inch-pounds $\left(\left[E_1 t_1 k \overline{EI}_y^2 + E_2 t_2 (1 - k \overline{EI}_y)^2 \right] h^2 \right)$
- G_1, G_2, G_C shear moduli of elasticity of lower-face, upper-face, and corrugated-core sheet materials, respectively, psi
- \overline{GA} unit shear stiffness of corrugated-core sandwich plate with respect to x- and y-directions (twist prevented), pounds per inch $\left(G_1 t_1 + \frac{G_C t_C^2}{A_C} + G_2 t_2 \right)$

- \overline{GJ} torsional stiffness, per unit width, of a beam cut from corrugated-core sandwich plate in x-direction, inch-pounds $\left(\left[G_1 t_1 k_{GJ}^2 + \frac{G_C t_C^2}{A_C} (k_{GJ} - k_C)^2 + G_2 t_2 (1 - k_{GJ})^2 \right] h^2 \right)$
- h distance between middle surfaces of face sheets, inches
- h_C depth of corrugation, measured vertically from center line at crest to center line at trough (see fig. D5 of appendix D), inches
- h_{EC} core thickness of sandwich plate (see fig. D5 of appendix D), inches
- I moment of inertia of width $2p$ of cross section parallel to yz-plane, taken about centroidal axis parallel to y-axis, inches⁴
- \overline{I}_C moment of inertia, per unit width, of corrugation cross section parallel to yz-plane, taken about centroidal axis of corrugation cross section, inches³
- $\left. \begin{array}{l} K_{A_y}, K_{A_z} \\ K_{L_y}, K_{L_z} \\ K_{L_{yz}} \\ K_L \\ K_{L_y}, K_{L_z} \\ K_{L_{yz}} \end{array} \right\}$ nondimensional integral parameters in equations for $B_3, B_4, B_6, B_7, C_1, C_2, \dots, C_7$, functions of corrugation cross-section geometry, defined by equations (D15) for general case and by equations (D21) and (D22) for corrugation having a cross-sectional center line consisting of straight lines and circular arcs
- k_y, k_z nondimensional parameters locating origin of y- and z-coordinates, respectively (see fig. D3 of appendix D)
- $k_I^h, k_{II}^h, k_{III}^h$ distances between middle surface of lower face and planes I, II, and III, respectively (see figs. B1 and C1 of appendixes B and C, respectively), inches
- k_{Ch} distance between middle surface of lower face and plane which cuts corrugation into lobes of equal area (also shear center of corrugation), inches
- $k_C = \frac{1}{2} \left(1 + \frac{A_1 - A_2}{2ph} \right)$

$k_{\bar{C}h}$ distance between middle surface of lower face and centroidal axis of corrugation cross section parallel to yz-plane, inches

$k_{\bar{E}I_x} h$ distance between middle surface of lower face and centroidal axis associated with $\bar{E}I_x$, inches

$$k_{\bar{E}I_x} = \frac{k_{\bar{C}} E_C \bar{A}_C + E_2 t_2}{\bar{E}A_x}$$

$k_{\bar{E}I_y} h$ distance between middle surface of lower face and centroidal axis associated with $\bar{E}I_y$, inches

$$k_{\bar{E}I_y} = \frac{E_2 t_2}{\bar{E}A_y}$$

$k_{\bar{G}J} h$ distance between middle surface of lower face and "zero-shear plane" associated with $\bar{G}J$, inches

$$k_{\bar{G}J} = \frac{\frac{G_C t_C^2}{\bar{A}_C} k_C + G_2 t_2}{\bar{G}A}$$

l length of one corrugation leg, measured along center line, inches

L distance between supports of test beam, inches

$2p$ corrugation pitch (see sketches in figs. 3 and 4), inches

P load applied to test beam, pounds

Q static moment about centroidal axis of cross-hatched portion of cross section shown in figure E1, inches³

S nondimensional coefficient in formula for D_{Q_y} ,

$$D_{Q_y} = \text{Sh} \left(\frac{E_C}{1 - \mu_C^2} \right) \left(\frac{t_C}{h_C} \right)^3$$

s coordinate measured along center line of corrugation cross sections parallel to yz-plane; see, for example, figures C2, D3, and E3, inches

t_1, t_2, t_c	thicknesses of lower-face, upper-face, and corrugated-core sheets, respectively, inches
θ	angle between face sheets and straight diagonal portion of corrugation leg (see sketches in figs. 3 and 4)
μ_1, μ_2, μ_c	Poisson's ratios for lower-face, upper-face, and corrugation materials, respectively
ψ	angle between face sheets and tangent to corrugation center line (see fig. D3)

Subscript

approx approximate value

APPENDIX B

DERIVATION OF FORMULAS FOR D_x , D_y , μ_x , μ_y , E_x , E_y ,
 μ'_x , μ'_y , C_{xx} , C_{xy} , C_{yx} , AND C_{yy}

In the derivation of the formulas for the elastic constants associated with bending and stretching an element of a corrugated-core sandwich plate is considered which is subjected to bending moments of intensity M_x and M_y and to horizontal resultant forces of intensity N_x and N_y at arbitrary distances $k_I h$ and $k_{II} h$, respectively, above the middle surfaces of the lower face. (See following fig.)

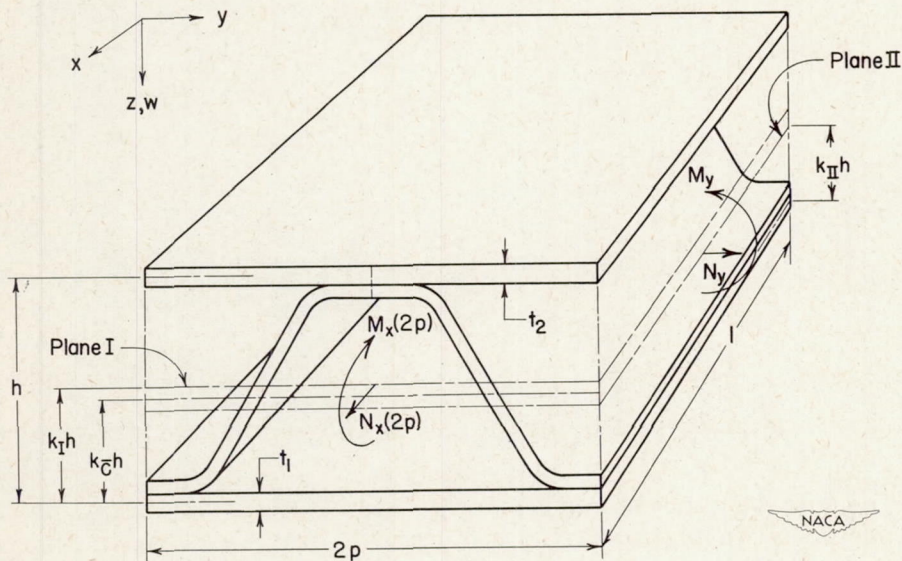


Figure B1

Equations are derived relating the distortions of this element to the forces and moments producing them; in these equations terms corresponding to D_x , D_y , μ_x , μ_y , E_x , E_y , μ'_x , μ'_y , C_{xx} , C_{xy} , C_{yx} , and C_{yy} are evident. The general formulas thus obtained are reduced for special applications.

The moment M_x and force N_x are assumed to be resisted by both the bending and extensional stiffnesses of the core and the extensional stiffnesses of the face sheets; the moment M_y and force N_y are assumed to be resisted only by the extensional stiffnesses of the face sheets.

Vertical lines drawn between middle-surface points in the upper and lower faces of the undistorted element are assumed to remain perpendicular to the faces and unchanged in length during distortion of the element. The distortion of the element as a whole will therefore

consist of curvatures $\frac{\partial^2 w}{\partial x^2}$ and $\frac{\partial^2 w}{\partial y^2}$. The middle surfaces of the faces will be strained in the x- and y-directions; it is convenient to imagine the existence of other horizontal planes in which the strains may be obtained by linear interpolation between the upper- and lower-face middle surfaces.

Inasmuch as the moment M_y and the force N_y are assumed to be resisted only by the extensional stiffnesses of the face sheets, the direct stresses in y-direction in the middle surfaces of the lower- and upper-face sheets σ_{y1} and σ_{y2} are statically determinate and are given, respectively, by

$$\sigma_{y1} = \frac{M_y}{t_1 h} + \frac{N_y}{t_1} (1 - k_{II}) \quad (B1)$$

$$\sigma_{y2} = - \frac{M_y}{t_2 h} + \frac{N_y}{t_2} k_{II} \quad (B2)$$

If, in addition, the middle-surface strains in the x-direction ϵ_{x1} and ϵ_{x2} in the lower- and upper-face sheets, respectively, were known, the state of deformation of the element would be completely fixed. These two strains can be determined from two conditions: namely, that the thrust intensity in the x-direction is N_x and the moment intensity in the x-direction about plane I is M_x , or

$$N_x = \sigma_{x1} t_1 + \sigma_{x2} t_2 + \bar{\sigma}_{x_C} \bar{A}_C \quad (B3)$$

$$M_x = \sigma_{x1} t_1 k_I h - \sigma_{x2} t_2 (1 - k_I) h + \bar{\sigma}_{x_C} \bar{A}_C (k_I - k_{\bar{C}}) h - E_C \bar{I}_C \frac{\partial^2 w}{\partial x^2} \quad (B4)$$

where

σ_{x_1} direct stress in the x-direction in the middle surface of lower face

σ_{x_2} direct stress in the x-direction in the middle surface of upper face

$\bar{\sigma}_{x_C}$ average direct stress in the x-direction in corrugation (also direct stress in the x-direction at centroid of corrugation)

The terms σ_{x_1} , σ_{x_2} , $\bar{\sigma}_{x_C}$, and $\frac{\partial^2 w}{\partial x^2}$ can be replaced by the following expressions in terms of ϵ_{x_1} and ϵ_{x_2} :

$$\begin{aligned}\sigma_{x_1} &= E_1 \epsilon_{x_1} + \mu_1 \sigma_{y_1} \\ &= E_1 \epsilon_{x_1} + \mu_1 \left[\frac{M_y}{t_1 h} + \frac{N_y (1 - k_{II})}{t_1} \right]\end{aligned}\quad (B5)$$

$$\begin{aligned}\sigma_{x_2} &= E_2 \epsilon_{x_2} + \mu_2 \sigma_{y_2} \\ &= E_2 \epsilon_{x_2} + \mu_2 \left(-\frac{M_y}{t_2 h} + \frac{N_y k_{II}}{t_2} \right)\end{aligned}\quad (B6)$$

$$\bar{\sigma}_{x_C} = E_C \left[\epsilon_{x_1} + k_{\bar{C}} (\epsilon_{x_2} - \epsilon_{x_1}) \right]\quad (B7)$$

$$\frac{\partial^2 w}{\partial x^2} = \frac{\epsilon_{x_2} - \epsilon_{x_1}}{h}\quad (B8)$$

Equations (B3) and (B4) then become

$$\epsilon_{x_1} \left[E_1 t_1 + E_C \bar{A}_C (1 - k_{\bar{C}}) \right] + \epsilon_{x_2} \left(E_2 t_2 + E_C \bar{A}_C k_{\bar{C}} \right) =$$

$$- \frac{M_y}{h} (\mu_1 - \mu_2) + N_x - N_y \left[\mu_1 (1 - k_{II}) + \mu_2 k_{II} \right] \quad (B9)$$

$$\epsilon_{x_1} \left[E_1 t_1 k_I + (1 - k_{\bar{C}}) E_C \bar{A}_C (k_I - k_{\bar{C}}) + \frac{E_C \bar{I}_C}{h^2} \right] -$$

$$\epsilon_{x_2} \left[E_2 t_2 (1 - k_I) - k_{\bar{C}} E_C \bar{A}_C (k_I - k_{\bar{C}}) + \frac{E_C \bar{I}_C}{h^2} \right] =$$

$$\frac{M_x}{h} - \frac{M_y}{h} \left[\mu_2 + (\mu_1 - \mu_2) k_I \right] + N_y \left[-\mu_1 (1 - k_{II}) k_I + \mu_2 k_{II} (1 - k_I) \right]$$

(B10)

Solution for ϵ_{x_1} and ϵ_{x_2} gives

$$\epsilon_{x_1} = \phi_{xx_1} \frac{M_x}{h} - \mu_1 \phi_{xy_1} \frac{M_y}{h} + \psi_{xx_1} N_x - \mu_1 \psi_{xy_1} N_y \quad (B11)$$

$$\epsilon_{x_2} = -\phi_{xx_2} \frac{M_x}{h} + \mu_2 \phi_{xy_2} \frac{M_y}{h} + \psi_{xx_2} N_x - \mu_2 \psi_{xy_2} N_y \quad (B12)$$

where

$$\begin{aligned}
 \phi_{xx1} &= \frac{k\bar{EI}_x h^2}{\bar{EI}_x} \\
 \phi_{xx2} &= \frac{(1 - k\bar{EI}_x)h^2}{\bar{EI}_x} \\
 \phi_{xy1} &= \frac{k\bar{EI}_x h^2}{\bar{EI}_x} - \left(1 - \frac{\mu_2}{\mu_1}\right) \left[\frac{(1 - k\bar{EI}_x)k\bar{EI}_x h^2}{\bar{EI}_x} - \frac{1}{EA_x} \right] \\
 \phi_{xy2} &= \frac{(1 - k\bar{EI}_x)h^2}{\bar{EI}_x} + \left(\frac{\mu_1}{\mu_2} - 1\right) \left[\frac{(1 - k\bar{EI}_x)k\bar{EI}_x h^2}{\bar{EI}_x} - \frac{1}{EA_x} \right] \\
 \psi_{xx1} &= \frac{1}{EA_x} + \left(k\bar{EI}_x - kI\right) \frac{k\bar{EI}_x h^2}{\bar{EI}_x} \\
 \psi_{xx2} &= \frac{1}{EA_x} - \left(k\bar{EI}_x - kI\right) \frac{(1 - k\bar{EI}_x)h^2}{\bar{EI}_x} \\
 \psi_{xy1} &= \frac{1}{EA_x} + \left(k\bar{EI}_x - k_{II}\right) \frac{k\bar{EI}_x h^2}{\bar{EI}_x} + \\
 &\quad k_{II} \left(1 - \frac{\mu_2}{\mu_1}\right) \left[\frac{(1 - k\bar{EI}_x)k\bar{EI}_x h^2}{\bar{EI}_x} - \frac{1}{EA_x} \right] \\
 \psi_{xy2} &= \frac{1}{EA_x} - \left(k\bar{EI}_x - k_{II}\right) \frac{(1 - k\bar{EI}_x)h^2}{\bar{EI}_x} - \\
 &\quad \left(1 - k_{II}\right) \left(\frac{\mu_1}{\mu_2} - 1\right) \left[\frac{(1 - k\bar{EI}_x)k\bar{EI}_x h^2}{\bar{EI}_x} - \frac{1}{EA_x} \right]
 \end{aligned}
 \tag{B13}$$

and

$$\left. \begin{aligned} \overline{EA}_x &= E_1 t_1 + E_C \bar{A}_C + E_2 t_2 \\ k_{\overline{EI}_x} &= \frac{k_C \bar{E}_C \bar{A}_C + E_2 t_2}{\overline{EA}_x} \\ \overline{EI}_x &= E_C \bar{I}_C + \left[E_1 t_1 k_{\overline{EI}_x}^2 + E_C \bar{A}_C (k_C - k_{\overline{EI}_x})^2 + E_2 t_2 (1 - k_{\overline{EI}_x})^2 \right] h^2 \end{aligned} \right\} \text{(B14)}$$

With the strains in the x-direction and the stresses in the y-direction known, the strains in the y-direction ϵ_{y1} and ϵ_{y2} in the middle surfaces of the lower and upper faces, respectively, are determined through the plane-stress relations:

$$\epsilon_{y1} = \left(\frac{1 - \mu_1^2}{E_1} \right) \sigma_{y1} - \mu_1 \epsilon_{x1} \tag{B15}$$

$$\epsilon_{y2} = \left(\frac{1 - \mu_2^2}{E_2} \right) \sigma_{y2} - \mu_2 \epsilon_{x2} \tag{B16}$$

or after elimination of σ_{y1} , σ_{y2} , ϵ_{x1} , and ϵ_{x2} by means of equations (B1), (B2), (B11), and (B12),

$$\epsilon_{y1} = \phi_{yy1} \frac{M_y}{h} - \mu_1 \phi_{xx1} \frac{M_x}{h} + \psi_{yy1} N_y - \mu_1 \psi_{xx1} N_x \tag{B17}$$

$$\epsilon_{y2} = - \phi_{yy2} \frac{M_y}{h} + \mu_2 \phi_{xx2} \frac{M_x}{h} + \psi_{yy2} N_y - \mu_2 \psi_{xx2} N_x \tag{B18}$$

where

$$\begin{aligned}
 \phi_{yy_1} &= (1 - \mu_1^2) \frac{k_{\overline{EI}_y} h^2}{\overline{EI}_y} + \mu_1^2 \phi_{xy_1} \\
 \phi_{yy_2} &= (1 - \mu_2^2) \frac{(1 - k_{\overline{EI}_y}) h^2}{\overline{EI}_y} + \mu_2^2 \phi_{xy_2} \\
 \psi_{yy_1} &= (1 - \mu_1^2) \left[\frac{1}{EA_y} + \frac{(k_{\overline{EI}_y} - k_{II}) k_{\overline{EI}_y} h^2}{\overline{EI}_y} \right] + \mu_1^2 \psi_{xy_1} \\
 \psi_{yy_2} &= (1 - \mu_2^2) \left[\frac{1}{EA_y} - \frac{(k_{\overline{EI}_y} - k_{II})(1 - k_{\overline{EI}_y}) h^2}{\overline{EI}_y} \right] + \mu_2^2 \psi_{xy_2}
 \end{aligned} \tag{B19}$$

and

$$\begin{aligned}
 \overline{EA}_y &= E_1 t_1 + E_2 t_2 \\
 k_{\overline{EI}_y} &= \frac{E_2 t_2}{EA_y} \\
 \overline{EI}_y &= \left[E_1 t_1 k_{\overline{EI}_y}^2 + E_2 t_2 (1 - k_{\overline{EI}_y})^2 \right] h^2
 \end{aligned} \tag{B20}$$

and ϕ_{xx_1} , ϕ_{xx_2} , ψ_{xx_1} , ψ_{xx_2} , ϕ_{xy_1} , ϕ_{xy_2} , ψ_{xy_1} , and ψ_{xy_2} are defined in equations (B13).

With the strains ϵ_{x_1} , ϵ_{x_2} , ϵ_{y_1} , and ϵ_{y_2} known and the assumption made that lines normal to the faces remain normal, the distortions of the element are completely defined. The curvatures can now be written as:

$$\begin{aligned} \frac{\partial^2 w}{\partial x^2} &= \frac{\epsilon_{x_2} - \epsilon_{x_1}}{h} \\ &= -\left(\phi_{xx_2} + \phi_{xx_1}\right) \frac{M_x}{h^2} + \left(\mu_2 \phi_{xy_2} + \mu_1 \phi_{xy_1}\right) \frac{M_y}{h^2} + \\ &\quad \left(\psi_{xx_2} - \psi_{xx_1}\right) \frac{N_x}{h} - \left(\mu_2 \psi_{xy_2} - \mu_1 \psi_{xy_1}\right) \frac{N_y}{h} \end{aligned} \tag{B21}$$

$$\begin{aligned} \frac{\partial^2 w}{\partial y^2} &= \frac{\epsilon_{y_2} - \epsilon_{y_1}}{h} \\ &= -\left(\phi_{yy_2} + \phi_{yy_1}\right) \frac{M_y}{h^2} + \left(\mu_2 \phi_{xx_2} + \mu_1 \phi_{xx_1}\right) \frac{M_x}{h^2} + \\ &\quad \left(\psi_{yy_2} - \psi_{yy_1}\right) \frac{N_y}{h} - \left(\mu_2 \psi_{xx_2} - \mu_1 \psi_{xx_1}\right) \frac{N_x}{h} \end{aligned} \tag{B22}$$

The strain in the x-direction in the plane of N_x is

$$\begin{aligned} \epsilon_x &= \epsilon_{x_1} + k_I (\epsilon_{x_2} - \epsilon_{x_1}) \\ &= \left[\psi_{xx_1} + k_I (\psi_{xx_2} - \psi_{xx_1}) \right] N_x - \left[\mu_1 \psi_{xy_1} + k_I (\mu_2 \psi_{xy_2} - \mu_1 \psi_{xy_1}) \right] N_y + \\ &\quad \left[\phi_{xx_1} - k_I (\phi_{xx_2} + \phi_{xx_1}) \right] \frac{M_x}{h} - \left[\mu_1 \phi_{xy_1} - k_I (\mu_2 \phi_{xy_2} + \mu_1 \phi_{xy_1}) \right] \frac{M_y}{h} \end{aligned} \tag{B23}$$

and the strain in the y-direction in the plane of N_y is

$$\begin{aligned} \epsilon_y &= \epsilon_{y1} + k_{II}(\epsilon_{y2} - \epsilon_{y1}) \\ &= \left[\psi_{yy1} + k_{II}(\psi_{yy2} - \psi_{yy1}) \right] N_y - \left[\mu_1 \psi_{xx1} + k_{II}(\mu_2 \psi_{xx2} - \mu_1 \psi_{xx1}) \right] N_x + \\ &\quad \left[\phi_{yy1} - k_{II}(\phi_{yy2} + \phi_{yy1}) \right] \frac{M_y}{h} - \left[\mu_1 \phi_{xx1} - k_{II}(\mu_2 \phi_{xx2} + \mu_1 \phi_{xx1}) \right] \frac{M_x}{h} \end{aligned} \quad (B24)$$

Comparison of equations (B21) to (B24) with equations (1') to (4'), respectively, permits identification of the following expressions for the elastic constants:

$$D_x = \bar{E}I_x \quad (B25)$$

$$\begin{aligned} D_y = \bar{E}I_y \left\{ 1 - \mu_2^2 \left(1 - \frac{\bar{E}I_y}{\bar{E}I_x} \right) - (\mu_1^2 - \mu_2^2) \left(k_{\bar{E}I_y} - k_{\bar{E}I_x} \frac{\bar{E}I_y}{\bar{E}I_x} \right) - \right. \\ \left. (\mu_1 - \mu_2)^2 \left[\left(1 - k_{\bar{E}I_x} \right) k_{\bar{E}I_x} \frac{\bar{E}I_y}{\bar{E}I_x} - \frac{\bar{E}I_y}{EA_x h^2} \right] \right\}^{-1} \end{aligned} \quad (B26)$$

$$\mu_x = \mu_2 + (\mu_1 - \mu_2) k_{\bar{E}I_x} \quad (B27)$$

$$\mu_y = \mu_x \frac{D_y}{D_x} \quad (B28)$$

$$E_x = \bar{E}A_x \left[1 + \left(k_{\bar{E}I_x} - k_I \right)^2 \frac{\bar{E}A_x h^2}{\bar{E}I_x} \right]^{-1} \quad (B29)$$

$$\begin{aligned}
 E_y = \bar{E}A_y \left\{ \left[1 + \left(k_{\bar{E}I_y} - k_{II} \right)^2 \frac{\bar{E}A_y h^2}{\bar{E}I_y} \right] \left(1 - \mu_1^2 \right) + \mu_1^2 \left[\frac{\bar{E}A_y}{\bar{E}A_x} + \right. \right. \\
 \left. \left. \left(k_{\bar{E}I_x} - k_{II} \right)^2 \frac{\bar{E}A_y h^2}{\bar{E}I_x} \right] + \left(\mu_1^2 - \mu_2^2 \right) \left[1 - \left(k_{\bar{E}I_y} - k_{II} \right) \left(1 - k_{\bar{E}I_y} \right) \frac{\bar{E}A_y h^2}{\bar{E}I_y} - \right. \right. \\
 \left. \left. \frac{\bar{E}A_y}{\bar{E}A_x} + \left(k_{\bar{E}I_x} - k_{II} \right) \left(1 - k_{\bar{E}I_x} \right) \frac{\bar{E}A_y h^2}{\bar{E}I_x} \right] k_{II} + \right. \\
 \left. \left. \left(\mu_1 - \mu_2 \right) \left(1 - k_{II} \right) k_{II} \left[\left(1 - k_{\bar{E}I_x} \right) k_{\bar{E}I_x} \frac{\bar{E}A_y h^2}{\bar{E}I_x} - \frac{\bar{E}A_y}{\bar{E}A_x} \right] \right\}^{-1} \quad (B30)
 \end{aligned}$$

$$\mu'_x = \frac{\mu_1 + \left(\mu_1 k_{\bar{E}I_x} - \mu_2 k_{II} \right) \left(k_{\bar{E}I_x} - k_I \right) \frac{\bar{E}A_x h^2}{\bar{E}I_x} - \left(\mu_1 - \mu_2 \right) \left[1 + \left(k_{\bar{E}I_x} - k_I \right) k_{\bar{E}I_x} \frac{\bar{E}A_x h^2}{\bar{E}I_x} \right] k_{II}}{1 + \left(k_{\bar{E}I_x} - k_I \right)^2 \frac{\bar{E}A_x h^2}{\bar{E}I_x}} \quad (B31)$$

$$\mu'_y = \mu'_x \frac{E_y}{E_x} \quad (B32)$$

$$C_{xx} = - \frac{(k\bar{EI}_x - k_I)h}{\bar{EI}_x} \quad (B33)$$

$$C_{xy} = \frac{\mu_2(k\bar{EI}_x - k_{II})h}{\bar{EI}_x} + (\mu_1 - \mu_2)(1 - k_{II})\frac{k\bar{EI}_x h}{\bar{EI}_x} \quad (B34)$$

$$C_{yx} = \frac{\mu_2(k\bar{EI}_x - k_I)h}{\bar{EI}_x} + (\mu_1 - \mu_2) \left[\frac{1}{\bar{EA}_x h} + \frac{(k\bar{EI}_x - k_I)k\bar{EI}_x h}{\bar{EI}_x} \right] \quad (B35)$$

$$C_{yy} = - \frac{(k\bar{EI}_y - k_{II})h}{\bar{EI}_y} + \mu_2^2 \left[\frac{(k\bar{EI}_y - k_{II})h}{\bar{EI}_y} - \frac{(k\bar{EI}_x - k_{II})h}{\bar{EI}_x} \right] +$$

$$(\mu_1^2 - \mu_2^2) \left[\frac{1}{\bar{EA}_y h} + \frac{(k\bar{EI}_y - k_{II})k\bar{EI}_y h}{\bar{EI}_y} - \frac{1}{\bar{EA}_x h} - \frac{(k\bar{EI}_x - k_{II})k\bar{EI}_x h}{\bar{EI}_x} \right] -$$

$$(\mu_1 - \mu_2) \left[\mu_2 + (\mu_1 - \mu_2)k_{II} \right] \left[\frac{(1 - k\bar{EI}_x)k\bar{EI}_x h}{\bar{EI}_x} - \frac{1}{\bar{EA}_x h} \right] \quad (B36)$$

For the usually encountered case in which the Poisson's ratios for the two face sheets are equal (that is, $\mu_2 = \mu_1$), the foregoing expressions for the elastic constants become appreciably simplified and are

$$D_x = \bar{EI}_x \quad (B25')$$

$$D_y = \bar{EI}_y \left[1 - \mu_1^2 \left(1 - \frac{\bar{EI}_y}{\bar{EI}_x} \right) \right]^{-1} \quad (B26')$$

$$\mu_x = \mu_1 \quad (B27')$$

$$\mu_y = \mu_x \frac{D_y}{D_x} \quad (\text{B28}')$$

$$E_x = \bar{E}A_x \left[1 + (k_{\bar{E}I_x} - k_I)^2 \frac{\bar{E}A_x h^2}{\bar{E}I_x} \right]^{-1} \quad (\text{B29}')$$

$$E_y = \bar{E}A_y \left\{ \left[1 + (k_{\bar{E}I_y} - k_{II})^2 \frac{\bar{E}A_y h^2}{\bar{E}I_y} \right] (1 - \mu_1^2) + \mu_1^2 \left[\frac{\bar{E}A_y}{\bar{E}A_x} + \right. \right. \\ \left. \left. (k_{\bar{E}I_x} - k_{II})^2 \frac{\bar{E}A_y h^2}{\bar{E}I_x} \right] \right\}^{-1} \quad (\text{B30}')$$

$$\mu'_x = \mu_1 \left[\frac{1 + (k_{\bar{E}I_x} - k_I)(k_{\bar{E}I_x} - k_{II}) \frac{\bar{E}A_x h^2}{\bar{E}I_x}}{1 + (k_{\bar{E}I_x} - k_I)^2 \frac{\bar{E}A_x h^2}{\bar{E}I_x}} \right] \quad (\text{B31}')$$

$$\mu'_y = \mu'_x \frac{E_y}{E_x} \quad (\text{B32}')$$

$$C_{xx} = - \frac{(k_{\bar{E}I_x} - k_I) h}{\bar{E}I_x} \quad (\text{B33}')$$

$$C_{xy} = \frac{\mu_1 (k_{\bar{E}I_x} - k_{II}) h}{\bar{E}I_x} \quad (\text{B34}')$$

$$C_{yx} = -\mu_1 C_{xx} \quad (\text{B35}')$$

$$C_{yy} = -(1 - \mu_1^2) \frac{(k_{\overline{EI}_y} - k_{II})h}{\overline{EI}_y} - \mu_1 C_{xy} \quad (B36')$$

It is evident from the preceding two sets of formulas that the values of the constants associated with stretching and also the values of the coupling constants depend upon the location of planes I and II in which the stretching forces N_x and N_y , respectively, are applied. Choosing planes I and II at the centroids of the transformed cross sections parallel to the yz- and xz-planes, respectively, (that is, letting $k_I = k_{\overline{EI}_x}$ and $k_{II} = k_{\overline{EI}_y}$) results in further simplification of the formulas and reduces two of the coupling constants to zero. Equations (B25') to (B36') become

$$D_x = \overline{EI}_x \quad (B25'')$$

$$D_y = \overline{EI}_y \left[1 - \mu_1^2 \left(1 - \frac{\overline{EI}_y}{\overline{EI}_x} \right) \right]^{-1} \quad (B26'')$$

$$\mu_x = \mu_1 \quad (B27'')$$

$$\mu_y = \mu_x \frac{D_y}{D_x} \quad (B28'')$$

$$E_x = \overline{EA}_x \quad (B29'')$$

$$E_y = \overline{EA}_y \left\{ 1 - \mu_1^2 \left[1 - \frac{\overline{EA}_y}{\overline{EA}_x} - \left(k_{\overline{EI}_x} - k_{\overline{EI}_y} \right)^2 \frac{\overline{EA}_y h^2}{\overline{EI}_x} \right] \right\}^{-1} \quad (B30'')$$

$$\mu'_x = \mu_1 \quad (B31'')$$

$$\mu'_{y'} = \mu'_{x'} \frac{E_y}{E_x} \quad (\text{B32"})$$

$$C_{xx} = 0 \quad (\text{B33"})$$

$$C_{xy} = \frac{\mu_1 (k_{\bar{E}I_x} - k_{\bar{E}I_y}) h}{\bar{E}I_x} \quad (\text{B34"})$$

$$C_{yx} = 0 \quad (\text{B35"})$$

$$C_{yy} = -\mu_1 C_{xy} \quad (\text{B36"})$$

APPENDIX C

DERIVATION OF FORMULAS FOR D_{xy} , G_{xy} , AND T

In the derivation of the formulas for D_{xy} , G_{xy} , and T , an element of a corrugated-core sandwich plate is considered which is subjected to shear flows q_1 , q_2 , and q_c in the middle surfaces of the lower-face, upper-face, and core sheet, respectively. (See following fig.)

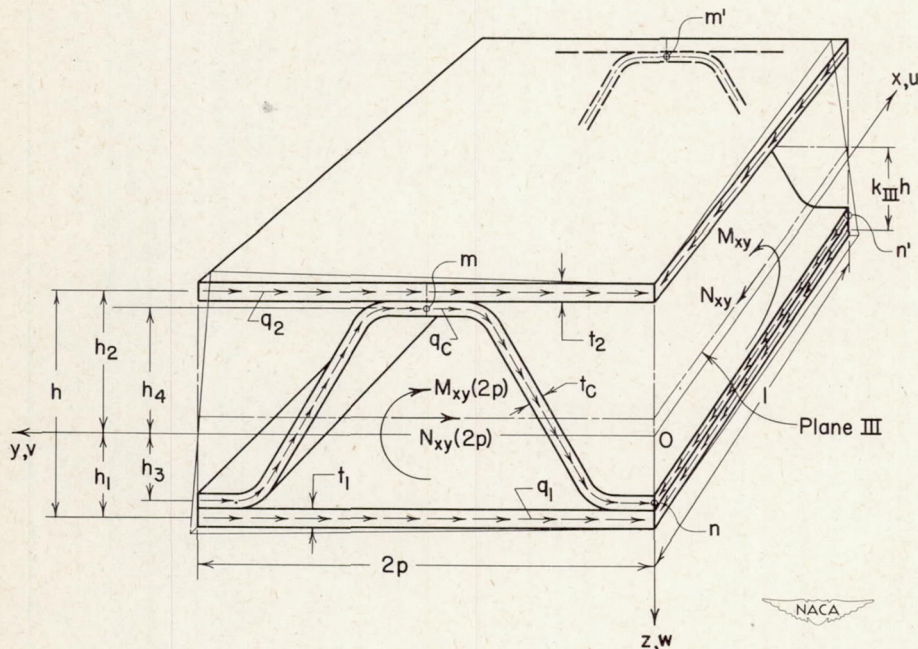


Figure C1

These shear flows may be represented by a resultant horizontal shear force of average intensity N_{xy} acting in some arbitrarily chosen plane, denoted as plane III, and a twisting moment of average intensity M_{xy} about this plane. The shear flows induce a twist $\frac{\partial^2 w}{\partial x \partial y}$ in the element as a whole and shear strains γ_1 , γ_2 , and γ_c in the middle surfaces of the face and core sheets. By linear interpolation (or extrapolation) between the middle surfaces of the face sheets, a shear strain for every horizontal plane can be defined. In this appendix equations are derived relating the twist $\frac{\partial^2 w}{\partial x \partial y}$ and the shear strain γ_{xy} of plane III to

the resultant forces of intensities M_{xy} and N_{xy} which produce them. From these equations general formulas for D_{xy} , G_{xy} , and T are obtained. These general formulas are then reduced to special forms for particular applications.

The orthogonal x- and y-axes are taken in the as yet undetermined plane of zero shear strain, as shown in the figure.

Assumptions.- Vertical lines drawn between middle-surface points in the upper and lower faces before twist are assumed to remain perpendicular to the faces and unchanged in length during twist. The shape of the corrugation in planes parallel to the yz-plane is assumed to be rigidly maintained, whereas displacements in x-direction of the corrugation between lines of attachment to the faces are freely permitted. In order to eliminate rigid-body displacements, the corner of the element ($x = 0$, $y = 0$) is assumed to be fixed in space, and the originally vertical line at the corner is assumed to remain vertical, that is, in coincidence with the z-axis. The distortion of the element is maintained only through the constant shear flows q_1 and q_2 in the faces and q_c in the corrugation; that is, the face and corrugation sheets are assumed to be so thin that twisting moments developed in them are negligible.

Displacements.- In terms of the twist $\frac{\partial^2 w}{\partial x \partial y}$ and the height h_1 of the xy-plane above the middle surface of the lower face, the horizontal displacements of points in the middle surface of the lower face u_1 and v_1 may be written as

$$u_1 = -h_1 y \frac{\partial^2 w}{\partial x \partial y} \quad (C1)$$

$$v_1 = -h_1 x \frac{\partial^2 w}{\partial x \partial y} \quad (C2)$$

The horizontal displacements of points in the middle surface of the upper face u_2 and v_2 are

$$u_2 = h_2 y \frac{\partial^2 w}{\partial x \partial y} \quad (C3)$$

$$v_2 = h_2 x \frac{\partial^2 w}{\partial x \partial y} \quad (C4)$$

The displacement in the x-direction of the corrugation middle-surface crest line mm' is

$$u_m = h_1 p \frac{\partial^2 w}{\partial x \partial y} \quad (C5)$$

and that of the trough line nn' is

$$u_n = 0 \quad (C6)$$

Vertical displacements are given by

$$w = xy \frac{\partial^2 w}{\partial x \partial y} \quad (C7)$$

Shear strains in the faces.- In terms of the foregoing displacements, the middle-surface shear strains in the faces γ_1 and γ_2 can be written as

$$\gamma_1 = \frac{\partial u_1}{\partial y} + \frac{\partial v_1}{\partial x} = -2h_1 \frac{\partial^2 w}{\partial x \partial y} \quad (C8)$$

$$\gamma_2 = \frac{\partial u_2}{\partial y} + \frac{\partial v_2}{\partial x} = 2h_2 \frac{\partial^2 w}{\partial x \partial y} \quad (C9)$$

Shear strain in the corrugation.- The shear strain in the corrugation can be determined by considering the portion between a crest and the adjacent trough as a beam which is being twisted about the x-axis at a constant rate $\frac{\partial^2 w}{\partial x \partial y}$, with the shape of the corrugation in planes perpendicular to the x-axis rigidly maintained. (See the following fig.)

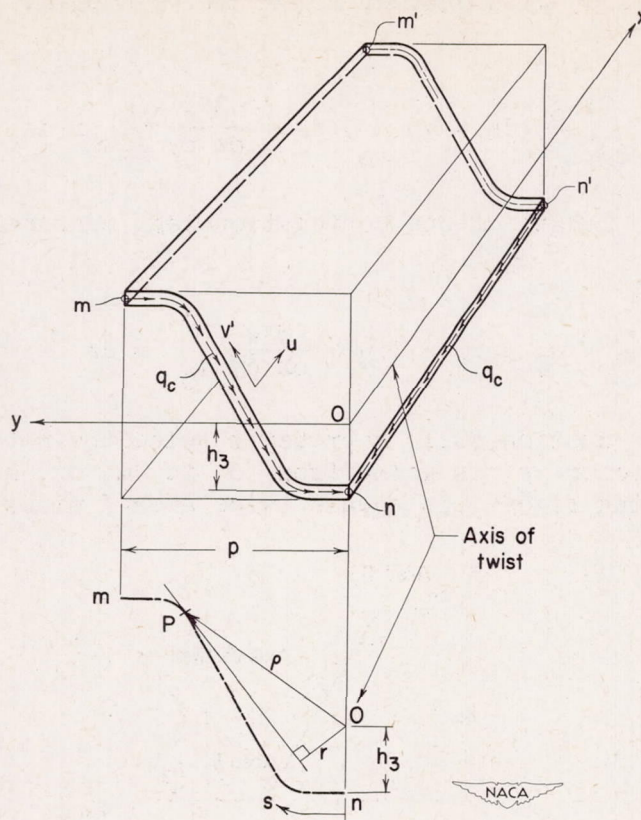


Figure C2

The constant shear strain γ_C in the corrugation must be such that continuity of displacements in the x-direction is maintained between the corrugation and the face sheets. With u and v' denoting axial and tangential displacements, respectively, of the corrugation middle surface and s denoting the distance from nm' measured along the corrugation center line, the shear strain in the corrugation at any point P may be written as

$$\begin{aligned} \gamma_C &= \frac{\partial u}{\partial s} + \frac{\partial v'}{\partial x} \\ &= \frac{\partial u}{\partial s} - r \frac{\partial^2 w}{\partial x \partial y} \end{aligned} \tag{C10}$$

where r is the perpendicular distance from the axis of twist Ox to the tangent at point P and is considered positive if the tangent passes below point O (as in fig.) and negative if it passes above.

Integration of (C10) with respect to s between points n and m gives

$$\int_0^l \frac{\partial u}{\partial s} ds = \gamma_C \int_0^l ds + \frac{\partial^2 w}{\partial x \partial y} \int_0^l r ds$$

where l is the length of one corrugation leg, measured along center line, or

$$u_m - u_n = l\gamma_C + \frac{\partial^2 w}{\partial x \partial y} \int_0^l r ds \quad (C11)$$

The integral in equation (C11) represents twice the net area swept out by the radius vector ρ in going from n to m , or, as can be seen from the following figure, it equals twice area I minus twice area II.

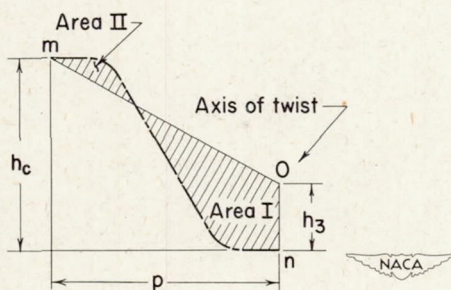


Figure C3

With

$$\text{Area I} - \text{Area II} \equiv \Delta A \quad (C12)$$

equation (C11) becomes

$$u_m - u_n = l\gamma_C + 2 \Delta A \frac{\partial^2 w}{\partial x \partial y} \quad (C13)$$

Continuity between core and faces requires that $u_m - u_n$ as given by equation (C13) be equal to $u_m - u_n$ as given by equations (C5) and (C6). Therefore,

$$l\gamma_C + 2 \Delta A \frac{\partial^2 w}{\partial x \partial y} = h_4 p \frac{\partial^2 w}{\partial x \partial y}$$

or

$$\begin{aligned} \gamma_C &= \left(h_4 p - 2 \Delta A \right) \frac{1}{l} \frac{\partial^2 w}{\partial x \partial y} \\ &= \left(h_4 - 2 \frac{\Delta A}{p} \right) \frac{t_C}{\bar{A}_C} \frac{\partial^2 w}{\partial x \partial y} \end{aligned} \tag{C14}$$

where \bar{A}_C equals $\frac{lt_C}{p}$, the corrugation cross-sectional area per unit width.

The area ΔA which appears in equation (C14) and is defined by equation (C12) depends simultaneously on the vertical location h_3 of the axis of twist and on the geometry of the corrugation. Through purely geometrical considerations, ΔA can be related to two other areas, one of which ph_3 depends only on the vertical location of the axis of twist and the other of which depends only on the geometry of the cross section. The relationship is

$$\Delta A = \frac{1}{2} h_3 p - \frac{1}{4} \left[A_1 - A_2 - p(t_1 - t_2) \right] \tag{C15}$$

where A_1 is the area, in width $2p$, lying between the corrugation center line and the lower-skin center line, and A_2 is similarly the area lying between the corrugation center line and the upper-skin center line. (See the following fig.)

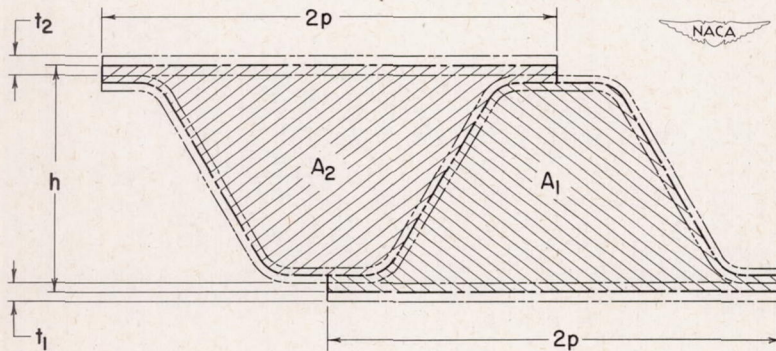


Figure C4

With ΔA in equation (C14) eliminated through equation (C15), the equation for γ_C becomes

$$\gamma_C = \left(h_2 - h_1 + \frac{A_1 - A_2}{2p} \right) \frac{t_C}{\bar{A}_C} \frac{\partial^2 w}{\partial x \partial y} \tag{C16}$$

Shear flows.- With the shear strains known through equations (C8), (C9), and (C16), the following expressions may be written for the shear flows:

$$q_1 = -2G_1 h_1 t_1 \frac{\partial^2 w}{\partial x \partial y} \quad (C17)$$

$$q_2 = 2G_2 h_2 t_2 \frac{\partial^2 w}{\partial x \partial y} \quad (C18)$$

$$q_C = G_C \left(h_2 - h_1 + \frac{A_1 - A_2}{2p} \right) \frac{t_C^2}{A_C} \frac{\partial^2 w}{\partial x \partial y} \quad (C19)$$

These expressions give the shear flows in terms of the twist $\frac{\partial^2 w}{\partial x \partial y}$ and the vertical location (h_1, h_2) of the plane of zero shear strain. In order to determine the elastic constants, the shear flows must be expressed in terms of the twist $\frac{\partial^2 w}{\partial x \partial y}$ and the shear strain γ_{xy} of plane III. The shear strain of any horizontal plane varies linearly with the distance from the xy -plane and must be consistent with the twist; hence,

$$\gamma_{xy} = (k_{III} h - h_1) \left(2 \frac{\partial^2 w}{\partial x \partial y} \right)$$

or

$$h_1 = k_{III} h - \frac{1}{2} \frac{\gamma_{xy}}{\frac{\partial^2 w}{\partial x \partial y}} \quad (C20)$$

and

$$\begin{aligned} h_2 &= h - h_1 \\ &= (1 - k_{III}) h + \frac{1}{2} \frac{\gamma_{xy}}{\frac{\partial^2 w}{\partial x \partial y}} \end{aligned} \quad (C21)$$

Using equations (C20) and (C21) to eliminate h_1 and h_2 from equations (C17) to (C19) gives the following expressions for the shear flows:

$$q_1 = -2G_1 t_1 \left(k_{III} h \frac{\partial^2 w}{\partial x \partial y} - \frac{1}{2} \gamma_{xy} \right) \tag{C22}$$

$$q_2 = 2G_2 t_2 \left[\left(1 - k_{III} \right) h \frac{\partial^2 w}{\partial x \partial y} + \frac{1}{2} \gamma_{xy} \right] \tag{C23}$$

$$q_C = \frac{G_C t_C^2}{A_C} \left\{ \left[\left(1 - 2k_{III} \right) h + \frac{A_1 - A_2}{2p} \right] \frac{\partial^2 w}{\partial x \partial y} + \gamma_{xy} \right\} \tag{C24}$$

The resultants of the shear flows, namely N_{xy} and M_{xy} , may now be evaluated.

Evaluation of N_{xy} . - The shear flows q_1 , q_2 , and q_C combine to give a resultant horizontal shear flow of

$$N_{xy} = q_1 + q_2 + q_C \tag{C25}$$

where q_1 , q_2 , and q_C are given by equations (C22) to (C24).

Evaluation of M_{xy} . - The average value of M_{xy} can be determined by taking moments, in the yz -plane, of q_1 , q_2 , and the horizontal components of q_C with respect to plane III. Use is made in this section of a horizontal plane which cuts the corrugation center line into lobes of equal area. This plane, which is shown as plane IV in the following sketch at a distance $k_C h$ above the middle surface of the lower face, is the centroid (or shear center) of the corrugation shear flows.

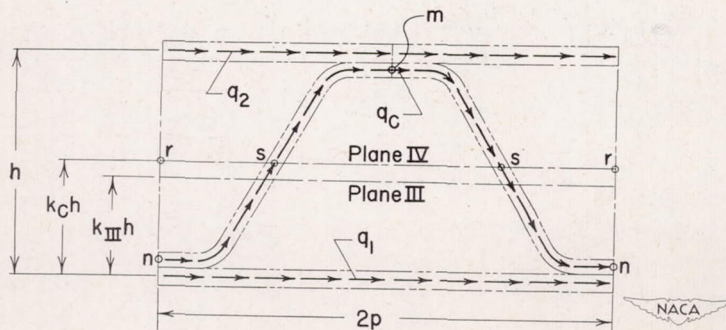


Figure C5

Taking moments with respect to plane III gives

$$M_{xy} = -q_1 k_{III} h + q_2 (1 - k_{III}) h + q_C (k_C - k_{III}) h \quad (C26)$$

where q_1 , q_2 , and q_C are given by equations (C22) to (C24).

Evaluation of N_{xy} and M_{xy} in terms of γ_{xy} and $\frac{\partial^2 w}{\partial x \partial y}$. - Substitution of equations (C22) to (C24) into equations (C25) and (C26) and elimination of $\frac{A_1 - A_2}{2ph}$ through the purely geometrical relationship

$$k_C = \frac{1}{2} \left(1 + \frac{A_1 - A_2}{2ph} \right) \quad (C27)$$

gives

$$N_{xy} = \gamma_{xy} \overline{GA} + 2 \frac{\partial^2 w}{\partial x \partial y} \overline{GA} (k_{GJ} - k_{III}) h \quad (C28)$$

$$M_{xy} = \gamma_{xy} \overline{GA} (k_{GJ} - k_{III}) h + 2 \frac{\partial^2 w}{\partial x \partial y} \left[\overline{GJ} + \overline{GA} (k_{GJ} - k_{III})^2 h^2 \right] \quad (C29)$$

where

$$\overline{GA} = G_1 t_1 + \frac{G_C t_C^2}{\overline{A_C}} + G_2 t_2 \quad (C30)$$

$$k_{GJ} = \frac{\frac{G_C t_C^2 k_C}{\overline{A_C}} + G_2 t_2}{\overline{GA}} \quad (C31)$$

$$\overline{GJ} = \left[G_1 t_1 k_{GJ}^2 + \frac{G_C t_C^2}{\overline{A_C}} (k_{GJ} - k_C)^2 + G_2 t_2 (1 - k_{GJ})^2 \right] h^2 \quad (C32)$$

Solution of equations (C28) and (C29) gives

$$\frac{\partial^2 w}{\partial x \partial y} = \frac{M_{xy}}{2\overline{GJ}} - N_{xy} \frac{(k_{\overline{GJ}} - k_{III})h}{2\overline{GJ}} \quad (C33)$$

$$\gamma_{xy} = -M_{xy} \frac{(k_{\overline{GJ}} - k_{III})h}{\overline{GJ}} + N_{xy} \left[\frac{1}{\overline{GA}} + \frac{(k_{\overline{GJ}} - k_{III})^2 h^2}{\overline{GJ}} \right] \quad (C34)$$

Comparison of equations (C33) and (C34) with equations (5') and (6') permits the identification of the following elastic constants:

$$D_{xy} = 2\overline{GJ} \quad (C35)$$

$$G_{xy} = \frac{\overline{GA}}{1 + \frac{\overline{GA}}{\overline{GJ}}(k_{\overline{GJ}} - k_{III})^2 h^2} \quad (C36)$$

$$T = -\frac{(k_{\overline{GJ}} - k_{III})h}{2\overline{GJ}} \quad (C37)$$

Choosing k_{III} equal to $k_{\overline{GJ}}$ reduces the foregoing equations to

$$D_{xy} = 2\overline{GJ} \quad (C35')$$

$$G_{xy} = \overline{GA} \quad (C36')$$

$$T = 0 \quad (C37')$$

APPENDIX D

DERIVATION OF FORMULA FOR D_{Q_y}

In this appendix a formula for the transverse shear stiffness D_{Q_y} is derived which is fundamentally the same as that given in reference 4 for the case of interference of flats neglected but extended slightly to include the effects of stretching of the corrugation and the prevention of anticlastic curvature. The general formula is reduced to special forms for specific applications.

The element of a corrugated-core sandwich shown in the following figure has unit width normal to the page and is in equilibrium under a small transverse shear of unit intensity ($Q_y = 1$) and horizontal forces Y of magnitude p/h . The corrugation is assumed to be fastened to the skins through rigid joints at its crests and troughs.

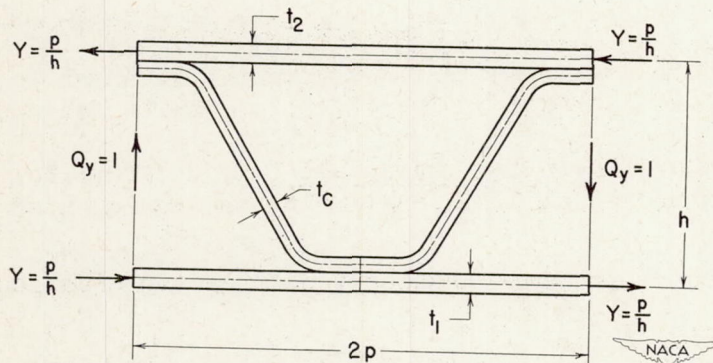


Figure D1

For small Q_y the relative distortions of the element are proportional to Q_y . These relative distortions δ_y and δ_z are shown in the following figure:

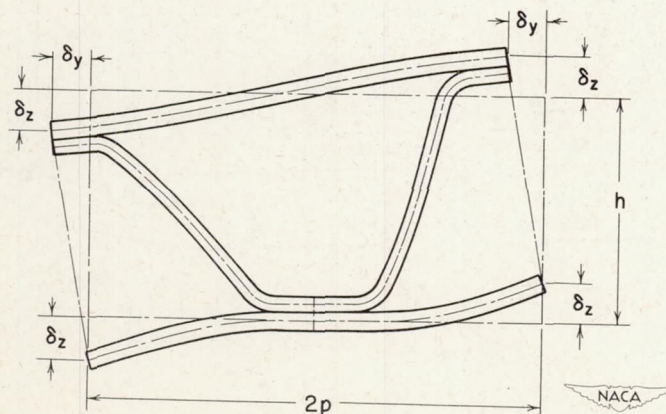


Figure D2

An average shear strain γ_y may be taken as $\frac{\delta_y}{h} - \frac{\delta_z}{p}$ and the transverse shear stiffness D_{Q_y} is then given by the ratio of shear intensity to shear strain, or

$$D_{Q_y} = \frac{1}{\gamma_y} = \frac{1}{\frac{\delta_y}{h} - \frac{\delta_z}{p}} \tag{D1}$$

The sandwich-plate element is now analyzed as a statically indeterminate structure to determine the displacements δ_y and δ_z . Substitution in equation (D1) then gives a general expression for the calculation of D_{Q_y} in any particular case. In the analysis of the unit-width element the assumption is made that the element is part of a sandwich having its width normal to the page equal to infinity. The corrugation and skin elements are therefore taken as beams in which anticlastic curvature is completely restrained, which amounts to multiplication of the beam flexural stiffnesses by factors of the type $\frac{1}{1 - \mu^2}$. In order to obtain values more consistent with experiments in which relatively narrow beams are used, the Poisson's ratios μ may be set equal to zero.

In the following figure are shown free-body diagrams for elements of the corrugation and skins. These elements are represented only by their center lines.

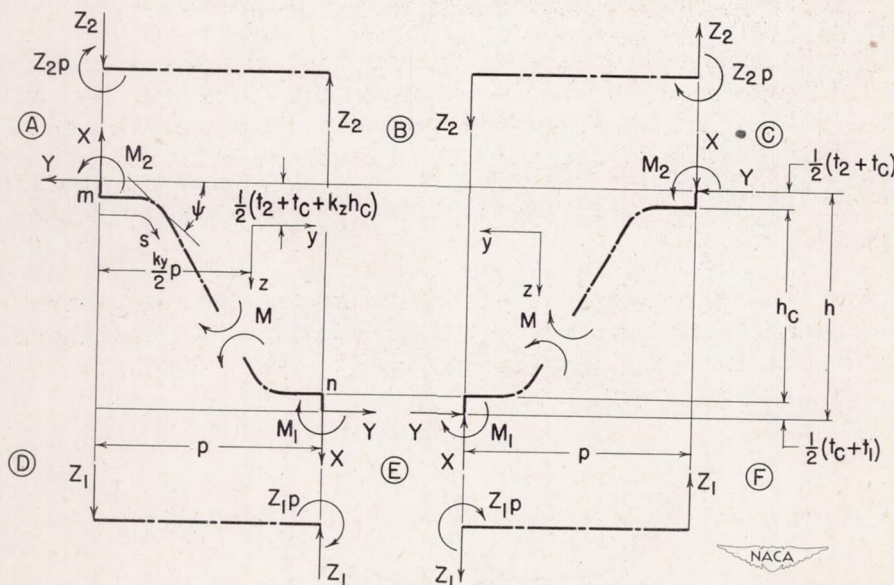


Figure D3

The distortions of the elements, assumed small, are shown in the following figure:

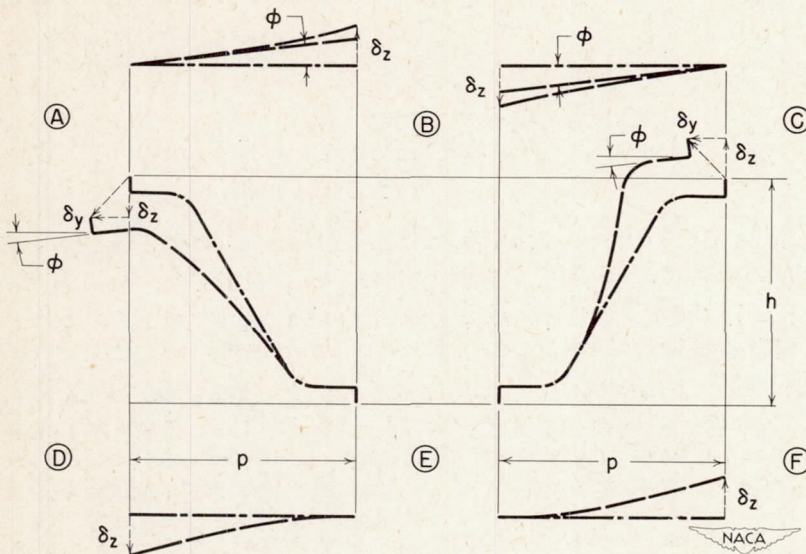


Figure D4

It should be noted that the forces Y on the corrugation elements are considered as acting in the midplanes of the skins and transmitted to the corrugation through short rigid projections. Similarly, the moments M_1 and M_2 are taken about points in these planes and are not the actual moments in the corrugation sheets at the joints.

Since the undeformed structure is symmetrical about any plane BE , all forces and deformations in the two corrugation elements EA and EC are equal, as likewise are those in the two skin elements ED and EF and in the two skin elements BA and BC . Then the skin moments at B , D , and F are zero, and each skin element is in equilibrium under its shear Z_1 or Z_2 and its moment Z_1p or Z_2p at one end.

Since a shear of unity is assumed to act on the sandwich, the relation between the shear carried by the corrugation X and the shears carried by the two skins Z_1 and Z_2 is

$$X - Z_1 - Z_2 = 1 \quad (D2)$$

Static equilibrium of the corrugation elements requires that

$$M_2 - M_1 + Yh - Xp = 0 \quad (D3)$$

Equilibrium of moments at joint E requires that

$$M_1 + Z_1 p + M_1 + Z_1 p = 0$$

or

$$M_1 = -Z_1 p \quad (D4)$$

Similarly, at an upper joint

$$M_2 = Z_2 p \quad (D5)$$

Finally, the internal moment M at any point in the corrugation sheet is given by

$$M = M_2 + Y \left[\frac{1}{2} (t_2 + t_C + k_z h_C) + z \right] - X \left(\frac{k_y p}{2} + y \right) \quad (D6)$$

The foregoing five equations are all the static relations needed.

With the rotation of A with respect to the horizontal tangent at E denoted as ϕ , the deformation δ_z may be written for the lower and upper skins, respectively, as

$$\delta_z = \frac{Z_1 p^3}{3E_1 I_1 / (1 - \mu_1^2)} \quad (D7)$$

$$\delta_z = \frac{Z_2 p^3}{3E_2 I_2 / (1 - \mu_2^2)} + p\phi \quad (D8)$$

Deformations in the corrugation sheet are due to both bending and stretching. The three components of the displacement at A or C with respect to the tangent at E are

$$\phi = \frac{1}{E_C I_C / (1 - \mu_C^2)} \int M ds \quad (D9)$$

$$\delta_y = \frac{1}{E_C I_C / (1 - \mu_C^2)} \int M \left[\frac{1}{2} (t_2 + t_C + k_z h_C) + z \right] ds + \frac{1}{E'_C t_C / (1 - \mu_C^2)} \int (Y \cos \psi + X \sin \psi) \cos \psi ds \quad (D10)$$

$$\delta_z = \frac{1}{E_C I_C / (1 - \mu_C^2)} \int M \left(\frac{k_y p}{2} + y \right) ds - \frac{1}{E'_C t_C / (1 - \mu_C^2)} \int (Y \cos \psi + X \sin \psi) \sin \psi ds \quad (D11)$$

where the integrals are taken over one corrugation leg, as from A to E or C to E (excluding the short rigid projections), s is the distance measured along the corrugation center line, and ψ is the angle between the tangent to the corrugation and the horizontal (see fig. D3). In equations (D10) and (D11) E'_C denotes the stretching modulus of elasticity of the core. It has been distinguished from the bending modulus E_C in order to permit identification of the terms representing the stretching contribution in the derivation. The Poisson's ratios associated with bending and with stretching of the core have, however, been assumed equal. In the rest of the derivation, the moments of inertia per unit width I_1 , I_2 , and I_C will in most cases be eliminated through the relations

$$\left. \begin{aligned} I_1 &= \frac{1}{12} t_1^3 \\ I_2 &= \frac{1}{12} t_2^3 \\ I_C &= \frac{1}{12} t_C^3 \end{aligned} \right\} \quad (D12)$$

The ten equations (D2) to (D11) contain ten unknowns for which they may be solved. The equations can first be reduced to the following four equations:

$$\left. \begin{aligned} a_{11}X + a_{12}Z_2 + a_{13} \delta_z + 0 &= r_1 \\ a_{21}X + a_{22}Z_2 + a_{23} \delta_z + 0 &= r_2 \\ a_{31}X + a_{32}Z_2 + a_{33} \delta_z + 0 &= r_3 \\ a_{41}X + a_{42}Z_2 + 0 + a_{44} \delta_y &= r_4 \end{aligned} \right\} \quad (D13)$$

where

$$a_{11} = 1$$

$$a_{21} = \frac{1}{h_C} \frac{h_C^3 (1 - \mu_C^2)}{E_C I_C} \left(K_{A_z} + \frac{k_y}{2} \frac{p}{h_C} K_L \right)$$

$$a_{31} = \frac{h_C^3 (1 - \mu_C^2)}{E_C I_C} \left[K_{I_z} + k_y \frac{p}{h_C} K_{A_z} + \left(\frac{k_y}{2} \frac{p}{h_C} \right)^2 K_L + \frac{1}{12} \frac{E_C}{E'_C} \left(\frac{t_C}{h_C} \right)^2 K_{L_z} \right]$$

$$a_{41} = \frac{h_C^3 (1 - \mu_C^2)}{E_C I_C} \left[\frac{1}{2} \left(\frac{t_2}{h_C} + \frac{t_C}{h_C} + k_z \right) \left(K_{A_z} + \frac{k_y}{2} \frac{p}{h_C} K_L \right) + K_{I_{yz}} + \frac{k_y}{2} \frac{p}{h_C} K_{A_y} - \frac{1}{12} \frac{E_C}{E'_C} \left(\frac{t_C}{h_C} \right)^2 K_{L_{yz}} \right]$$

$$a_{12} = -1$$

$$a_{22} = -\frac{1}{h_C} \frac{h_C^3 (1 - \mu_C^2)}{E_C I_C} \left[K_L + \frac{1}{3} \frac{E_C}{E_2} \frac{1 - \mu_2^2}{1 - \mu_C^2} \left(\frac{t_C}{t_2} \right)^3 \left(\frac{p}{h_C} \right) \frac{p}{h_C} \right] \quad (D14)$$

$$a_{32} = -\frac{h_C^3 (1 - \mu_C^2)}{E_C I_C} \left(K_{A_z} + \frac{k_y}{2} \frac{p}{h_C} K_L \right) \frac{p}{h_C}$$

$$a_{42} = -\frac{h_C^3 (1 - \mu_C^2)}{E_C I_C} \left[K_{A_y} + \frac{1}{2} \left(\frac{t_2}{h_C} + \frac{t_C}{h_C} + k_z \right) K_L \right] \frac{p}{h_C}$$

$$a_{13} = -\frac{3E_1 I_1}{(1 - \mu_1^2) p^3}$$

$$a_{23} = \frac{1}{p}$$

$$a_{33} = a_{44} = r_1 = 1$$

Equation (D14) continued on next page

$$\begin{aligned}
 r_2 &= \frac{1}{h} \frac{h_C^3 (1 - \mu_C^2)}{E_C I_C} \left[K_{A_y} + \frac{1}{2} \left(\frac{t_2}{h_C} + \frac{t_C}{h_C} + k_z \right) K_L \right] \frac{p}{h_C} \\
 r_3 &= \frac{h_C}{h} \frac{h_C^3 (1 - \mu_C^2)}{E_C I_C} \left[K_{I_{yz}} + \frac{1}{2} \left(\frac{t_2}{h_C} + \frac{t_C}{h_C} + k_z \right) \left(K_{A_z} + \frac{k_y}{2} \frac{p}{h_C} K_L \right) + \right. \\
 &\quad \left. \frac{k_y}{2} \frac{p}{h_C} K_{A_y} - \frac{1}{12} \frac{E_C}{E'_C} \left(\frac{t_C}{h_C} \right)^2 K_{L_{yz}} \right] \frac{p}{h_C} \\
 r_4 &= \frac{h_C}{h} \frac{h_C^3 (1 - \mu_C^2)}{E_C I_C} \left\{ K_{I_y} + \left(\frac{t_2}{h_C} + \frac{t_C}{h_C} + k_z \right) \left[K_{A_y} + \right. \right. \\
 &\quad \left. \left. \frac{1}{4} \left(\frac{t_2}{h_C} + \frac{t_C}{h_C} + k_z \right) K_L \right] + \frac{1}{12} \frac{E_C}{E'_C} \left(\frac{t_C}{h_C} \right)^2 K_{L_y} \right\} \frac{p}{h_C}
 \end{aligned}
 \tag{D14} \text{ Concluded}$$

The quantities K_{I_y} , K_{I_z} , . . . and so on are nondimensional functions of the corrugation shape and the origin location. They are defined by the following integrals taken along one leg of the corrugation center line from the crest to the trough; that is, from m to n in figure D3:

$$\left. \begin{aligned}
 K_{I_z} &= \frac{1}{h_C^3} \int y^2 ds \\
 K_{I_{yz}} &= \frac{1}{h_C^3} \int yz ds \\
 K_{I_y} &= \frac{1}{h_C^3} \int z^2 ds \\
 K_{A_z} &= \frac{1}{h_C^2} \int y ds \\
 K_{A_y} &= \frac{1}{h_C^2} \int z ds
 \end{aligned} \right\} \tag{D15}$$

Equation (D15) continued on next page

$$\left. \begin{aligned}
 K_L &= \frac{1}{h_C} \int ds \\
 K_{L_y} &= \frac{1}{h_C} \int \cos^2 \psi ds \\
 K_{L_{yz}} &= \frac{1}{h_C} \int \sin \psi \cos \psi ds \\
 K_{L_z} &= \frac{1}{h_C} \int \sin^2 \psi ds
 \end{aligned} \right\} \begin{array}{l} \text{(D15)} \\ \text{Concluded} \end{array}$$

Equations (D13) may be solved for δ_y and δ_z . Substitution in equation (D1) then furnishes the following expression for D_{Q_y} :

$$D_{Q_y} = \text{Sh} \left(\frac{E_C}{1 - \mu_C^2} \right) \left(\frac{t_C}{h_C} \right)^3 \tag{D16}$$

where

$$S = \frac{3 \frac{h_C}{p} c_7 (c_2^2 - c_1 c_3) - c_3 + \frac{p}{h_C} (2c_2 - \frac{p}{h_C} c_1)}{\left\{ \begin{aligned}
 &2 \frac{p}{h_C} \left[\frac{p}{h_C} (c_1 c_4 - c_2 c_5) - (c_2 c_4 - c_3 c_5) \right] + \frac{h_C}{h} \left\{ 3c_7 \left[c_4 (c_1 c_4 - 2c_2 c_5) + \right. \right. \\
 &12 \left. \left. c_3 c_5^2 - c_6 (c_1 c_3 - c_2^2) \right] + \frac{p}{h_C} (c_4^2 - c_3 c_6) + 2 \left(\frac{p}{h_C} \right)^2 (c_2 c_6 - c_4 c_5) + \right. \\
 &\left. \left. \left(\frac{p}{h_C} \right)^3 (c_5^2 - c_1 c_6) \right\} + \frac{h}{h_C} \frac{p}{h_C} (c_2^2 - c_1 c_3) \right\}
 \end{aligned} \right\} \tag{D17}$$

and

$$\begin{aligned}
 C_1 &= K_L + \frac{1}{3} \frac{E_C (1 - \mu_2^2)}{E_2 (1 - \mu_C^2)} \left(\frac{t_C}{t_2} \right)^3 \frac{p}{h_C} \\
 C_2 &= K_{A_z} + \frac{k_y}{2} \frac{p}{h_C} K_L \\
 C_3 &= K_{I_z} + k_y \frac{p}{h_C} \left(K_{A_z} + \frac{k_y}{4} \frac{p}{h_C} K_L \right) + \frac{1}{12} \frac{E_C}{E'_C} \left(\frac{t_C}{h_C} \right)^2 K_{L_z} \\
 C_4 &= K_{I_{yz}} + \frac{1}{2} \left[k_z + \left(1 + \frac{t_2}{t_C} \right) \frac{t_C}{h_C} \right] \left(K_{A_z} + \frac{k_y}{2} \frac{p}{h_C} K_L \right) + \frac{k_y}{2} \frac{p}{h_C} K_{A_y} - \\
 &\quad \frac{1}{12} \frac{E_C}{E'_C} \left(\frac{t_C}{h_C} \right)^2 K_{L_{yz}} \\
 C_5 &= K_{A_y} + \frac{1}{2} \left[k_z + \left(1 + \frac{t_2}{t_C} \right) \frac{t_C}{h_C} \right] K_L \\
 C_6 &= K_{I_y} + \left[k_z + \left(1 + \frac{t_2}{t_C} \right) \frac{t_C}{h_C} \right] \left\{ K_{A_y} + \frac{1}{4} \left[k_z + \left(1 + \frac{t_2}{t_C} \right) \frac{t_C}{h_C} \right] K_L \right\} + \\
 &\quad \frac{1}{12} \frac{E_C}{E'_C} \left(\frac{t_C}{h_C} \right)^2 K_{L_y} \\
 C_7 &= \frac{E_1}{E_C} \frac{1 - \mu_C^2}{1 - \mu_1^2} \left(\frac{t_1}{t_C} \right)^3
 \end{aligned} \tag{D18}$$

Special Cases

Symmetrical corrugation.- The evaluation of the terms K_{I_y} , K_{I_z} , . . . and so on in the formula for D_{Q_y} depends upon the location of the origin of coordinates, that is, on the choice of k_y and k_z . For the frequently encountered case in which the corrugation is symmetrical, computational advantages are gained by letting $k_y = k_z = 1$, that is, by choosing the origin at the midpoint of the corrugation leg. As a result the parameters K_{A_y} and K_{A_z} vanish.

Symmetrical sandwich.- For the case of the symmetrical corrugated-core sandwich, elimination of K_{A_y} and K_{A_z} by choosing $k_y = k_z = 1$ is again advantageous. In addition, however, the numerator and denominator in equation (D17) for S contain a common factor. Cancellation of this factor yields the following simplified expression for S to replace equation (D17):

$$S = \frac{6 \frac{h_C}{p} B_3 B_7 + \left(\frac{p}{h_C}\right)^2}{12 \left\{ -2 \left(\frac{p}{h_C}\right)^2 B_4 + \frac{h_C}{h} \left[6 B_7 (B_3 B_6 - B_4^2) + \left(\frac{p}{h_C}\right)^3 B_6 \right] + \frac{h}{h_C} \frac{p}{h_C} B_3 \right\}} \quad (D19)$$

where

$$\left. \begin{aligned} B_3 &= K_{I_z} + \frac{1}{12} \frac{E_C}{E'_C} \left(\frac{t_C}{h_C}\right)^2 K_{L_z} \\ B_4 &= K_{I_{yz}} - \frac{1}{12} \frac{E_C}{E'_C} \left(\frac{t_C}{h_C}\right)^2 K_{L_{yz}} \\ B_6 &= K_{I_y} + \frac{1}{12} \frac{E_C}{E'_C} \left(\frac{t_C}{h_C}\right)^2 K_{L_y} \\ B_7 &= C_7 = \frac{E_1}{E_C} \frac{1 - \mu_C^2}{1 - \mu_1^2} \left(\frac{t_1}{t_C}\right)^3 \end{aligned} \right\} \quad (D20)$$

Corrugation center line consisting of straight lines and circular arcs.- The center line of a corrugation leg in many cases consists of three straight-line segments (two flats and one diagonal element) separated from each other by two circular arcs. The following figure

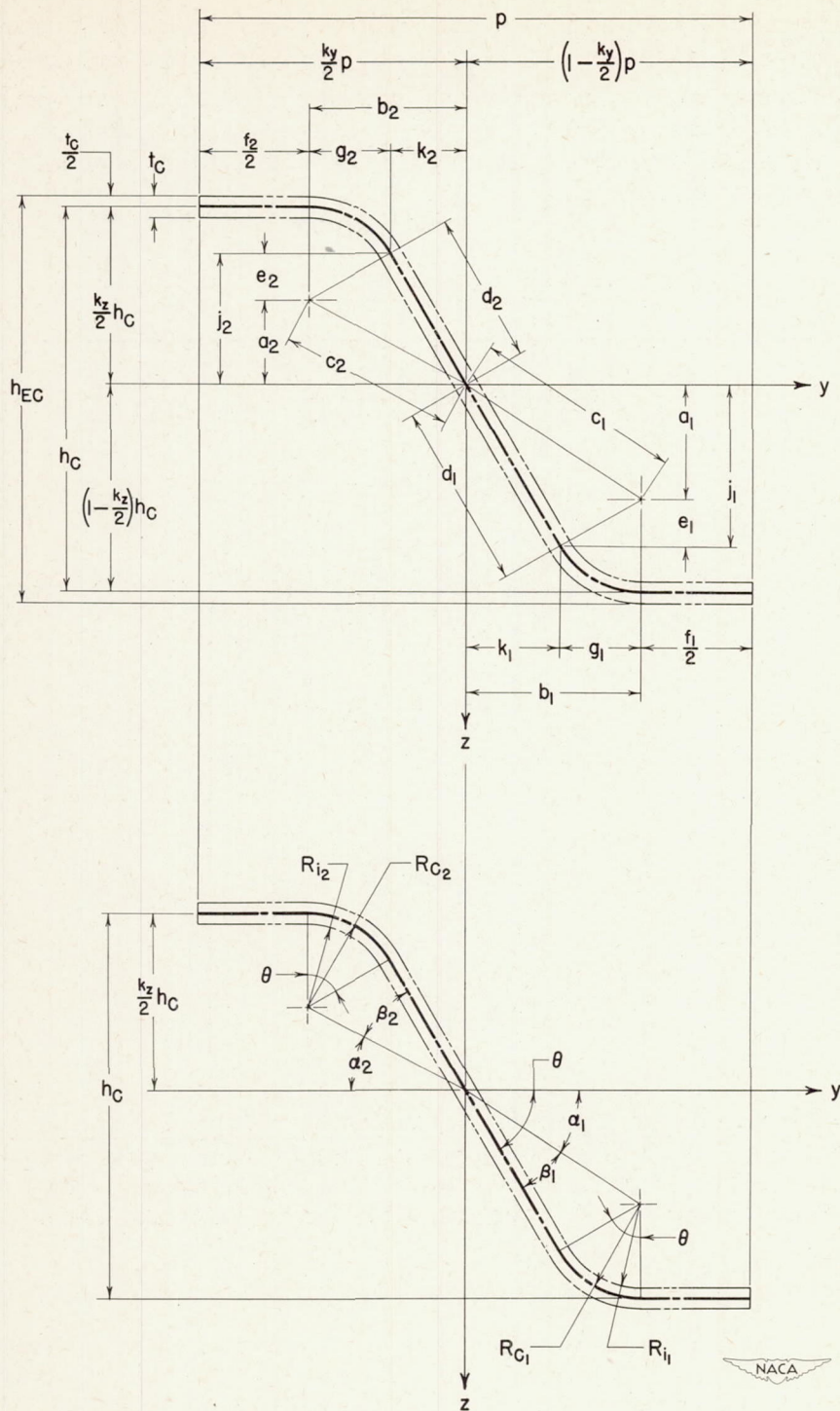


Figure D5

shows such a corrugation leg with its dimensions. If the integrals in equations (D15) are evaluated for this shape, with the origin of x and y chosen along the straight diagonal portion as shown in the figure, the results are

$$\begin{aligned}
 K_{I_z} &= \frac{1}{3} \left[\left(\frac{k_1}{h_c} \right)^2 \frac{d_1}{h_c} + \left(\frac{k_2}{h_c} \right)^2 \frac{d_2}{h_c} \right] + \frac{1}{3} \left[\left(1 - \frac{k_y}{2} \right)^3 \left(\frac{p}{h_c} \right)^3 - \left(\frac{b_1}{h_c} \right)^3 + \right. \\
 &\quad \left. \frac{k_y^3}{8} \left(\frac{p}{h_c} \right)^3 - \left(\frac{b_2}{h_c} \right)^3 \right] + \frac{R_{C1}}{h_c} \left\{ \frac{b_1}{h_c} \left[\theta \frac{b_1}{h_c} - 2 \left(\frac{R_{C1}}{h_c} - \frac{e_1}{h_c} \right) \right] + \right. \\
 &\quad \left. \frac{1}{2} \left[\theta \left(\frac{R_{C1}}{h_c} \right)^2 - \frac{g_1}{h_c} \frac{e_1}{h_c} \right] \right\} + \frac{R_{C2}}{h_c} \left\{ \frac{b_2}{h_c} \left[\theta \frac{b_2}{h_c} - 2 \left(\frac{R_{C2}}{h_c} - \frac{e_2}{h_c} \right) \right] + \right. \\
 &\quad \left. \frac{1}{2} \left[\theta \left(\frac{R_{C2}}{h_c} \right)^2 - \frac{g_2}{h_c} \frac{e_2}{h_c} \right] \right\} \\
 \\
 K_{I_{yz}} &= \frac{1}{3} \left(\frac{j_1}{h_c} \frac{k_1}{h_c} \frac{d_1}{h_c} + \frac{j_2}{h_c} \frac{k_2}{h_c} \frac{d_2}{h_c} \right) + \frac{1}{4} \left\{ 2 \left(1 - \frac{k_z}{2} \right) \left[\left(1 - \frac{k_y}{2} \right)^2 \left(\frac{p}{h_c} \right)^2 - \right. \right. \\
 &\quad \left. \left. \left(\frac{b_1}{h_c} \right)^2 \right] + k_z \left[\frac{k_y^2}{4} \left(\frac{p}{h_c} \right)^2 - \left(\frac{b_2}{h_c} \right)^2 \right] \right\} + \frac{R_{C1}}{h_c} \left[\frac{a_1}{h_c} \left(\theta \frac{b_1}{h_c} + \frac{e_1}{h_c} - \frac{R_{C1}}{h_c} \right) + \right. \\
 &\quad \left. \frac{g_1}{h_c} \left(\frac{b_1}{h_c} - \frac{1}{2} \frac{g_1}{h_c} \right) \right] + \frac{R_{C2}}{h_c} \left[\frac{a_2}{h_c} \left(\theta \frac{b_2}{h_c} + \frac{e_2}{h_c} - \frac{R_{C2}}{h_c} \right) + \frac{g_2}{h_c} \left(\frac{b_2}{h_c} - \frac{1}{2} \frac{g_2}{h_c} \right) \right] \quad (D21) \\
 \\
 K_{I_y} &= \frac{1}{3} \left[\left(\frac{j_1}{h_c} \right)^2 \left(\frac{d_1}{h_c} \right) + \left(\frac{j_2}{h_c} \right)^2 \frac{d_2}{h_c} \right] + \frac{1}{8} \left[4 \left(1 - \frac{k_z}{2} \right)^2 \frac{f_1}{h_c} + k_z^2 \frac{f_2}{h_c} \right] + \\
 &\quad \frac{R_{C1}}{h_c} \left\{ \frac{a_1}{h_c} \left(\theta \frac{a_1}{h_c} + 2 \frac{g_1}{h_c} \right) + \frac{1}{2} \left[\theta \left(\frac{R_{C1}}{h_c} \right)^2 + \frac{g_1}{h_c} \frac{e_1}{h_c} \right] \right\} + \\
 &\quad \frac{R_{C2}}{h_c} \left\{ \frac{a_2}{h_c} \left(\theta \frac{a_2}{h_c} + 2 \frac{g_2}{h_c} \right) + \frac{1}{2} \left[\theta \left(\frac{R_{C2}}{h_c} \right)^2 + \frac{g_2}{h_c} \frac{e_2}{h_c} \right] \right\}
 \end{aligned}$$

Equation (D21) continued on next page

$$\begin{aligned}
 K_{A_z} &= \frac{1}{2} \left(\frac{k_1}{h_c} \frac{d_1}{h_c} - \frac{k_2}{h_c} \frac{d_2}{h_c} \right) + \frac{1}{2} \left[\frac{f_1}{h_c} \left(\frac{b_1}{h_c} + \frac{1}{4} \frac{f_1}{h_c} \right) - \frac{f_2}{h_c} \left(\frac{b_2}{h_c} + \frac{1}{4} \frac{f_2}{h_c} \right) \right] + \\
 &\quad \frac{RC_1}{h_c} \left(\theta \frac{b_1}{h_c} + \frac{e_1}{h_c} - \frac{RC_1}{h_c} \right) - \frac{RC_2}{h_c} \left(\theta \frac{b_2}{h_c} + \frac{e_2}{h_c} - \frac{RC_2}{h_c} \right) \\
 K_{A_y} &= \frac{1}{2} \left(\frac{j_1}{h_c} \frac{d_1}{h_c} - \frac{j_2}{h_c} \frac{d_2}{h_c} \right) + \frac{1}{4} \left[2 \left(1 - \frac{k_z}{2} \right) \frac{f_1}{h_c} - k_z \frac{f_2}{h_c} \right] + \\
 &\quad \frac{RC_1}{h_c} \left(\theta \frac{a_1}{h_c} + \frac{g_1}{h_c} \right) - \frac{RC_2}{h_c} \left(\theta \frac{a_2}{h_c} + \frac{g_2}{h_c} \right) \\
 K_L &= \frac{d_1}{h_c} + \frac{d_2}{h_c} + \theta \left(\frac{RC_1}{h_c} + \frac{RC_2}{h_c} \right) + \frac{1}{2} \left(\frac{f_1}{h_c} + \frac{f_2}{h_c} \right) \\
 K_{L_y} &= \frac{1}{2} \left(\frac{f_1}{h_c} + \frac{f_2}{h_c} \right) + \left(\frac{d_1}{h_c} + \frac{d_2}{h_c} \right) \cos^2 \theta + \frac{1}{2} \left(\frac{RC_1}{h_c} + \frac{RC_2}{h_c} \right) (\theta + \sin \theta \cos \theta) \\
 K_{L_{yz}} &= \left(\frac{d_1}{h_c} + \frac{d_2}{h_c} \right) \sin \theta \cos \theta + \frac{1}{2} \left(\frac{RC_1}{h_c} + \frac{RC_2}{h_c} \right) \sin^2 \theta \\
 K_{L_z} &= \left(\frac{d_1}{h_c} + \frac{d_2}{h_c} \right) \sin^2 \theta + \frac{1}{2} \left(\frac{RC_1}{h_c} + \frac{RC_2}{h_c} \right) (\theta - \sin \theta \cos \theta)
 \end{aligned}
 \tag{D21} \text{ Con-cluded}$$

If, in addition to consisting of straight lines and circular arcs, the corrugation is symmetrical (that is, $RC_2 = RC_1$, $b_2 = b_1$, and so on) and the origin of y and z is chosen at the midpoint of the corrugation leg (that is, $k_y = k_z = 1$), then equations (D21) become

$$\begin{aligned}
K_{I_z} &= \frac{2}{3} \left(\frac{k_1}{h_c} \right)^2 \frac{d_1}{h_c} + \frac{2}{3} \left[\frac{1}{8} \left(\frac{p}{h_c} \right)^3 - \left(\frac{b_1}{h_c} \right)^3 \right] + \\
&\quad \left. 2 \frac{R_{C1}}{h_c} \left[\frac{b_1}{h_c} \left[\theta \frac{b_1}{h_c} - 2 \left(\frac{R_{C1}}{h_c} - \frac{e_1}{h_c} \right) \right] + \frac{1}{2} \left[\theta \left(\frac{R_{C1}}{h_c} \right)^2 - \frac{g_1}{h_c} \frac{e_1}{h_c} \right] \right] \right\} \\
K_{I_{yz}} &= \frac{2}{3} \frac{J_1}{h_c} \frac{k_1}{h_c} \frac{d_1}{h_c} + \frac{1}{2} \left[\frac{1}{4} \left(\frac{p}{h_c} \right)^2 - \left(\frac{b_1}{h_c} \right)^2 \right] + \\
&\quad 2 \frac{R_{C1}}{h_c} \left[\frac{a_1}{h_c} \left(\theta \frac{b_1}{h_c} + \frac{e_1}{h_c} - \frac{R_{C1}}{h_c} \right) + \frac{g_1}{h_c} \left(\frac{b_1}{h_c} - \frac{1}{2} \frac{g_1}{h_c} \right) \right] \\
K_{I_y} &= \frac{2}{3} \left(\frac{J_1}{h_c} \right)^2 \frac{d_1}{h_c} + \frac{1}{4} \frac{f_1}{h_c} + \\
&\quad 2 \frac{R_{C1}}{h_c} \left\{ \frac{a_1}{h_c} \left(\theta \frac{a_1}{h_c} + 2 \frac{g_1}{h_c} \right) + \frac{1}{2} \left[\theta \left(\frac{R_{C1}}{h_c} \right)^2 + \frac{g_1}{h_c} \frac{e_1}{h_c} \right] \right\} \\
K_{A_z} &= K_{A_y} = 0 \\
K_L &= 2 \frac{d_1}{h_c} + 2\theta \frac{R_{C1}}{h_c} + \frac{f_1}{h_c} \\
K_{L_y} &= \frac{f_1}{h_c} + 2 \frac{d_1}{h_c} \cos^2 \theta + \frac{R_{C1}}{h_c} (\theta + \sin \theta \cos \theta) \\
K_{L_{yz}} &= 2 \frac{d_1}{h_c} \sin \theta \cos \theta + \frac{R_{C1}}{h_c} \sin^2 \theta \\
K_{L_z} &= 2 \frac{d_1}{h_c} \sin^2 \theta + \frac{R_{C1}}{h_c} (\theta - \sin \theta \cos \theta)
\end{aligned} \tag{D22}$$

The dimensions that have to be inserted in the right-hand sides of equations (D21) and (D22) can be obtained from a few basic dimensions

(p , h_{EC} , R_{i_1} , R_{i_2} , f_1 , f_2 , and t_C) through the following sequence of computations:

$$\begin{aligned}
 h_C &= h_{EC} - t_C \\
 R_{C_1} &= R_{i_1} + \frac{t_C}{2} & R_{C_2} &= R_{i_2} + \frac{t_C}{2} \\
 a_1 &= \left(1 - \frac{k_z}{2}\right) h_C - R_{C_1} & a_2 &= k_z \frac{h_C}{2} - R_{C_2} \\
 b_1 &= \left(1 - \frac{k_y}{2}\right) p - \frac{f_1}{2} & b_2 &= \frac{1}{2} (k_y p - f_2) \\
 c_1 &= \left(a_1^2 + b_1^2\right)^{1/2} & c_2 &= \left(a_2^2 + b_2^2\right)^{1/2} \\
 \alpha_1 &= \arctan \frac{a_1}{b_1} & \alpha_2 &= \arctan \frac{a_2}{b_2} \\
 \beta_1 &= \arcsin \frac{R_{C_1}}{c_1} & \beta_2 &= \arcsin \frac{R_{C_2}}{c_2} \\
 d_1 &= \left(c_1^2 - R_{C_1}^2\right)^{1/2} & d_2 &= \left(c_2^2 - R_{C_2}^2\right)^{1/2} \\
 \theta &= \alpha_1 + \beta_1 = \alpha_2 + \beta_2 \\
 e_1 &= R_{C_1} \cos \theta & e_2 &= R_{C_2} \cos \theta \\
 g_1 &= R_{C_1} \sin \theta & g_2 &= R_{C_2} \sin \theta \\
 j_1 &= a_1 + e_1 & j_2 &= a_2 + e_2 \\
 k_1 &= b_1 - g_1 & k_2 &= b_2 - g_2
 \end{aligned} \tag{D23}$$

These dimensions required in equations (D21) and (D22) can also be obtained from a different set of basic dimensions (p , h_{EC} , R_{i1} , R_{i2} , θ , and t_C) through the following sequence of computations:

$$\begin{array}{rcl}
 & h_C = h_{EC} - t_C & \\
 R_{C1} = R_{i1} + \frac{t_C}{2} & & R_{C2} = R_{i2} + \frac{t_C}{2} \\
 a_1 = \left(1 - \frac{k_z}{2}\right)h_C - R_{C1} & & a_2 = k_z \frac{h_C}{2} - R_{C2} \\
 e_1 = R_{C1} \cos \theta & & e_2 = R_{C2} \cos \theta \\
 g_1 = R_{C1} \sin \theta & & g_2 = R_{C2} \sin \theta \\
 j_1 = a_1 + e_1 & & j_2 = a_2 + e_2 \\
 k_1 = j_1 \cot \theta & & k_2 = j_2 \cot \theta \\
 d_1 = j_1 \csc \theta & & d_2 = j_2 \csc \theta \\
 b_1 = k_1 + g_1 & & b_2 = k_2 + g_2 \\
 f_1 = 2 \left[\left(1 - \frac{k_y}{2}\right)p - b_1 \right] & & f_2 = 2 \left(\frac{k_y}{2} p - b_2 \right)
 \end{array} \quad (D24)$$

APPENDIX E

DERIVATION OF FORMULA FOR D_{Q_x}

In the derivation of the transverse shear stiffness D_{Q_x} , an element of corrugated-core sandwich plate of length dx and width $2p$ under a transverse shear V is considered. (See following fig.)

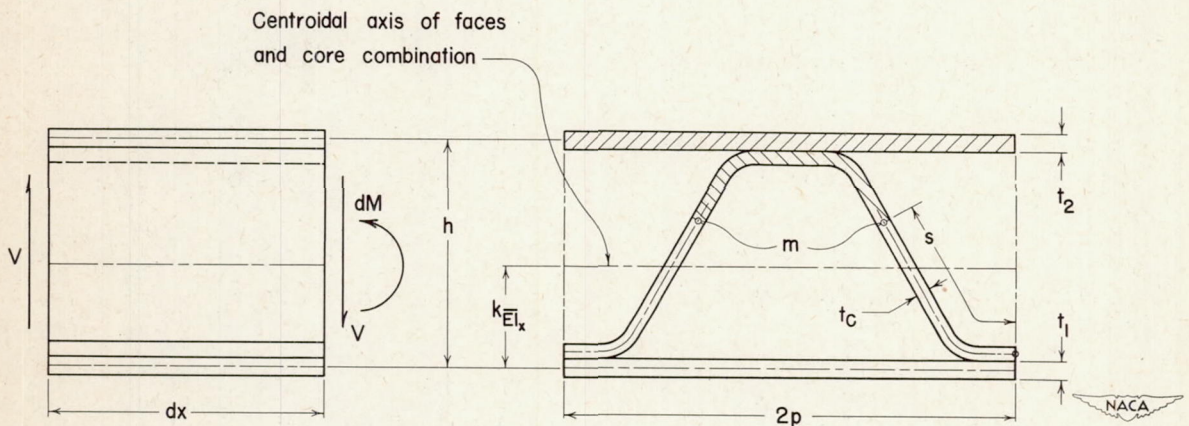


Figure E1

The transverse shear is equilibrated by a change in bending moment dM from one end of the element to the other. From the equation relating the distortions of this element to the shear V , a general formula for D_{Q_x} is obtained. A more practicable approximate formula is then obtained by assuming that the core carries no direct stress.

General derivation.- The direct stresses produced in the element by the bending moment dM are assumed to vary linearly through the thickness. Assuming the only flexibility to be that of the corrugation in shear gives the following picture of the relative distortions of the element:

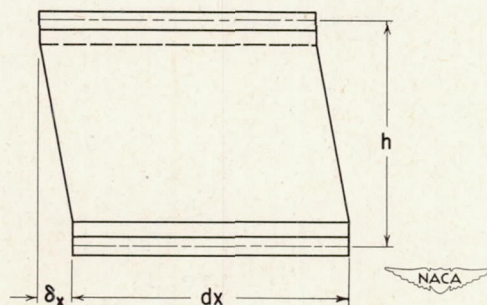


Figure E2

The angle $\frac{\delta_x}{h}$ is taken as an average shear strain γ_x for the cross section, and the transverse shear stiffness D_{Q_x} is then given by

$$D_{Q_x} = \frac{Q_x}{\gamma_x} = \frac{V/2p}{\delta_x/h} \quad (E1)$$

An expression is now derived for δ_x as a linear function of V for substitution in equation (E1).

Elementary considerations give the shear stress in the corrugation at a point such as m (see fig. E1) as

$$\tau_C = \frac{VQ}{2It_C} \quad (E2)$$

where

Q static moment of cross-hatched area about neutral axis, inches³

I moment of inertia of cross section of width $2p$ about centroidal axis, inches⁴

(If faces and core are not all of the same material, a transformed cross section should be used in calculating Q and I .) The shear strain in the corrugation sheet is

$$\begin{aligned} \gamma_C &= \frac{\tau_C}{G_C} \\ &= \frac{VQ}{2G_C It_C} \end{aligned} \quad (E3)$$

Integration of γ_C along one corrugation-leg center line (see the following fig.)

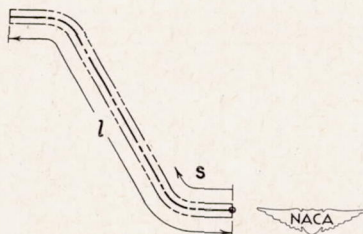


Figure E3

gives the relative displacement δ_x of one face with respect to the other, or

$$\begin{aligned}\delta_x &= \int_0^l \gamma_x \, ds \\ &= \frac{V}{2G_C I t_C} \int_0^l Q \, ds\end{aligned}\quad (E4)$$

Substitution of expression (E4) in (E1) gives the following general expression for D_{Q_x} :

$$D_{Q_x} = \frac{G_C I t_C h}{p \int_0^l Q \, ds}\quad (E5)$$

Approximation.- If, as is usual, the corrugation carries only a small portion of the bending moment M , then an accurate approximation to D_{Q_x} may be obtained by assuming that the entire bending moment is resisted by the faces and, therefore, that the corrugation carries no normal stress. The resulting formula for D_{Q_x} will be the same as equation (E5) but with the effect of the corrugation omitted in calculating I , $\int_0^l Q \, ds$, and the centroidal-axis location $(k_{\overline{EI}_x} h)$; that is,

$$I \approx 2pt_1(k_{\overline{EI}_x} h)^2 + \frac{E_2}{E_1}(2p)t_2(1 - k_{\overline{EI}_x})^2 h^2\quad (E6)$$

$$\int_0^l Q \, ds \approx \left[\frac{E_2}{E_1}(2p)t_2(1 - k_{\overline{EI}_x})h \right] l\quad (E7a)$$

or

$$\int_0^l Q \, ds \approx 2pt_1 k_{\overline{EI}_x} h l\quad (E7b)$$

$$k_{EI_x} \approx \frac{\frac{E_2}{E_1} t_2}{t_1 + \frac{E_2}{E_1} t_2} \quad (E8)$$

Substitution of the approximate expressions (E6), (E7), and (E8) in equation (E5) gives the following approximation to D_{Q_x} :

$$D_{Q_x} \approx \frac{G_C t_C h^2}{p l} = \frac{G_C t_C^2}{\bar{A}_C} \left(\frac{h}{p} \right)^2 \quad (E9)$$

where the corrugation cross-sectional area per unit width $\bar{A}_C = \frac{t_C}{p}$.

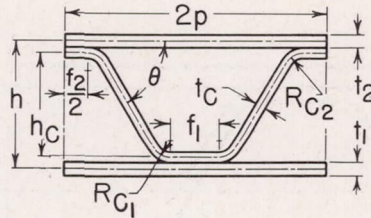
REFERENCES

1. Shanley, F. R.: Cardboard-Box Wing Structures. Jour. Aero. Sci., vol. 14, no. 12, Dec. 1947, pp. 713-715.
2. Libove, Charles, and Batdorf, S. B.: A General Small-Deflection Theory for Flat Sandwich Plates. NACA Rep. 899, 1948.
3. Stein, Manuel, and Mayers, J.: A Small-Deflection Theory for Curved Sandwich Plates. NACA TN 2017, 1950.
4. Heilbron, C. H., and Foster, H.: Chordwise Shear Theory, Double-Skin Construction. Rep. No. 2326, Lockheed Aircraft Corp., Sept. 4, 1941.
5. Kennedy, W. B., Jr., and Troxell, W. W.: Study of Compression Panel, Supported on Four Edges, Formed of Corrugated Sheet with Flat Skin on Both Sides. NACA ARR 5B03, 1945.
6. Timoshenko, S.: Strength of Materials. Part I - Elementary Theory and Problems. Second ed., D. Van Nostrand Co., Inc., 1940, pp. 269-270.

TABLE I.- RESULTS OF NUMERICAL SURVEY OF ACCURACY OF APPROXIMATE FORMULAS FOR D_y , E_y ,

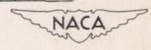
D_{xy} , AND D_{Q_x} . ($k_{II} = k_{EI_y}$)

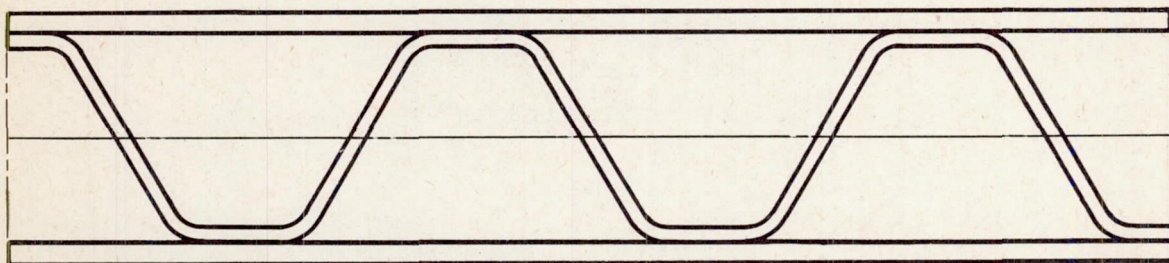
$[E_1 = E_2 = E_C; G_1 = G_2 = G_C; \mu_1 = \mu_2 = \frac{1}{3}; f_1 = f_2; \text{ and } R_{C1} = R_{C2} = 0.18h_C]$



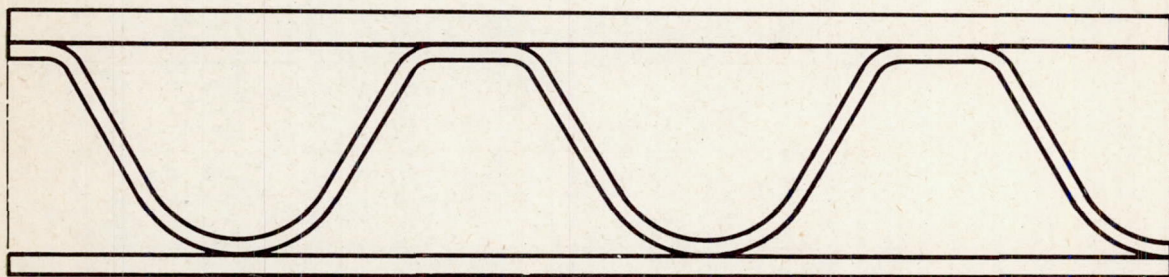
Ratio		$\frac{D_{y,approx}}{D_y}$				$\frac{E_{y,approx}}{E_y}$				$\frac{(D_{Q_x})_{approx}}{D_{Q_x}}$				$\frac{(D_{xy})_{approx}}{D_{xy}}$				
		60		90		60		90		60		90		60		90		
		$\frac{h_C}{t_C}$	$\frac{p}{h_C}$	$\frac{h_C}{t_C}$	$\frac{p}{h_C}$	$\frac{h_C}{t_C}$	$\frac{p}{h_C}$	$\frac{h_C}{t_C}$	$\frac{p}{h_C}$	$\frac{h_C}{t_C}$	$\frac{p}{h_C}$	$\frac{h_C}{t_C}$	$\frac{p}{h_C}$	$\frac{h_C}{t_C}$	$\frac{p}{h_C}$	$\frac{h_C}{t_C}$	$\frac{p}{h_C}$	
1.00	10	0.30	0.99	0.99	0.99	0.99	0.98	0.98	0.97	0.98	1.01	1.00	1.01	1.00	1	1	1	1
		1.00	.98	.97	.97	.97	.95	.95	.94	.95	1.01	.97	.97	.94	1	1	1	1
		1.25	.97	.97	.96	.96	.94	.95	.94	.94	1.01	.96	.96	.93	1	1	1	1
	25	.30	.99	.99	.99	.99	.98	.98	.97	.98	1.00	.99	.98	.98	1	1	1	1
		1.00	.97	.97	.96	.96	.95	.95	.94	.95	.99	.95	.93	.91	1	1	1	1
		1.25	.97	.96	.96	.96	.94	.95	.94	.94	.99	.93	.92	.89	1	1	1	1
	40	.30	.99	.99	.99	.99	.98	.98	.97	.98	1.00	.98	.98	.97	1	1	1	1
		1.00	.97	.97	.96	.96	.95	.95	.94	.95	.98	.94	.92	.90	1	1	1	1
		1.25	.97	.96	.95	.96	.94	.95	.94	.94	.98	.93	.91	.88	1	1	1	1
.80	10	.30	.99	.99	.99	.99	.98	.98	.97	.98	1.01	1.00	1.01	.99	1.00	1.00	1.00	1.00
		1.00	.97	.97	.96	.97	.95	.95	.94	.95	1.01	.97	.96	.94	1.00	1.00	1.00	1.00
		1.25	.97	.97	.96	.96	.94	.95	.93	.94	1.01	.96	.95	.92	1.00	1.00	1.00	1.00
	25	.30	.99	.99	.98	.99	.98	.98	.97	.98	1.00	.99	.98	.97	1.00	1.00	1.00	1.00
		1.00	.97	.97	.96	.96	.95	.95	.94	.95	.99	.94	.93	.90	1.00	1.00	1.00	1.00
		1.25	.97	.96	.95	.95	.94	.95	.93	.94	.99	.93	.91	.88	1.00	1.00	1.00	1.00
	40	.30	.99	.99	.98	.98	.98	.98	.97	.98	1.00	.98	.97	.96	1.00	1.00	1.00	1.00
		1.00	.97	.97	.96	.96	.95	.95	.94	.95	.98	.93	.91	.89	1.00	1.00	1.00	1.00
		1.25	.96	.96	.95	.95	.94	.95	.93	.94	.98	.92	.90	.87	1.00	1.00	1.00	1.00
.50	10	.30	.99	.99	.98	.98	.97	.98	.97	.97	1.01	.99	.99	.98	.98	.98	.98	.98
		1.00	.96	.96	.95	.96	.94	.95	.94	.95	1.01	.96	.94	.92	.96	.96	.96	.96
		1.25	.96	.96	.95	.95	.94	.94	.93	.94	1.01	.95	.94	.90	.96	.95	.96	.95
	25	.30	.98	.98	.98	.98	.97	.98	.97	.97	1.00	.98	.97	.96	.98	.98	.99	.98
		1.00	.96	.96	.95	.95	.94	.94	.94	.94	.98	.93	.91	.88	.96	.96	.96	.96
		1.25	.96	.95	.94	.94	.94	.94	.93	.94	.98	.91	.90	.87	.96	.95	.96	.96
	40	.30	.98	.98	.98	.98	.97	.98	.97	.97	.99	.97	.96	.95	.98	.98	.99	.98
		1.00	.96	.96	.95	.95	.94	.95	.94	.94	.98	.92	.90	.87	.96	.96	.97	.96
		1.25	.95	.95	.94	.94	.94	.94	.93	.94	.97	.91	.89	.86	.96	.95	.96	.96

^aApproximate and exact values are identical for a symmetrical sandwich ($\frac{t_1}{t_2} = 1.00$).



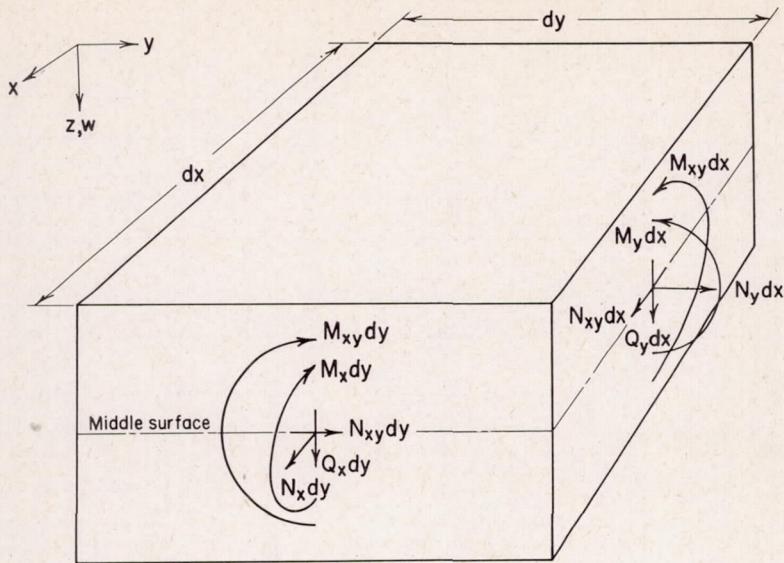


(a) Symmetrical.

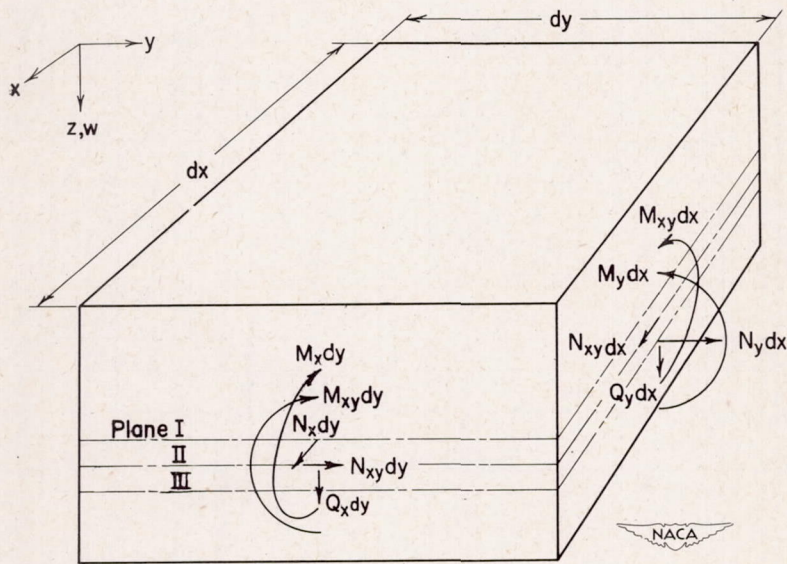


(b) Unsymmetrical.

Figure 1.- Two types of corrugated-core sandwich plate.

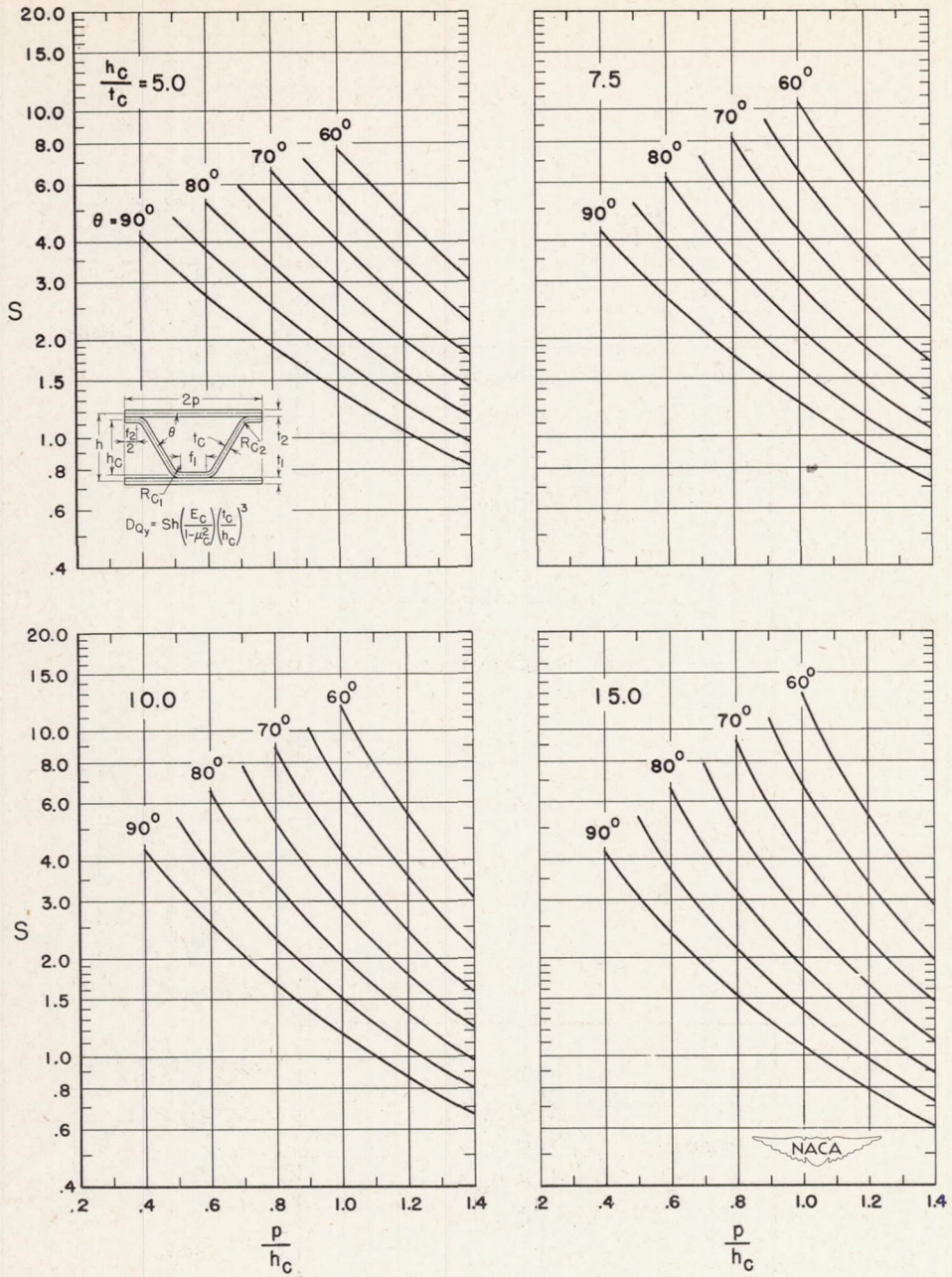


(a) Symmetrical loading.



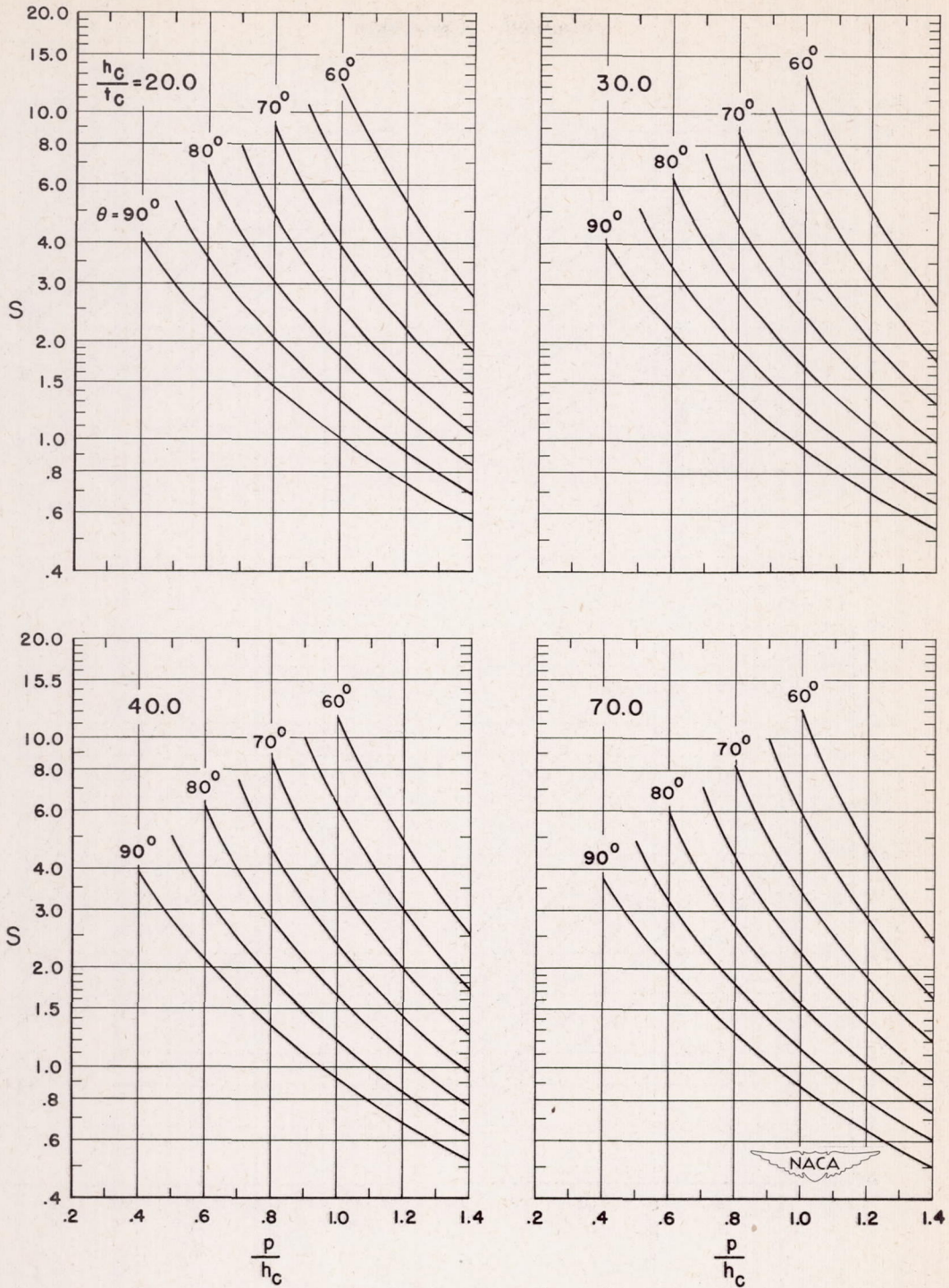
(b) General loading.

Figure 2.- Forces and moments acting on infinitesimal sandwich-plate element.



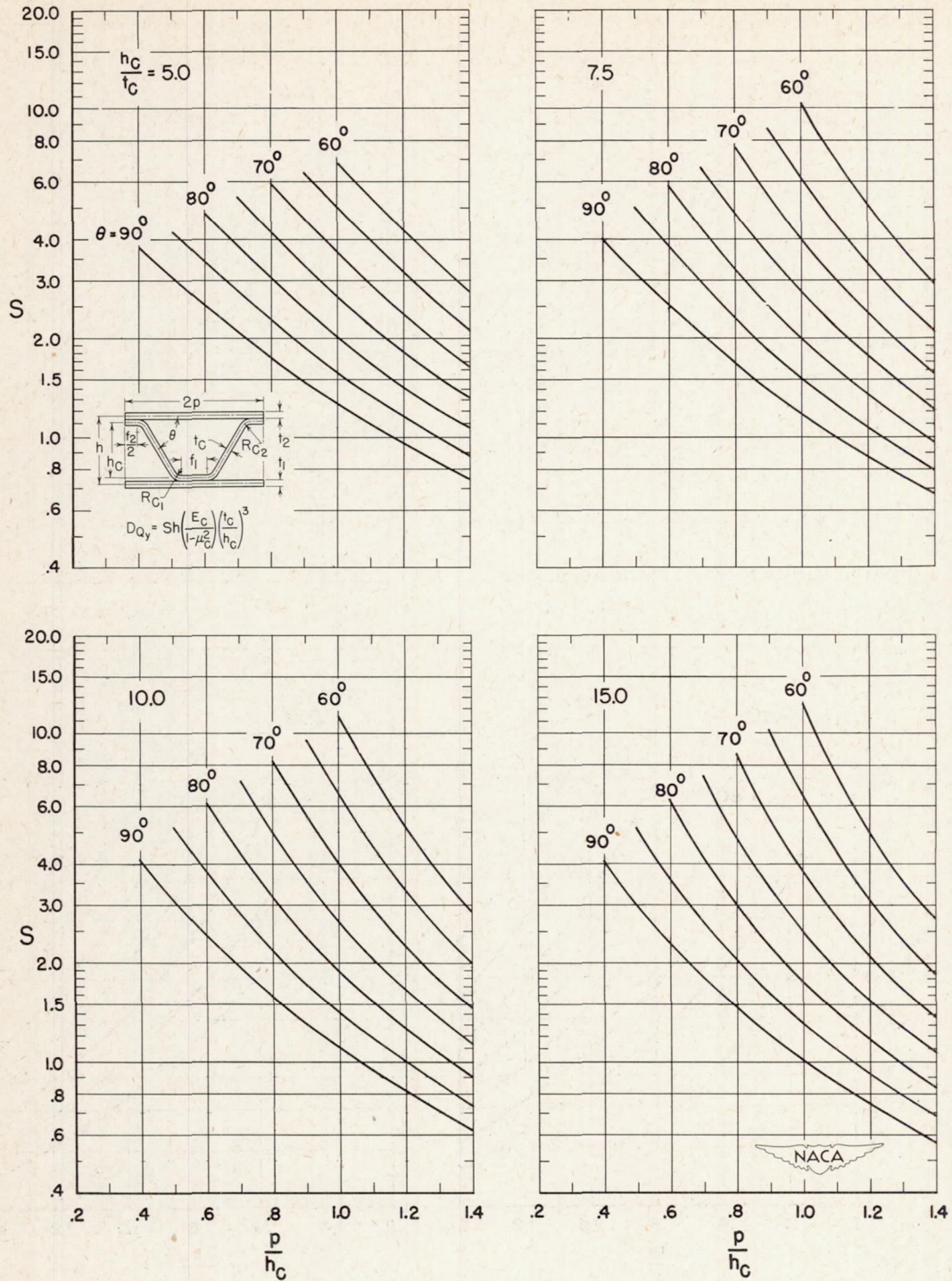
(a) $\frac{t_c}{t_1} = 0.30$.

Figure 3.- Charts for evaluating coefficient S in formula for D_{Qy} for homogeneous symmetrical sandwich with corrugation cross section composed of straight lines and circular arcs ($E_2 = E_C = E_1$; $\mu_2 = \mu_C = \mu_1$; $t_2 = t_1$; $f_2 = f_1$; $R_{C2} = R_{C1} = 0.18h_c$).



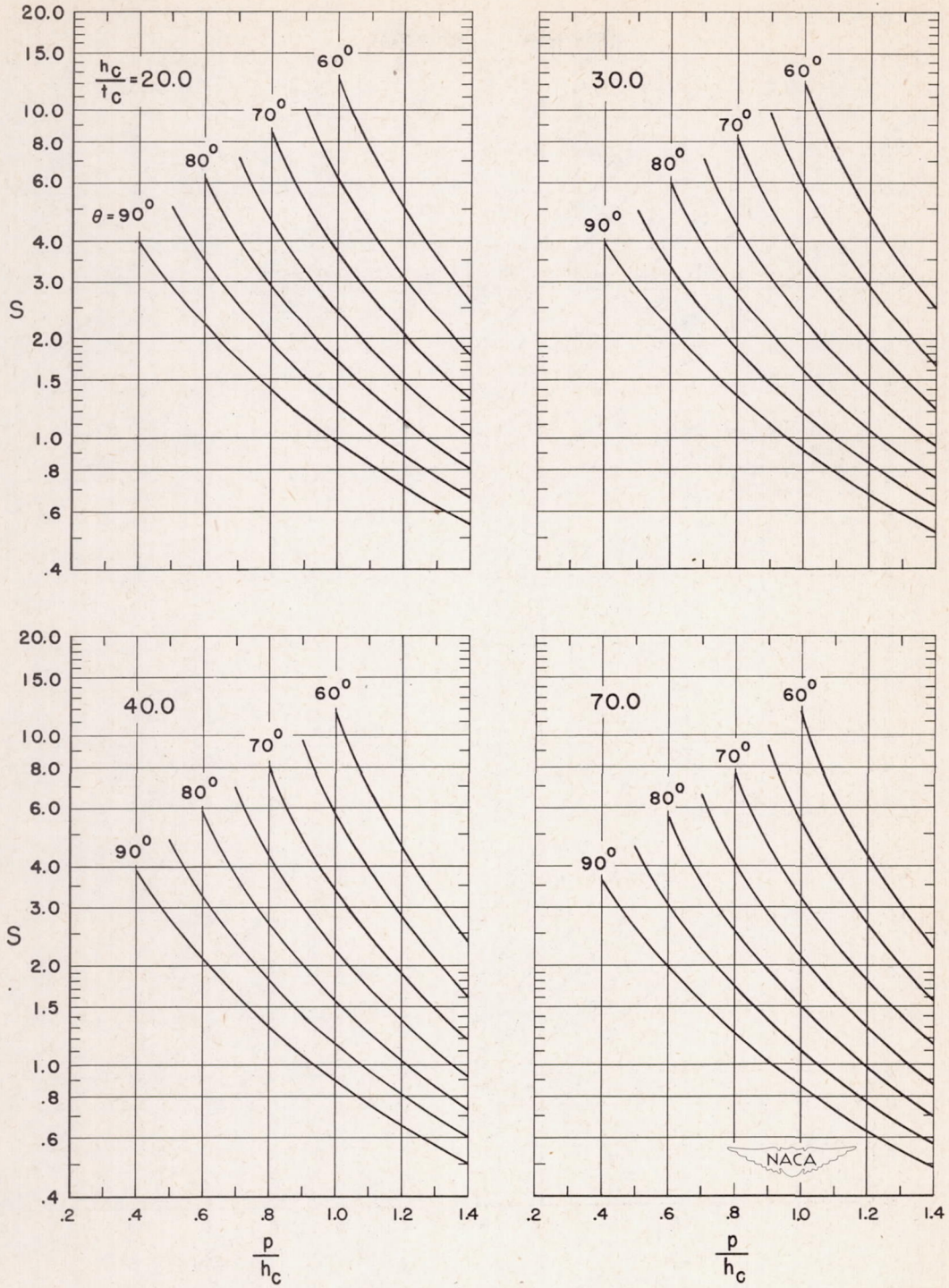
(a) Concluded.

Figure 3.- Continued.



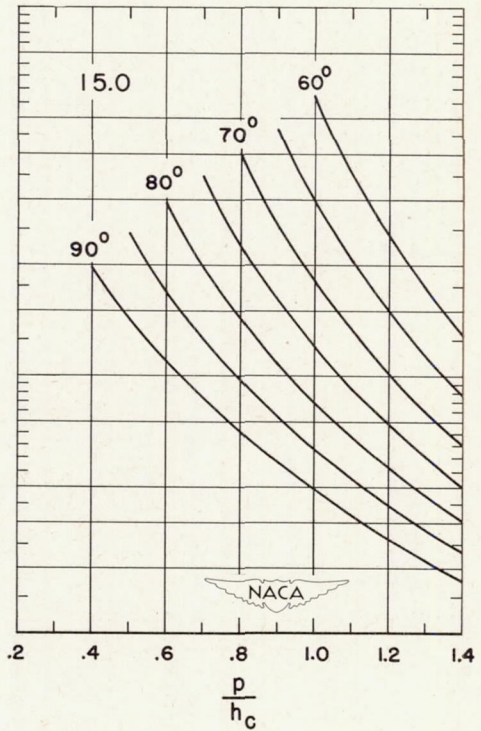
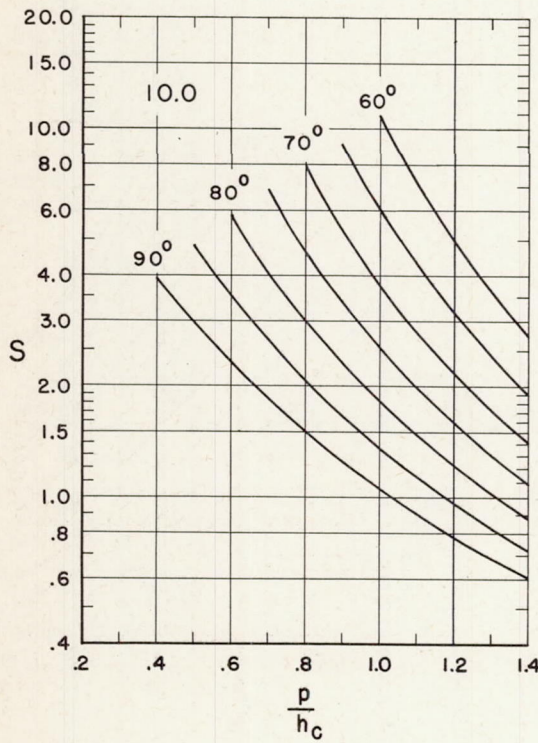
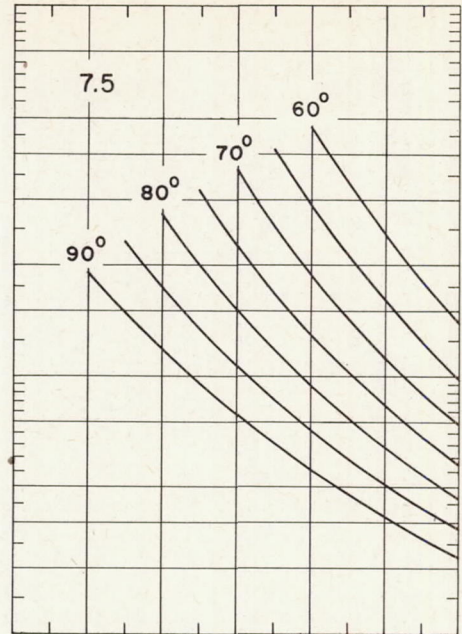
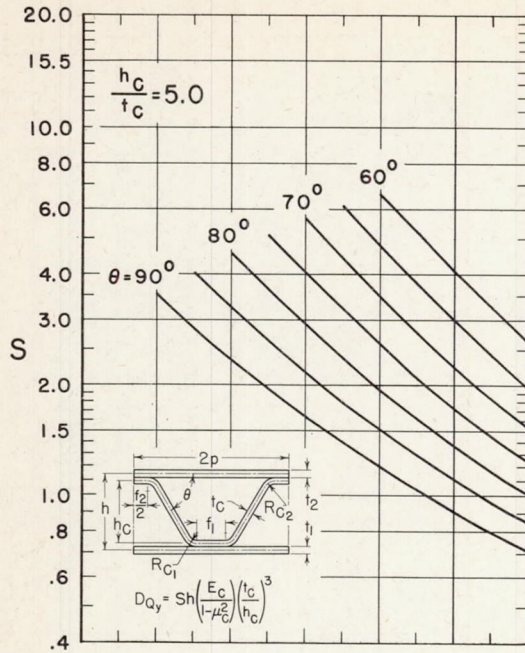
(b) $\frac{t_c}{t_1} = 0.40$.

Figure 3.- Continued.



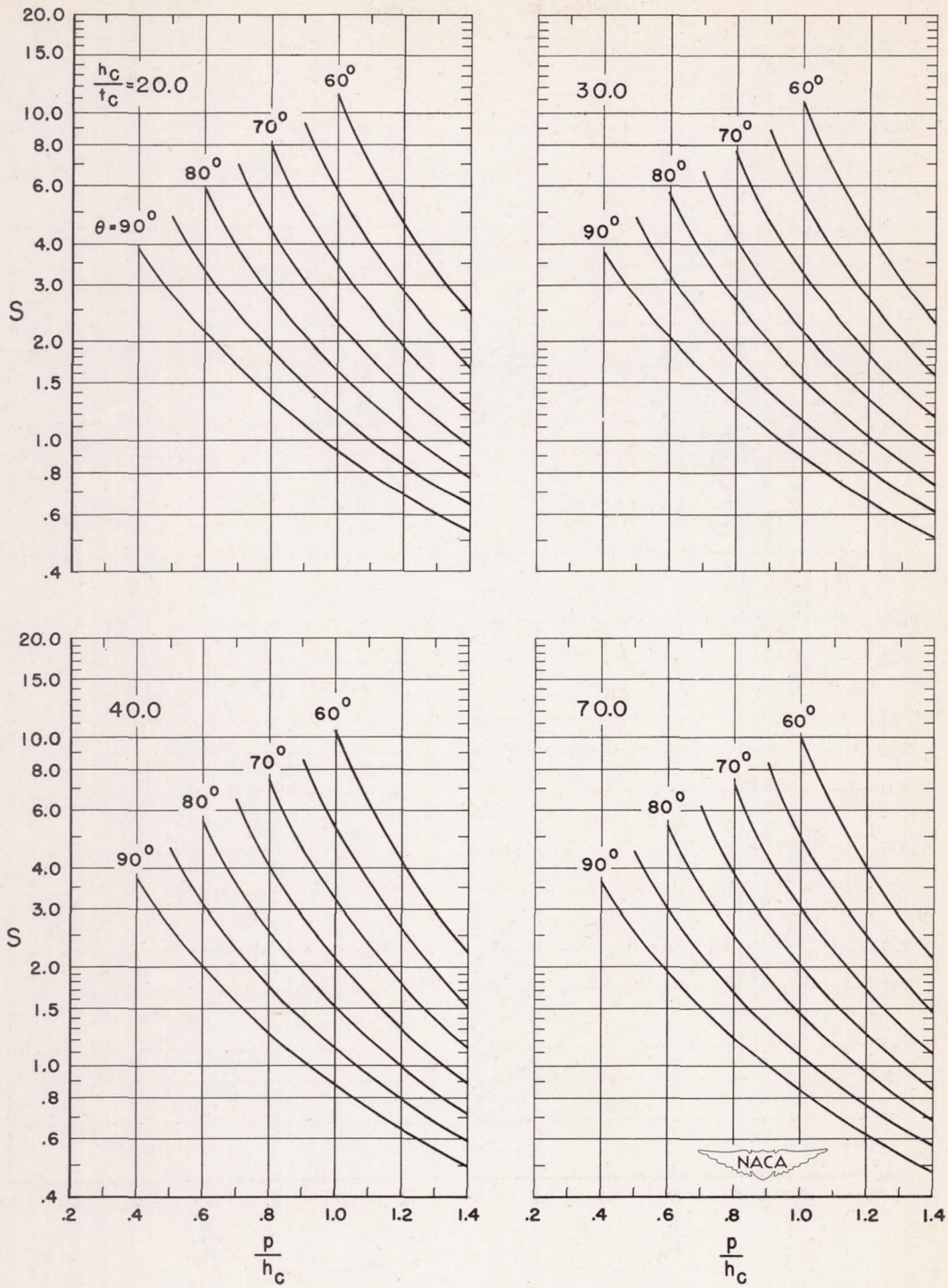
(b) Concluded.

Figure 3.- Continued.



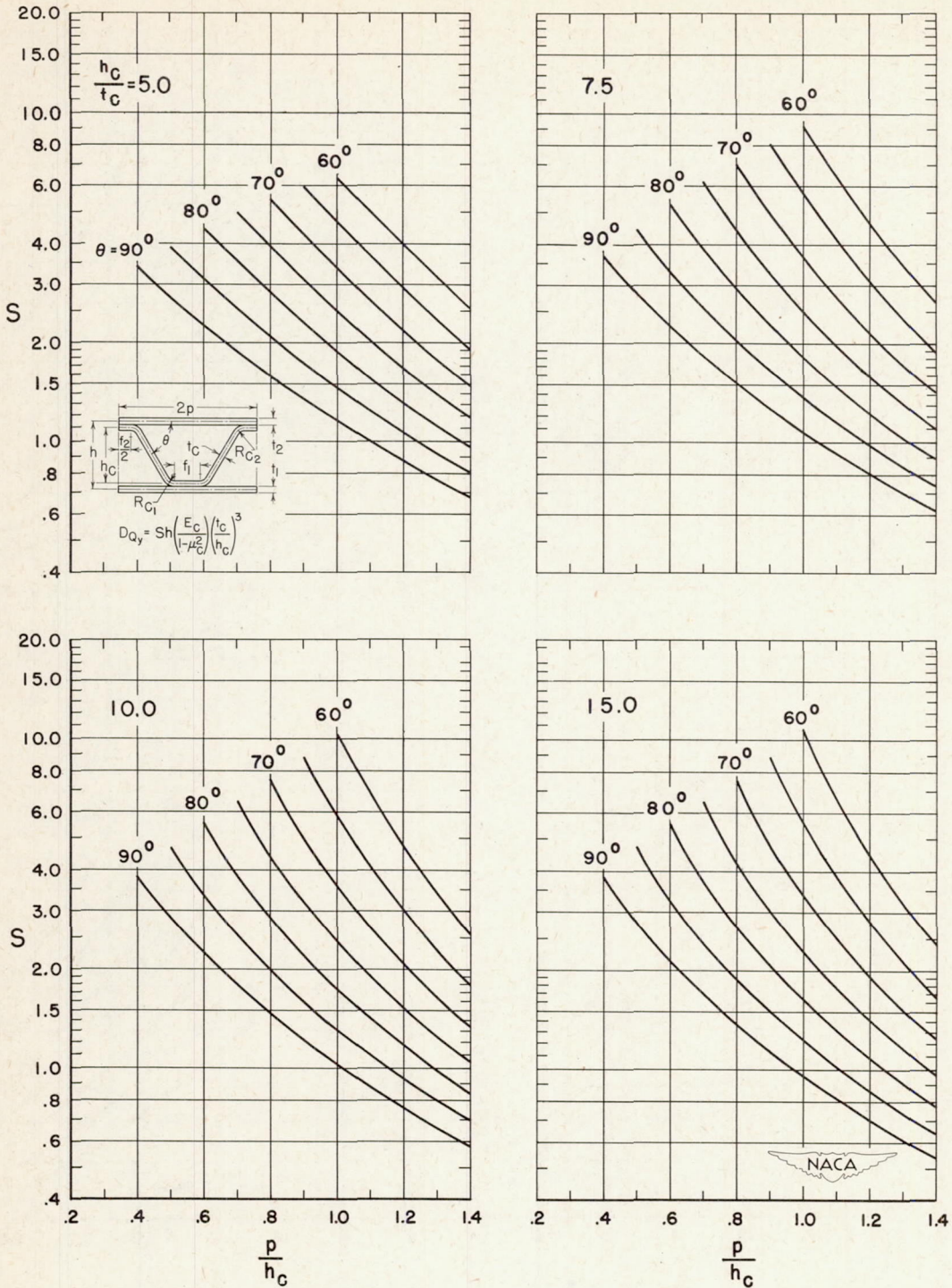
(c) $\frac{t_c}{t_1} = 0.50.$

Figure 3.- Continued.



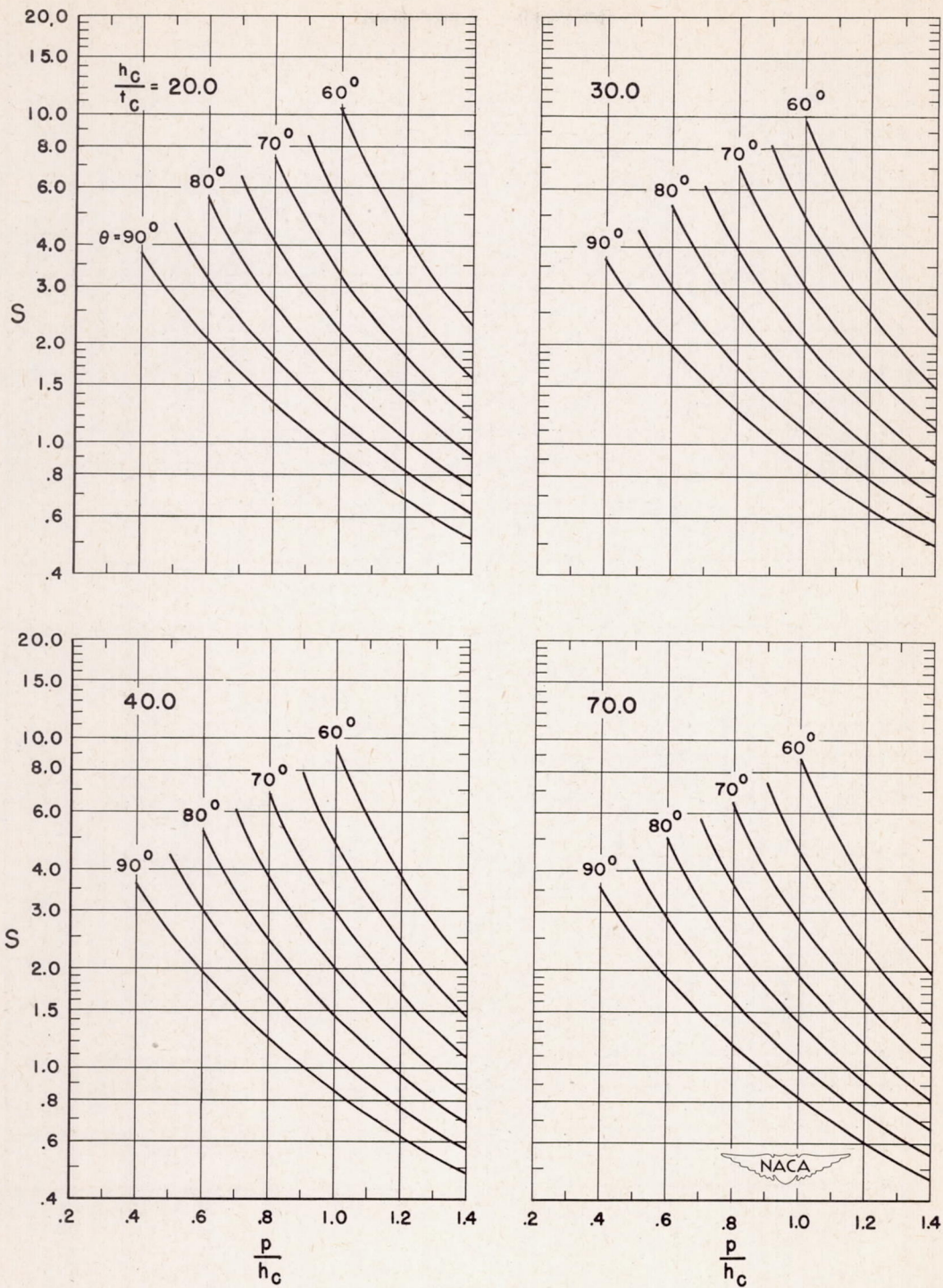
(c) Concluded.

Figure 3.- Continued.



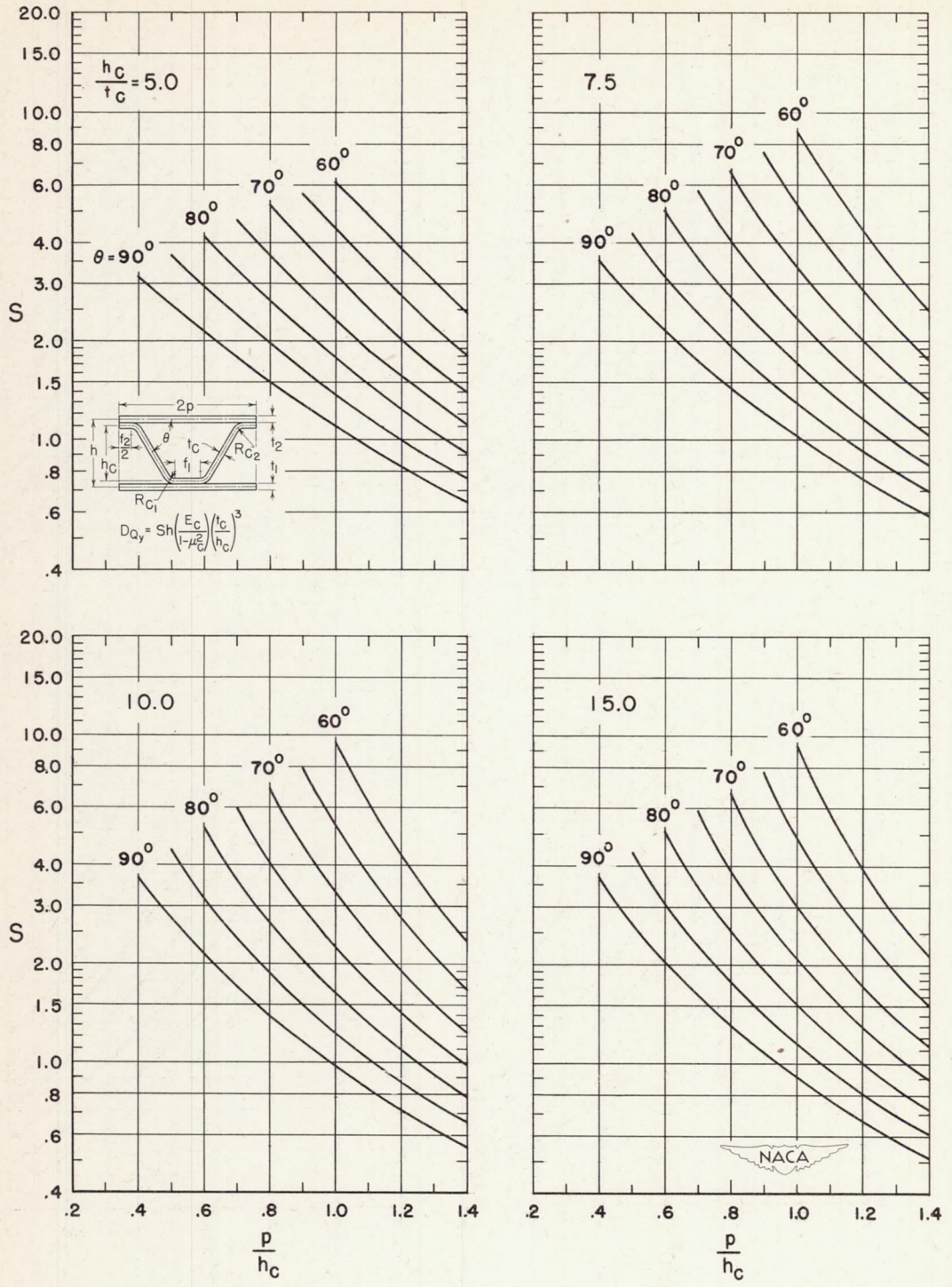
(d) $\frac{t_c}{t_1} = 0.60.$

Figure 3.- Continued.



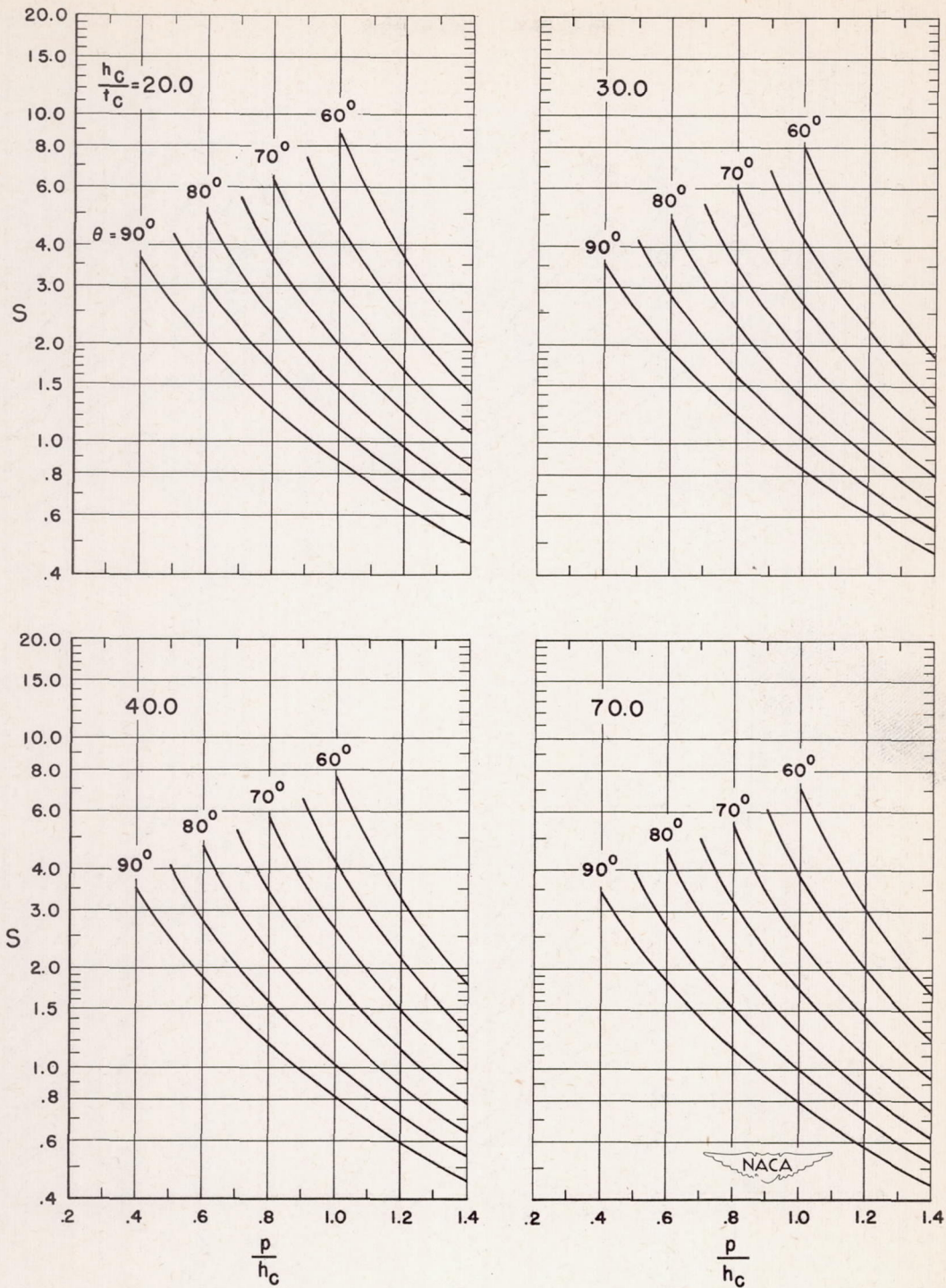
(d) Concluded.

Figure 3.- Continued.



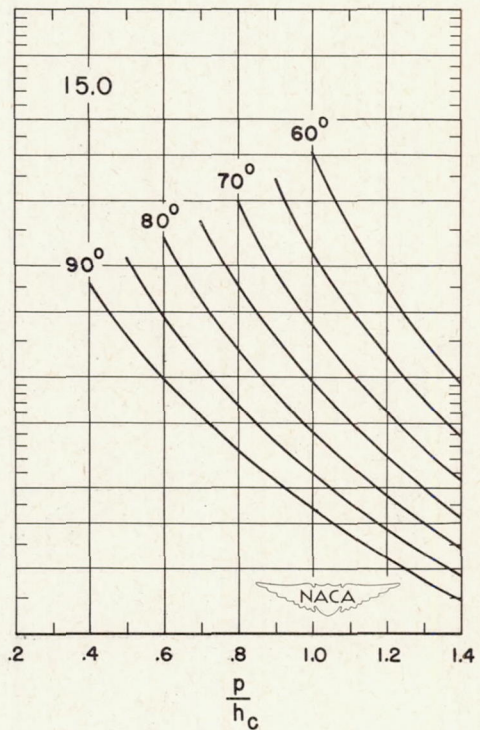
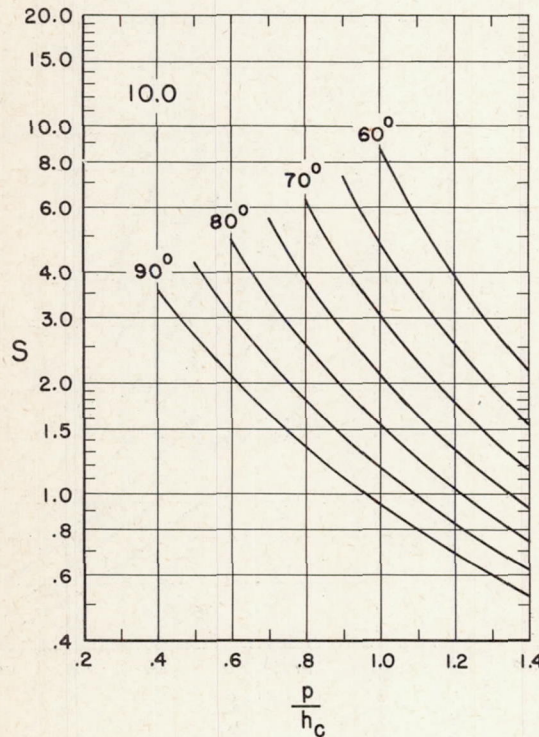
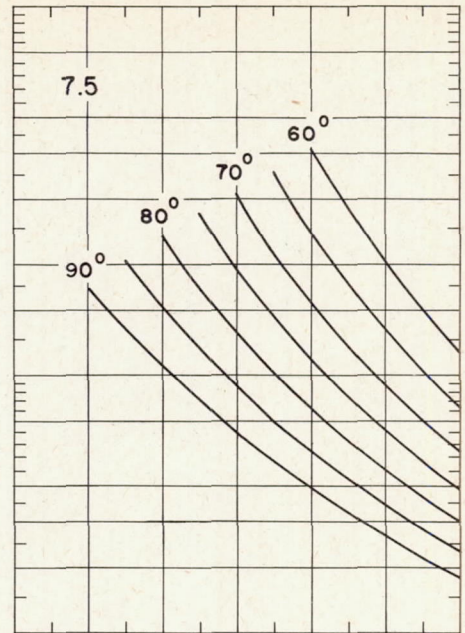
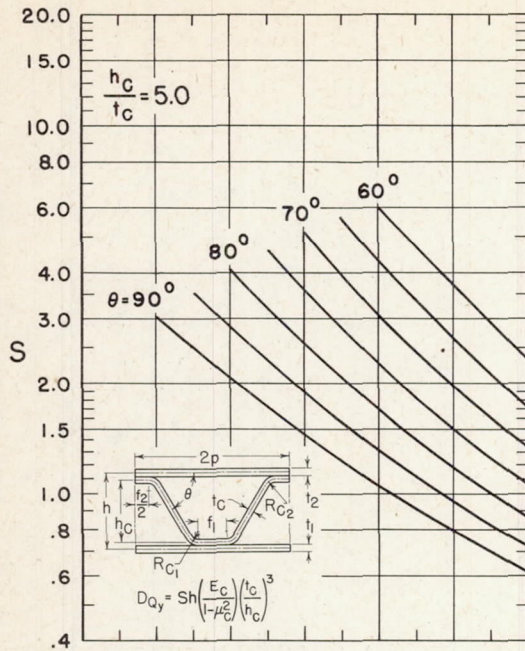
(e) $\frac{t_c}{t_1} = 0.80.$

Figure 3.- Continued.



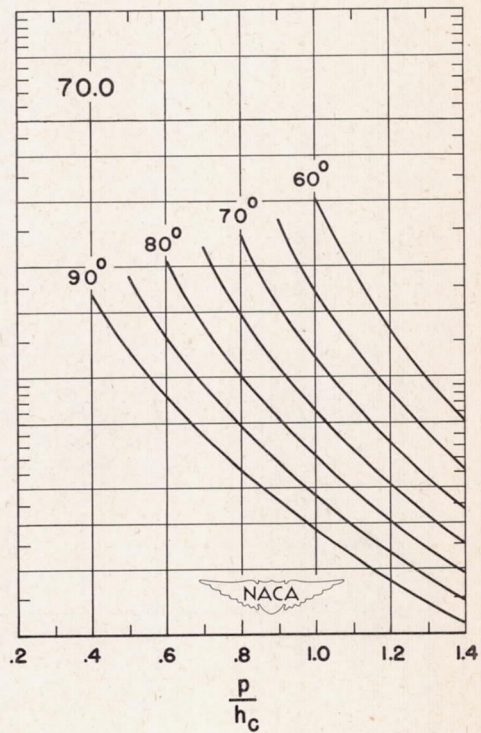
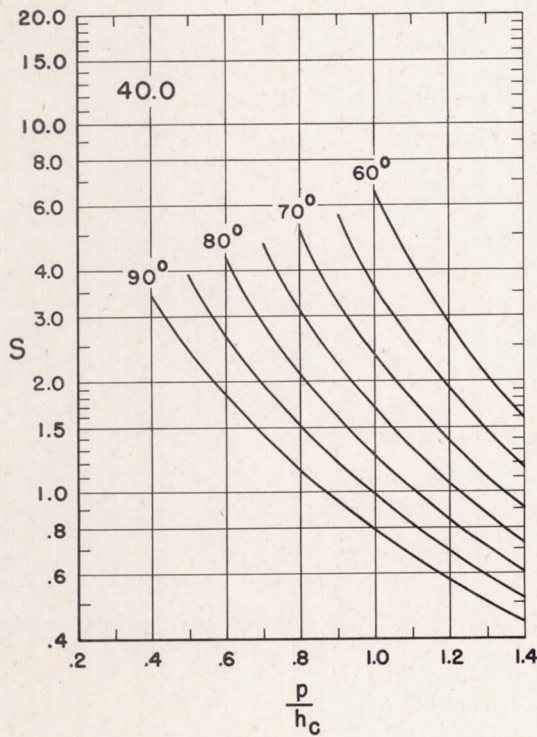
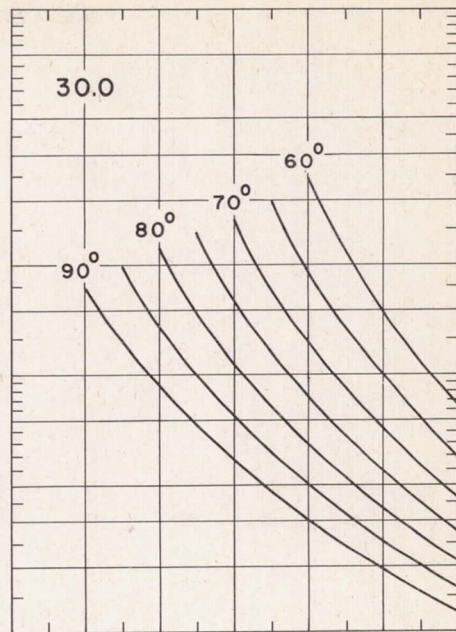
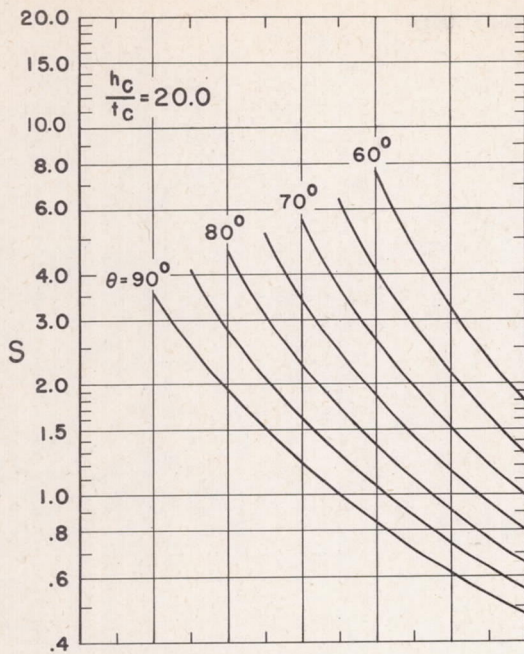
(e) Concluded.

Figure 3.- Continued.



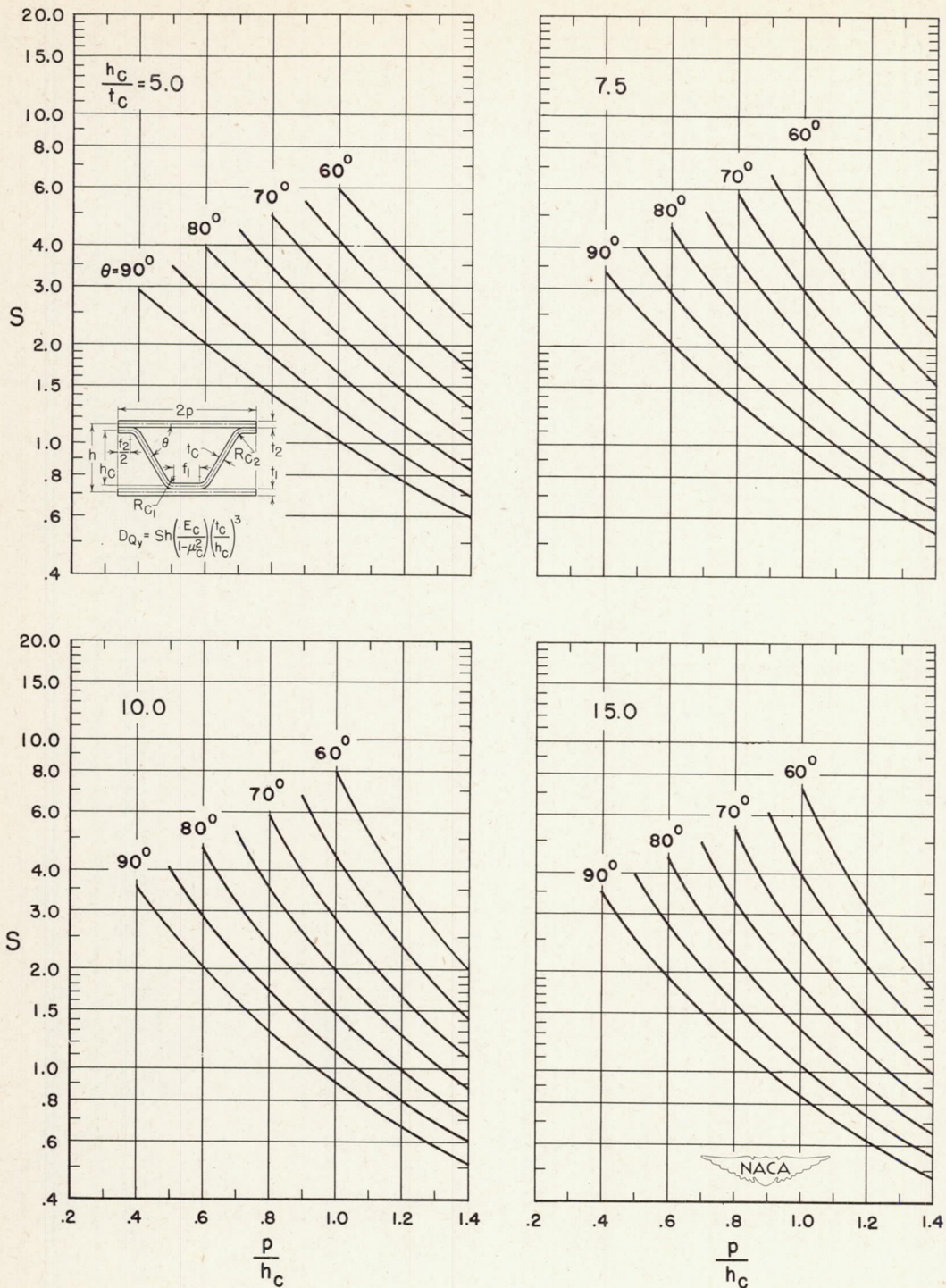
(f) $\frac{t_c}{t_1} = 1.00.$

Figure 3.- Continued.



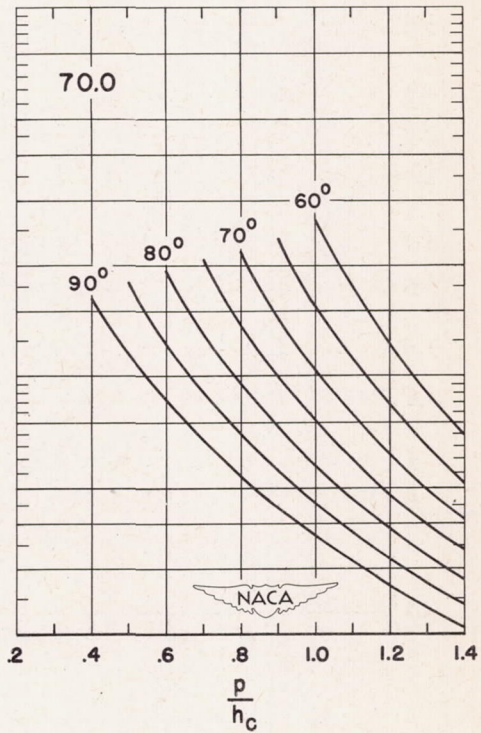
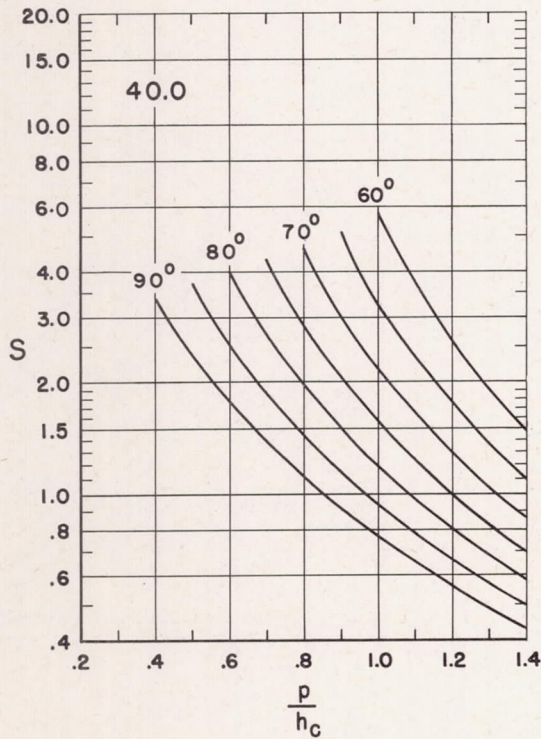
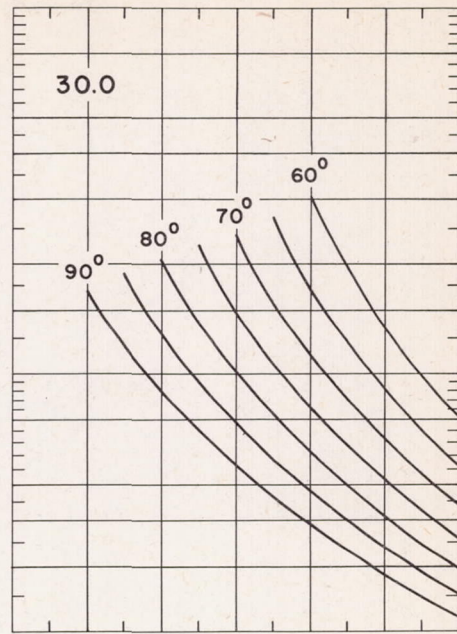
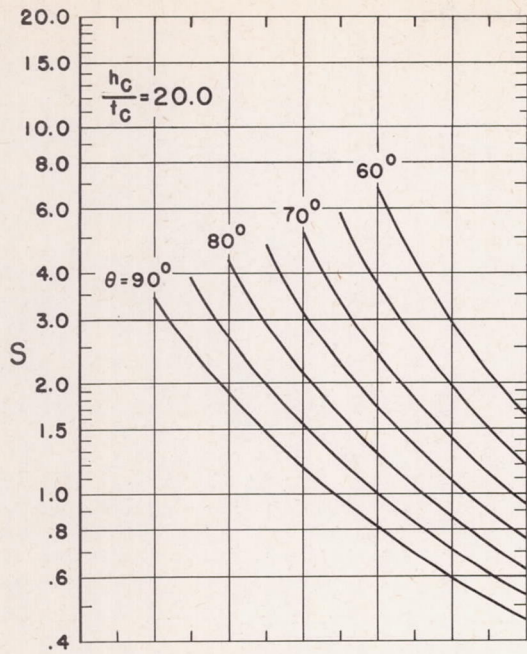
(f) Concluded.

Figure 3.- Continued.



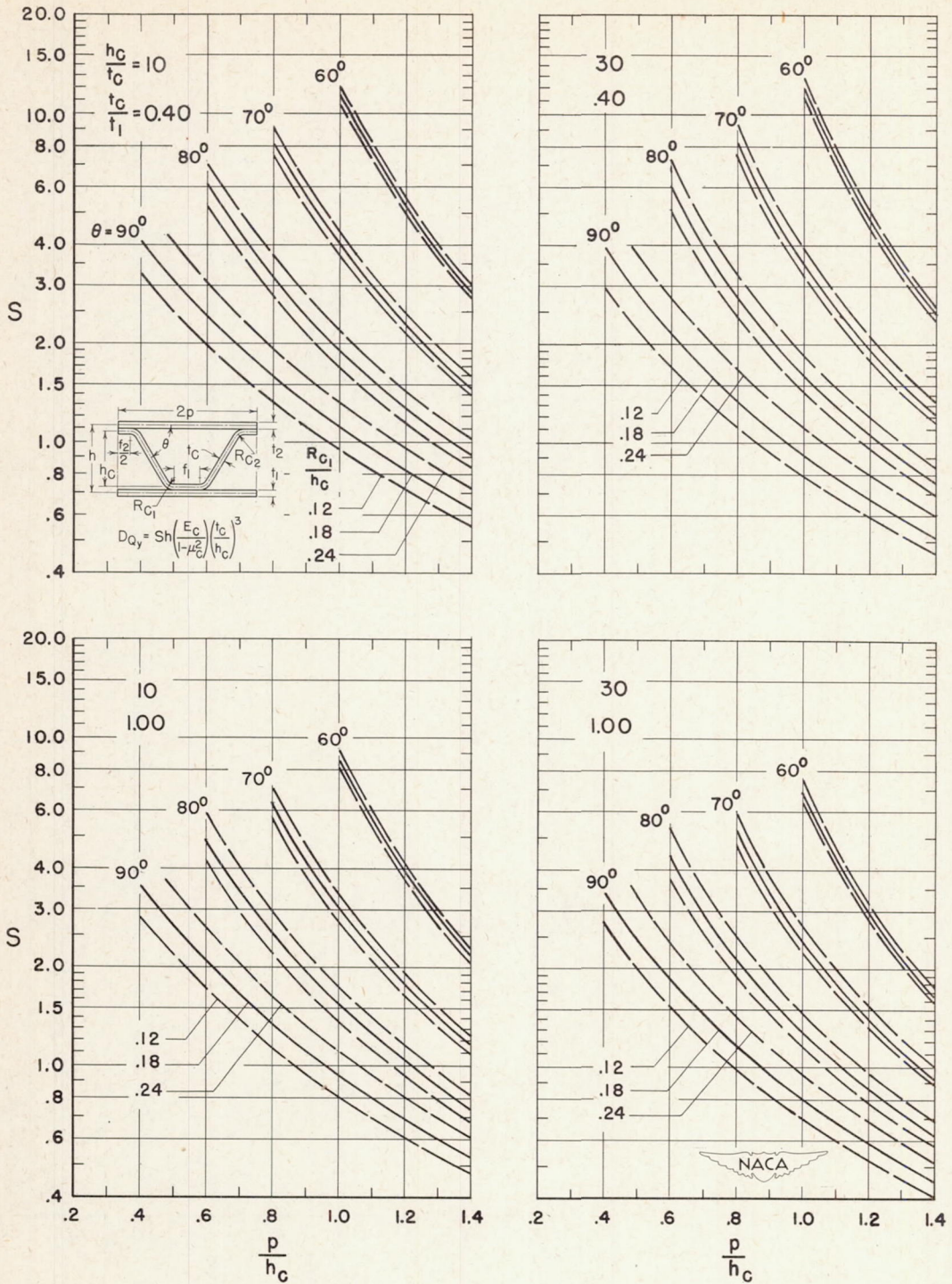
(g) $\frac{t_c}{t_1} = 1.25.$

Figure 3.- Continued.



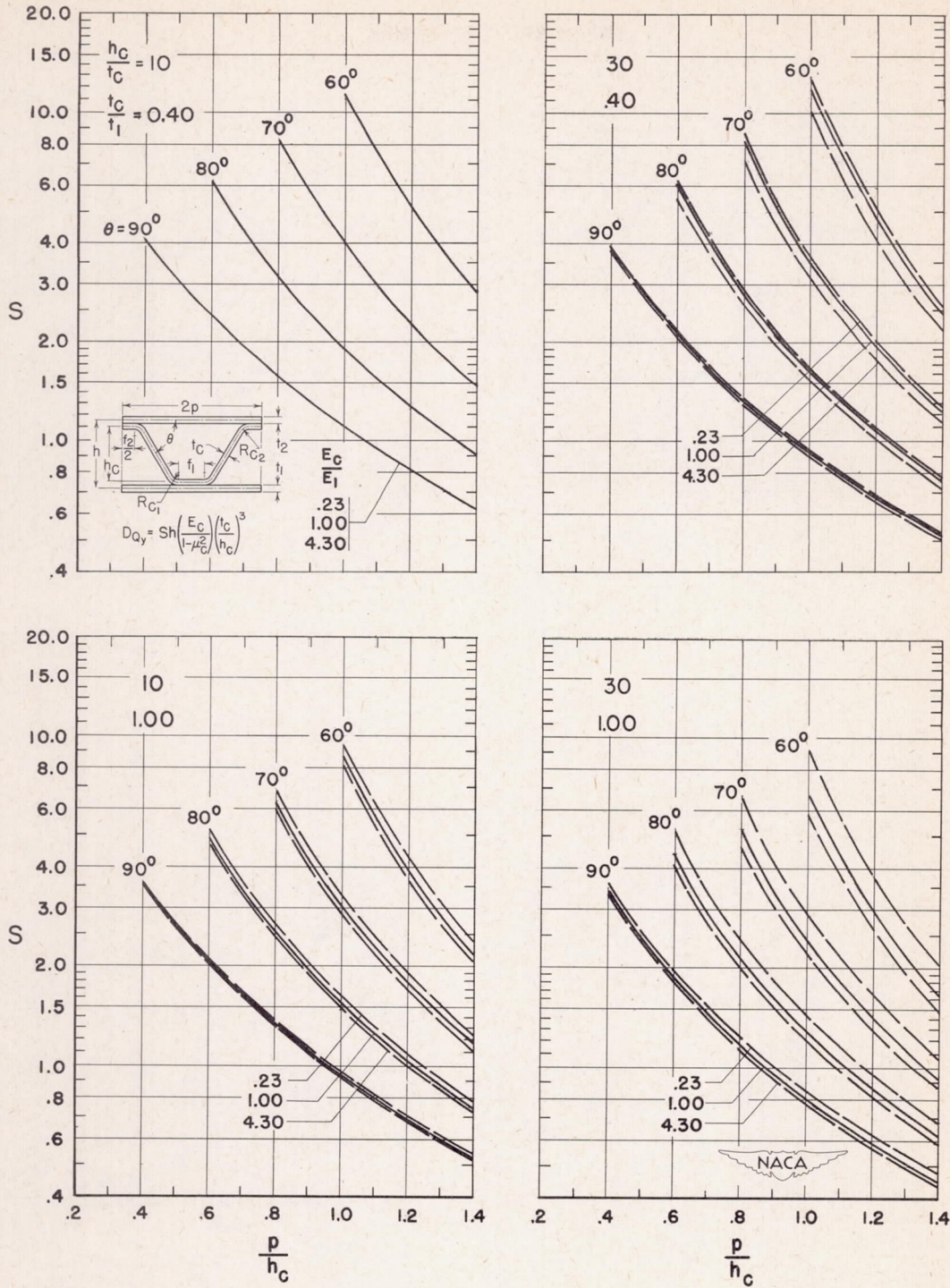
(g) Concluded.

Figure 3.- Concluded.



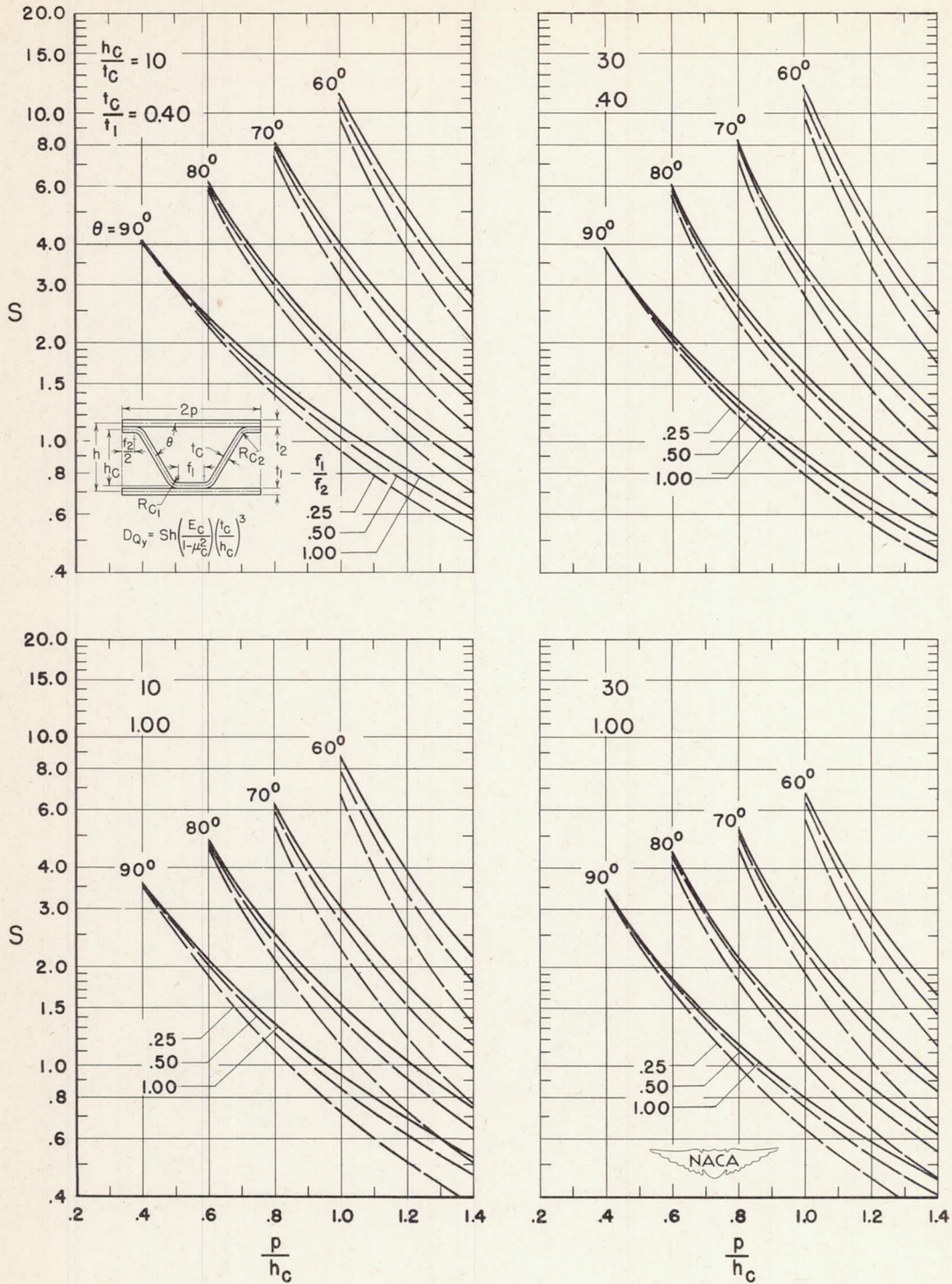
(a) $R_{C1} = R_{C2} \neq 0.18h_c$.

Figure 4.- Charts showing effects on S of four departures from the conditions of figure 3.



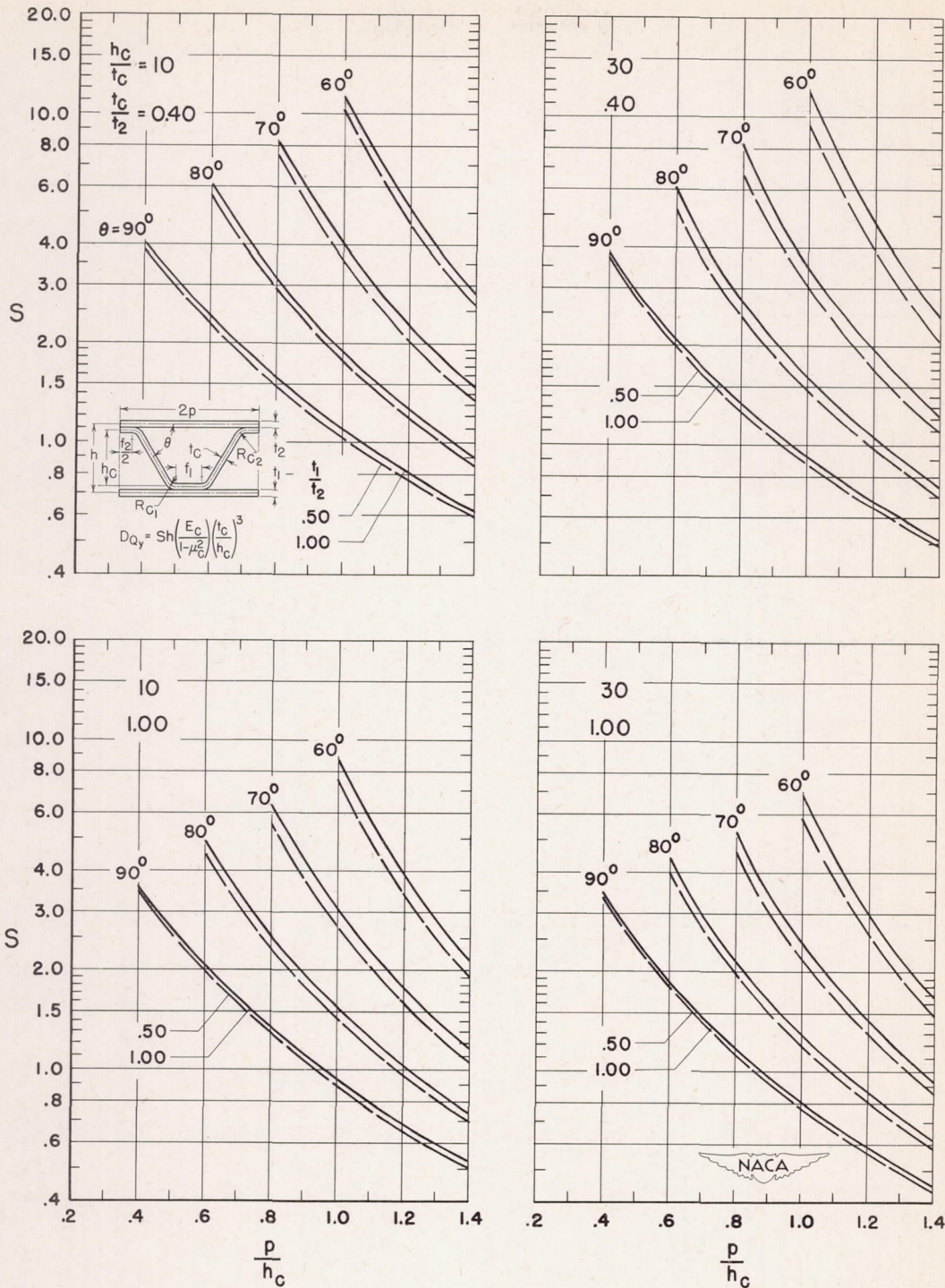
(b) $E_1 = E_2 \neq E_c$.

Figure 4.- Continued.



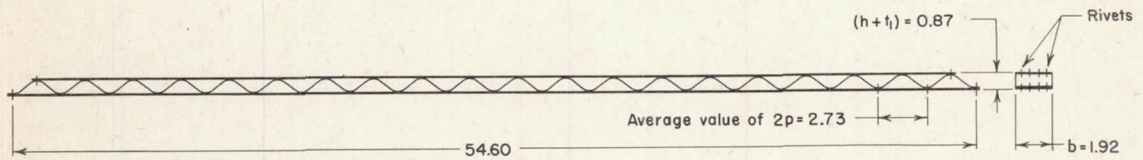
(c) $f_2 \neq f_1$.

Figure 4.- Continued.

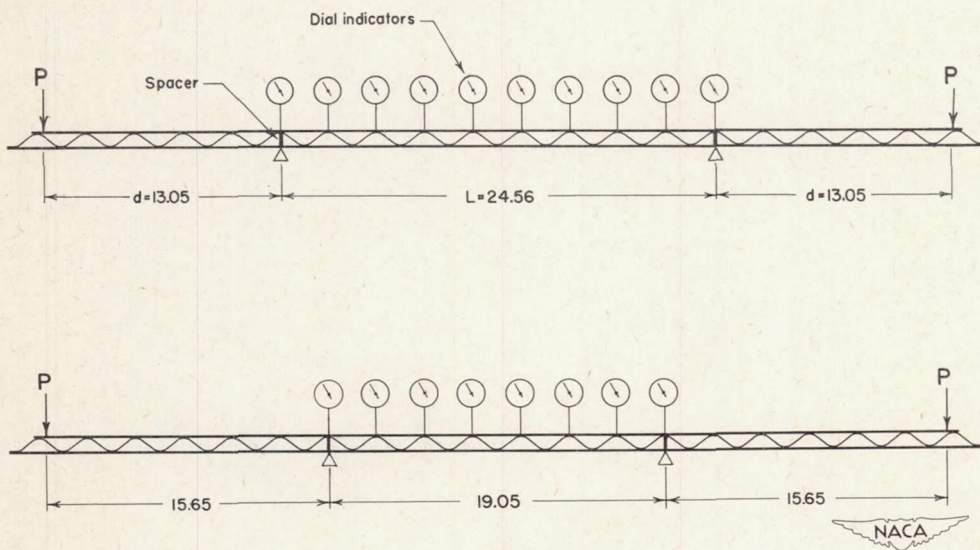


(d) $t_2 \neq t_1$.

Figure 4.- Concluded.

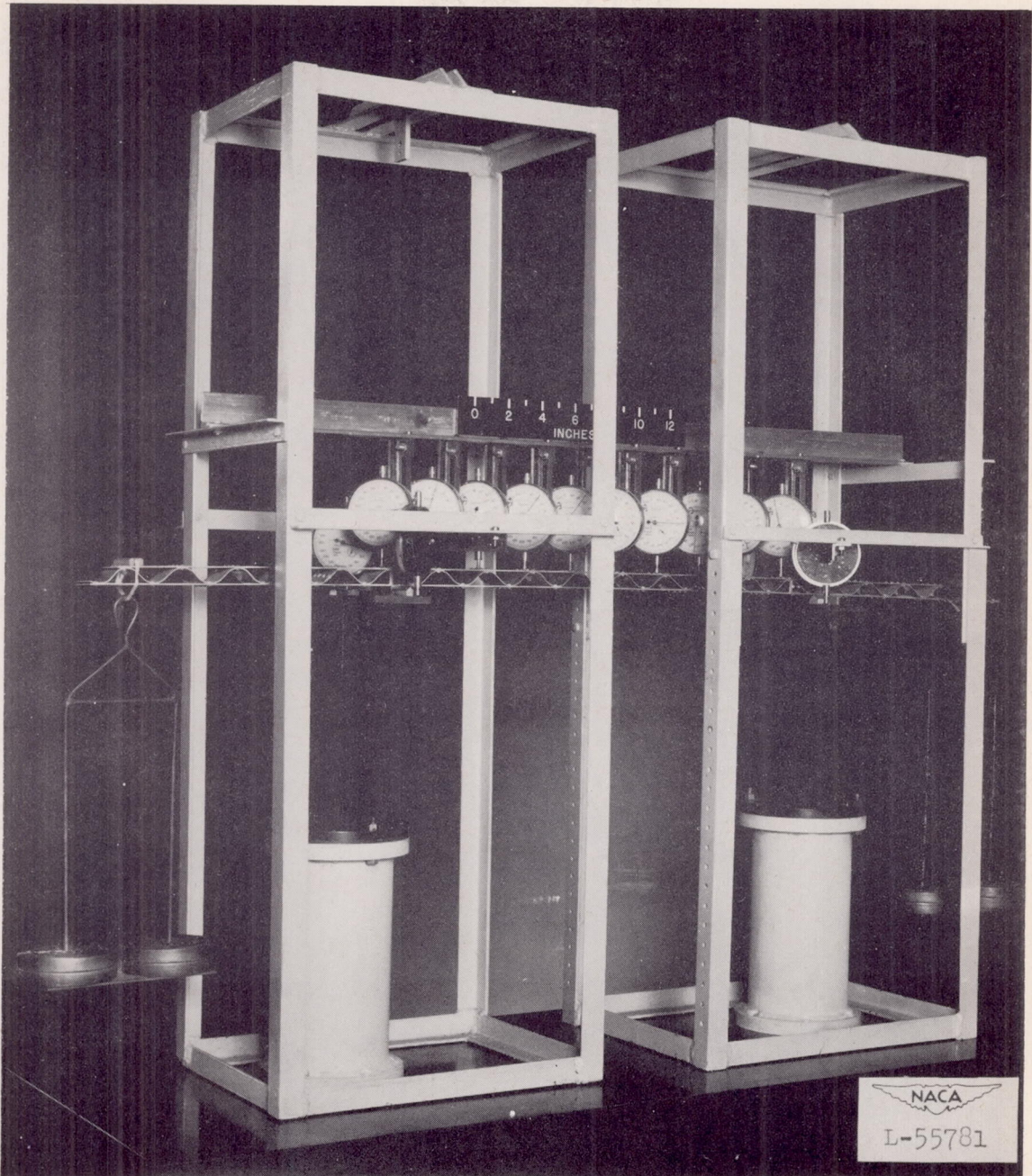


(a) Dimensions of beam test specimen.



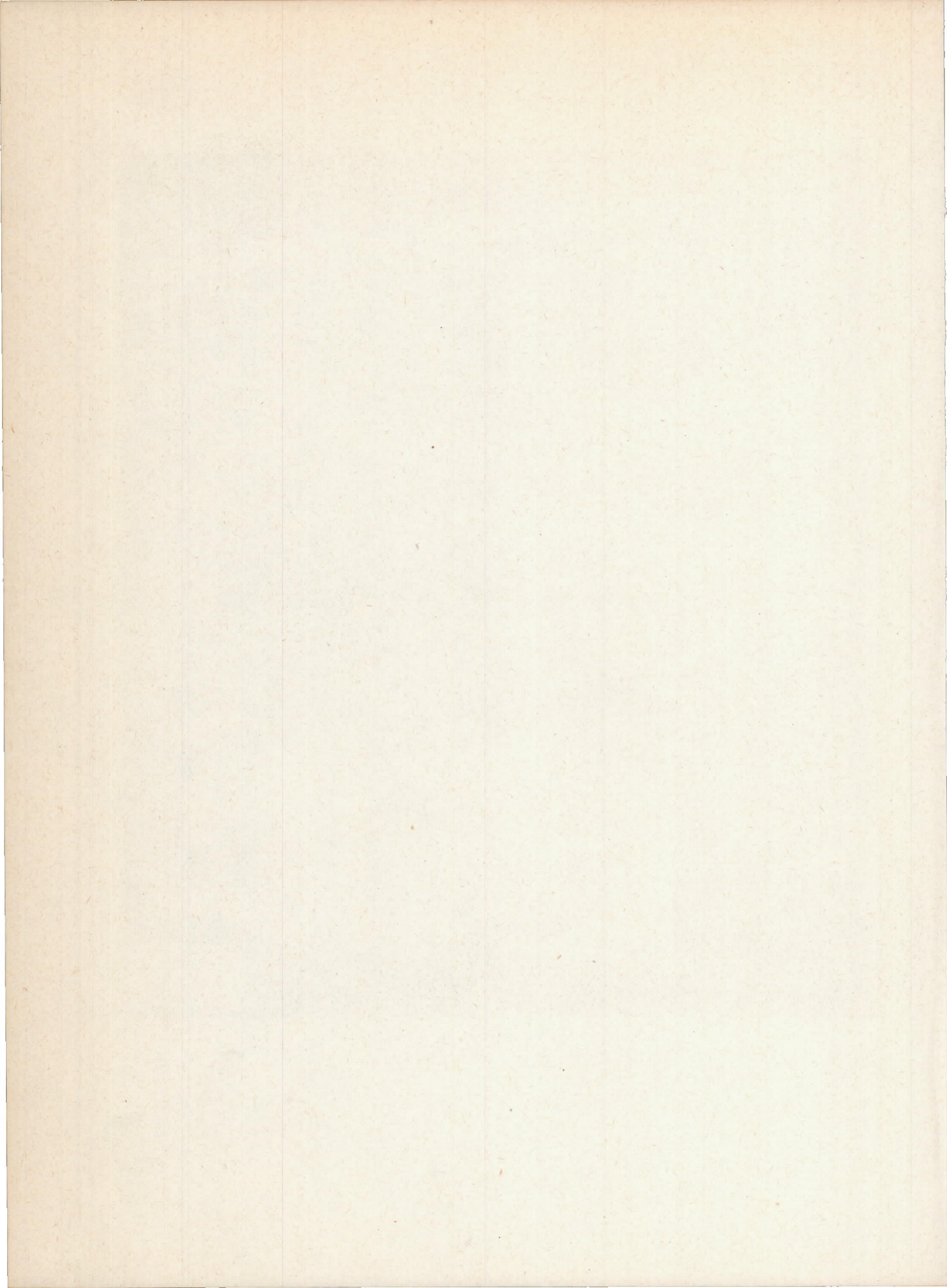
(b) Loadings and gage locations.

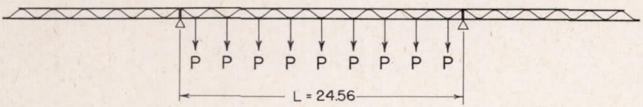
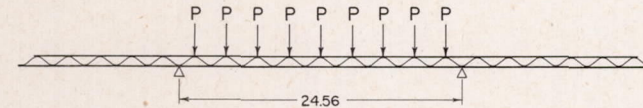
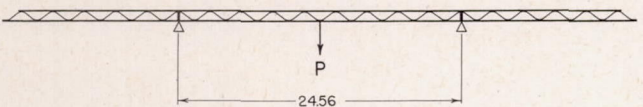
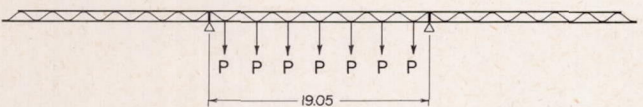
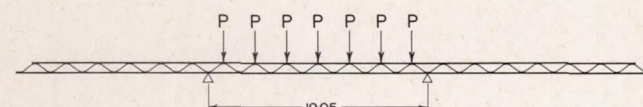
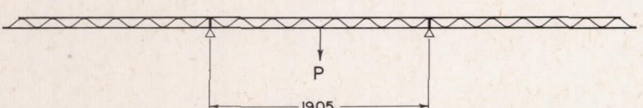
Figure 5.- Specimen and test setup used in experimental determination of D_y .

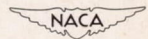


(c) Photograph of typical test setup.

Figure 5.- Concluded.

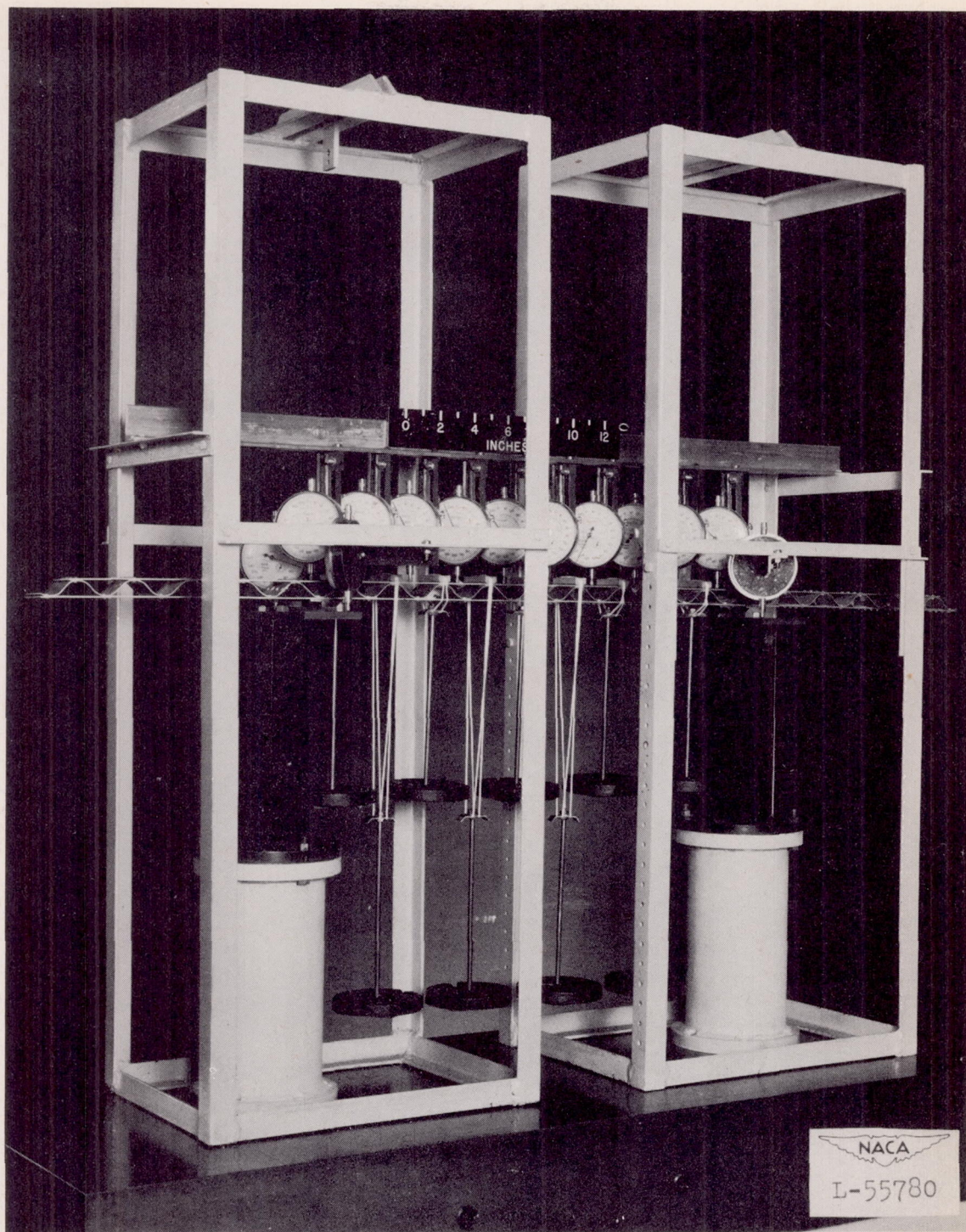


Type of loading	Maximum value of P (lb)	Load increment in P (lb)	Experimental value of D_{Q_y} (lb/in.)
	10	2	4310
	15	3	4040
	60	10	4040
	25	5	4250
	25	5	4010
	100	20	4150



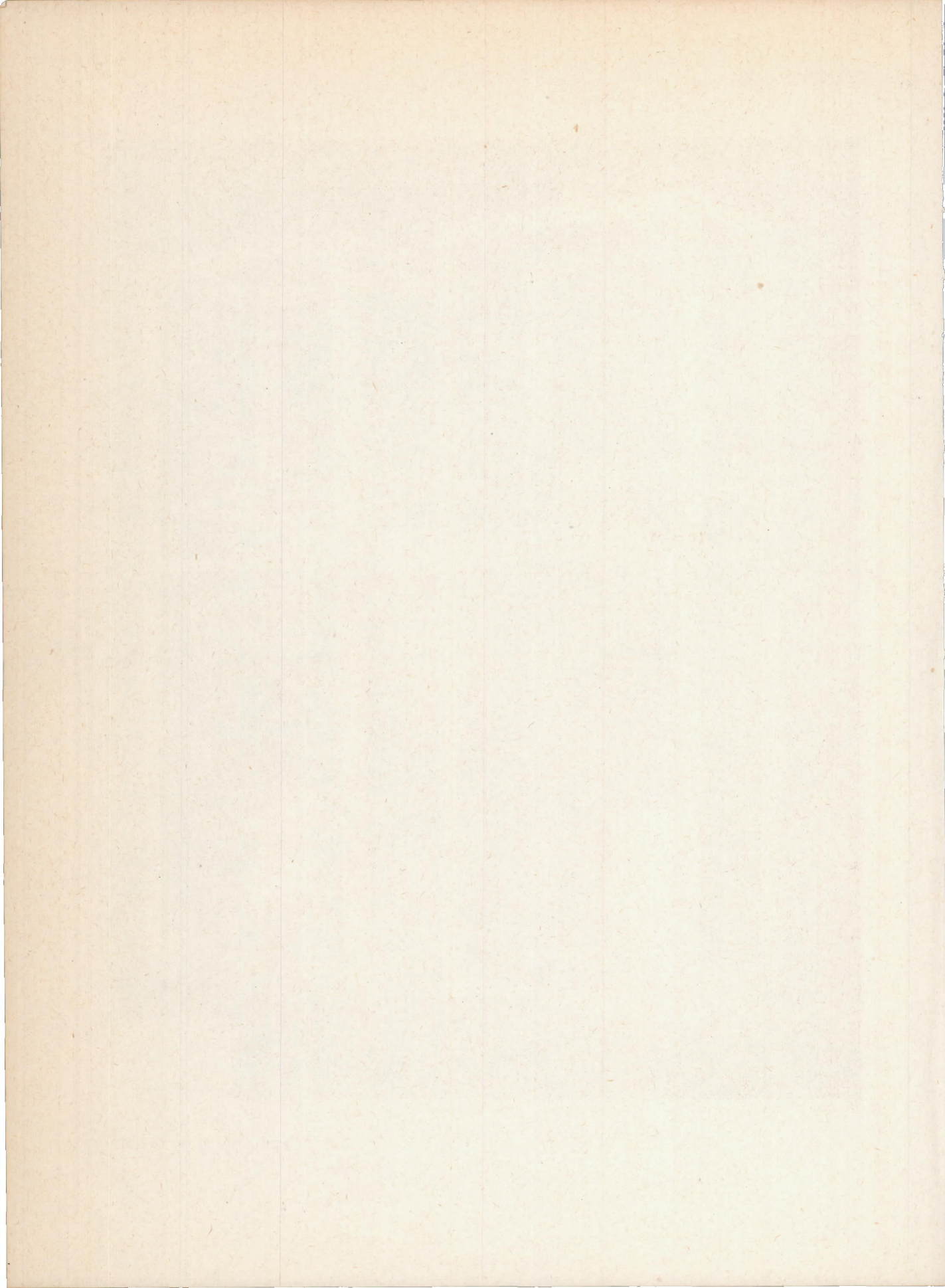
(a) Loadings and resulting values of D_{Q_y} .

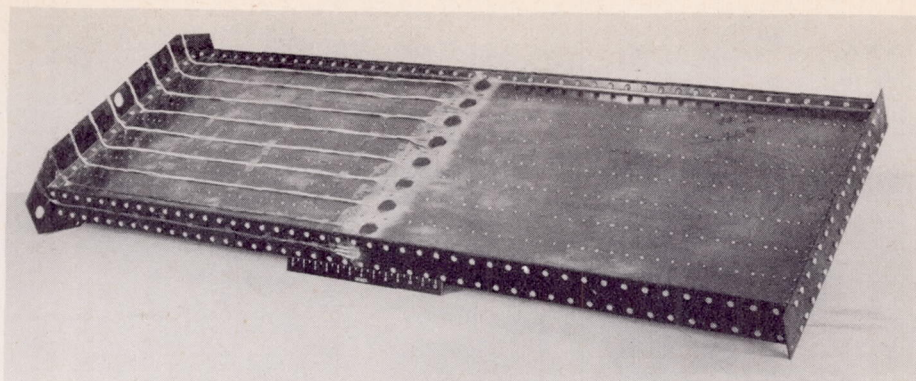
Figure 6.- Test setups used in experimental determination of D_{Q_y} .



(b) Photograph of typical test setup.

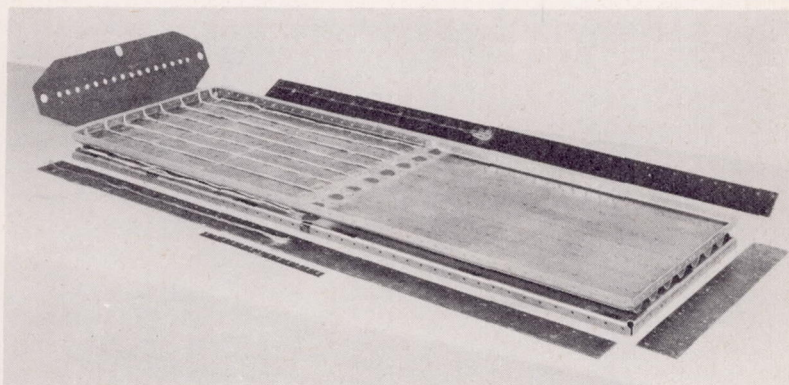
Figure 6.- Concluded.





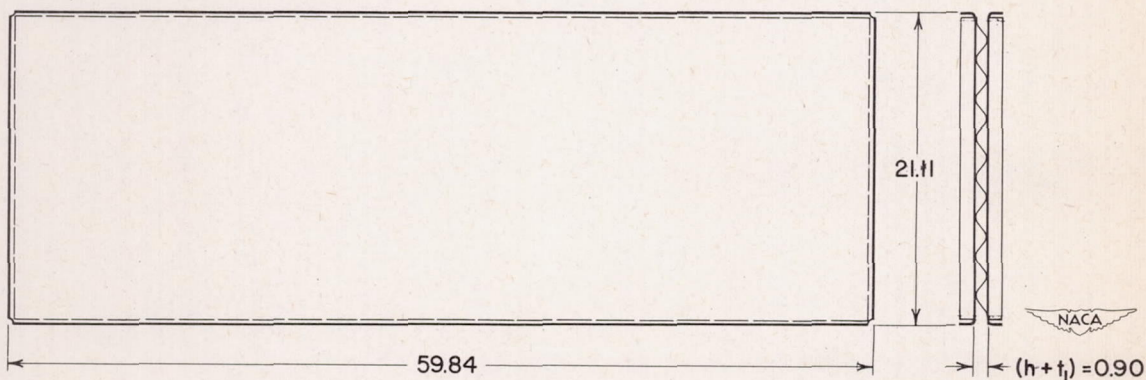
NACA
L-66801

(a) Photograph of test specimen and steel side and end plates assembled.



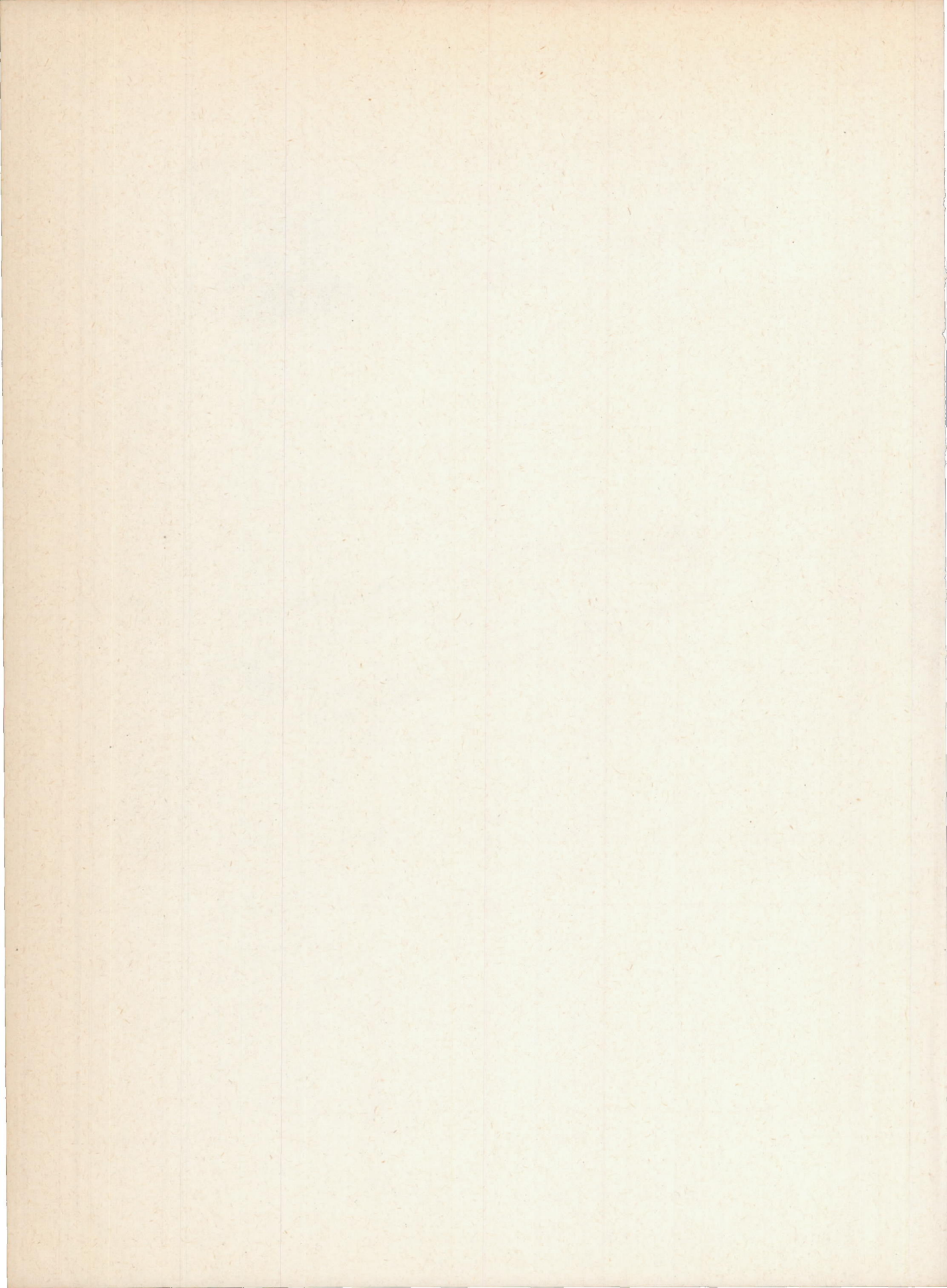
NACA
L-66802.1

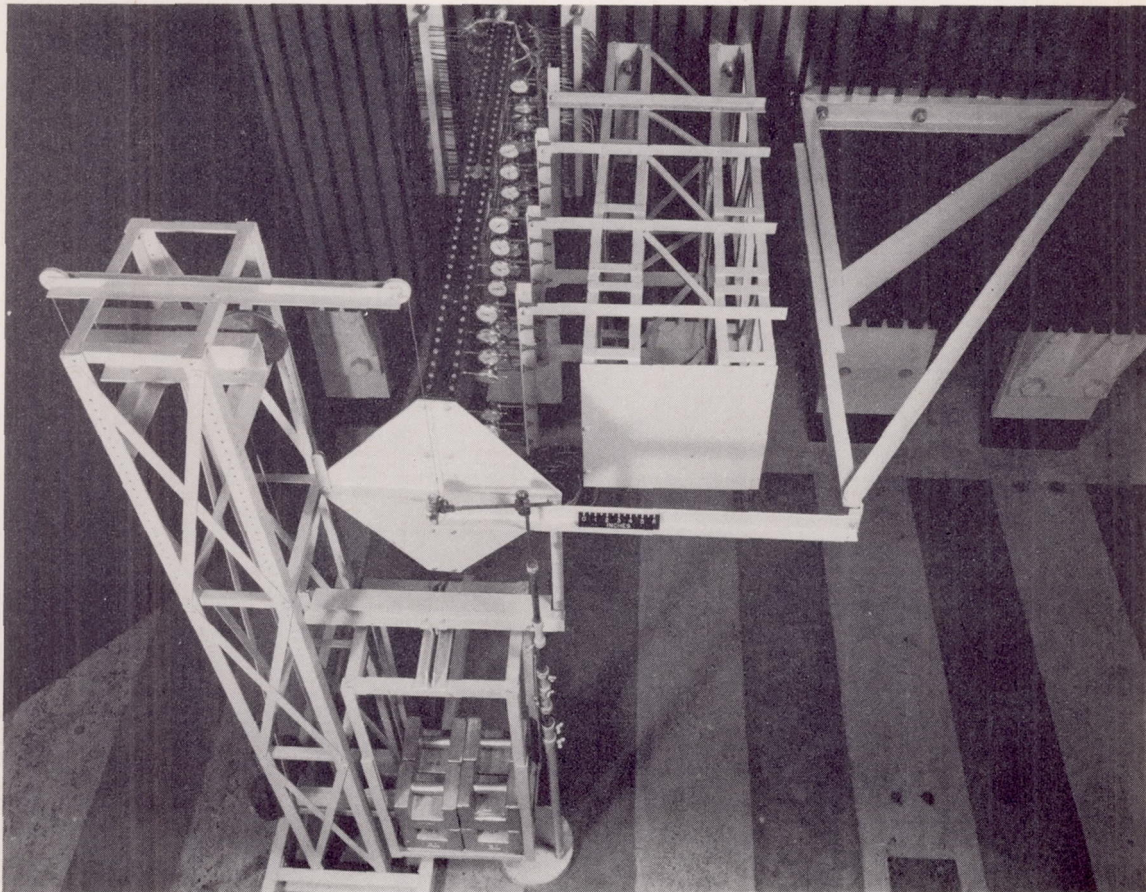
(b) Photograph of test specimen and steel side and end plates disassembled.



(c) Dimensions of twisting test specimen.

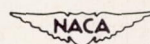
Figure 7.- Specimen and test setup used in experimental determination of D_{xy} .





(d) Photograph of test setup.

Figure 7.- Concluded.



L-58058

